EFFECTS OF THE MELANOCORTIN AGONIST MELANOTAN II, CENTRAL PRO-OPIOMELANOCORTIN AND INTERLEUKIN-6 GENE THERAPIES ON THE REGULATION OF BODY WEIGHT AND ENERGY HOMEOSTASIS

By

GANG LI

A DISSERTATION PRESENTED TO THE GRADUATE SCHOOL
OF THE UNIVERSITY OF FLORIDA IN PARTIAL FULFILLMENT
OF THE REQUIREMENTS FOR THE DEGREE OF
DOCTOR OF PHILOSOPHY

UNIVERSITY OF FLORIDA

2003

This dissertation is dedicated to my wife Qin Dong, my mother Xuehua Tang and my father Yantang Li.

ACKNOWLEDGMENTS

This dissertation has been made possible through the support and encouragement I have received from faculty, friends and family here in Gainesville and back in China. I first want to give my deepest gratitude to my mentor, Dr. Philip J. Scarpace, for all the time and effort he has invested on me. I am very grateful to him for having faith in me and accepting me to be his graduate student, and I also cherish the four years under his guidance. His keen insights in the field of obesity research have made my research much easier, and his consideration and trust have made me, a foreign graduate student feel at home. Dr. Scarpace has been both a mentor and a friend for me. I also want to acknowledge Dr. Nihal Tümer for unofficially comentoring me in my Ph.D. endeavors. She has been kind and considerate at all times, willing to help me on both academic and personal issues. My committee members Dr. Stephen Baker and Dr. William Millard have assisted me to grow gradually by their great suggestions and comments over the last several years, and I thank them. I also want to thank Dr. Ron Klein from Dr. Edwin Meyer's lab for many enthusiastic discussions and his expertise on viral-mediated gene therapy, and to Dr. Michael King for his help on fluorescent microscopy.

My special thanks also go to my colleagues in the laboratory, both past and present; in particular Michael Matheny, the lab manager and a senior scientist, who taught me all the fundamentals when I started, and I can always count on him when I face an unexpected technical problem. Dr. Yi Zhang, who in addition to her scientific input in my projects and manuscript preparations, has been my big sister and always ready to give me

a hand. Jared T. Wilsey, my fellow graduate student, and dear friend, has been a reliable source of humor, American history and standard English grammar whenever I need them. I also want to thank Dr. Min Li, Kit-Yan Cheng and Constanza Frase for their wonderful support and help in daily work.

I want to thank my wife from the bottom of my heart. Without her love and support I would never have reached this far. Lastly, I thank my parents, my parents-in-law and my sister who have been wonderful and supportive at all times.

TABLE OF CONTENTS

Page

LIST OF TABLES

Table page

LIST OF FIGURES

Figure page

Abstract of Dissertation Presented to the Graduate School
of the University of Florida in Partial Fulfillment of the
Requirements for the Degree of Doctor of Philosophy

EFFECTS OF THE MELANOCORTIN AGONIST MELANOTAN II, CENTRAL PRO-OPIOMELANOCORTIN AND INTERLEUKIN-6 GENE THERAPIES ON THE REGULATION OF BODY WEIGHT AND ENERGY HOMEOSTASIS

By

Gang Li

August 2003

Chair: Philip J. Scarpace
Major Department: Pharmacology and Therapeutics

Leptin, an adipocyte-derived hormone, reduces food intake and increases energy expenditure via the hypothalamus. Obese animals and humans are associated with elevated serum leptin and leptin resistance. Recent evidence suggests the central melanocortin (MC) system may be located downstream of the hypothalamic leptin signal pathway. We hypothesize direct activation of the central MC system will circumvent leptin resistance and reduce body weight in leptin-resistant animals.

MC3/4-receptor agonist melanotan II (MTII) was infused centrally for six days in chow-fed (CH) and high-fat (HF) diet-induced obese (DIO) Sprague-Dawley rats. MTII reduced body weight and visceral adiposity and suppressed caloric intake in CH and DIO rats. The initial anorexic and thermogenic responses were enhanced in DIO. In both diet groups, MTII reduced serum insulin and cholesterol. HF feeding increased brown adipose tissue (BAT) uncoupling protein 1 (UCP1), which was further elevated by MTII

treatment. MTII also appeared to increase fat metabolism in muscle of DIO rats. Hypothalamic MC3/4-receptor expression levels were reduced in DIO.

We employed a recombinant adeno-associated virus encoding pro-opiomelanocortin (rAAV-POMC) to enhance POMC expression in hypothalami of obese Zucker rats with defective leptin receptors. POMC gene therapy resulted in a sustained reduction in food intake, a moderate attenuation of weight gain and a decrease in visceral adiposity. It increased BAT UCP1 and decreased fasting serum leptin, insulin and cholesterol levels.

Interleukin-6 (IL-6) is produced in adipose tissues and shares a similar signaling pathway with leptin. A rAAV expressing murine IL-6 (rAAV-IL-6) was delivered into hypothalami of normal Sprague-Dawley rats. The treatment suppressed weight gain and visceral adiposity and enhanced BAT UCP1 without affecting food intake. Unilateral denervation of BAT abolished weight-reducing effect of rAAV-IL-6 and prevented increases in UCP1 mRNA and protein levels in the denervated BAT pad.

Our studies demonstrate that MTII and POMC gene therapy activate the central MC system, reduce body weight and visceral adiposity, and improve glucose and cholesterol metabolism in leptin-resistant DIO and obese Zucker rats, respectively. Both hypophagia and increased energy expenditure are the likely underlying mechanisms. IL-6 also has a potential role in energy regulation, which involves sympathetic induction of UCP1 in BAT.

CHAPTER 1
LITERATURE REVIEW

Obesity is a pressing health problem in Western and developing countries. The latest survey shows more than 60% of the US adults are overweight and over one-third obese (Flegal et al., 2002). Obesity is not only disfiguring but also associated with a series of life-threatening complications such as type 2 diabetes, hypertension, heart diseases, stroke, certain cancers, and arthritis (Visscher and Seidell, 2001). The etiology of obesity is still unknown, and many genetic and epidemiological studies suggest that there are multiple causes of obesity involving diet, genes and psychological factors.

Homeostatic Energy Regulation: Biased Toward Weight Gain?

The regulation of body weight can be considered a homeostatic system, and a delicate balance between food intake and energy expenditure is needed to maintain a steady body weight for each normal individual. However, this energy regulation system may have evolved to be biased toward weight gain and storage of fat in times of plenty in order to be protected against famine. Conversely, there is little evolutionary pressure to suppress food intake or burn off excess calories as heat when energy stores are replete (Schwartz et al., 2003). This inherently biased system may account for the dramatic surge in obesity in the present calorie-oversupplied environment.

White Adipose Tissue: More Than a Storage Depot for Fat?

Unraveling the diverse hormonal and neuroendocrine systems that regulate energy expenditure and body fat has been a long-standing challenge in the fields of obesity and metabolic research. A great number of hormones or factors have been discovered to be

involved in the positive or negative regulation of body weight. Although white adipose tissue (WAT) was once thought of as merely a storage depot for fat, we now know that WAT is a vital endocrine organ that is actively involved in whole body homeostasis. WAT secretes a family of hormones collectively known as adipokines, including leptin, adiponectin, tumor necrosis factor (TNF)-α, resistin and interleukin-6, many of which have endocrine functions in modulating food intake and energy expenditure (Saltiel, 2001).

Leptin

Leptin, the ob gene product, is a 16 kDa soluble hormone primarily produced in white adipocytes. Since the discovery of leptin in 1994, our understanding of neuroendocrine regulation of body weight and food intake has been greatly expanded (Jequier, 2002). Leptin, synthesized and secreted by fat cells in proportion to total body fat mass, has been implicated as one of the adiposity signals—afferent, blood-borne signals that convey information about the status of body fat stores to the brain. Once it enters the central nervous system (CNS), leptin acts on hypothalamic satiety and appetite centers to both reduce food consumption and increase energy expenditure. While obesity, insulin, TNF-α and glucocorticoids induce leptin expression, fasting and sympathetic stimulation reduce its synthesis (Sweeney, 2002). The details of the action and effects of leptin on energy regulation will be discussed later.

Interleukin-6

Interleukin-6 (IL-6) is a multifunctional, proinflammatory cytokine that acts on a wide range of tissues influencing cell growth and differentiation. It is now understood that both immune and nonimmune cells synthesize IL-6. Interestingly, systemic

concentrations of IL-6 have been shown to be positively correlated with body mass index (Vozarova et al., 2001), and as much as a third of total circulating IL-6 originates from adipose tissue (Mohamed-Ali et al., 1997). Furthermore, IL-6 and its receptor share many structural and functional similarities with leptin (Schobitz et al., 1992; Tartaglia et al., 1995). In this regard, similar to leptin, IL-6 may be both an autocrine and paracrine regulator of adipocyte function. However, it is unclear whether IL-6 serves as an adiposity signal to the CNS like leptin does.

Hypothalamic Neural Circuits Controlled by Leptin

Food intake and body weight are regulated by multiple factors and involving several brain areas. However, the hypothalamus is still regarded as the main regulatory center for feeding and energy expenditure. Leptin, one of the most important adiposity signals, interacts with leptin receptors on two populations of first order hypothalamic neurons. One population of neurons synthesizes and releases two orexigenic (feeding inducing) neuropeptides: neuropeptide Y (NPY) and agouti-related peptide (AgRP). These neurons are referred to as NPY neurons, and leptin acts on these neurons to reduce the expression of NPY and AgRP (Spiegelman and Flier, 2001). Another population of neurons expresses pro-opiomelanocortin (POMC), the precursor for the anorexigenic peptide α melanocyte-stimulating hormone (α-MSH). These neurons, designed as POMC neurons, also express cocaine and amphetamine-related transcript (CART). Leptin induces the expression of these two anorexigenic peptides (α-MSH and CART) (Spiegelman and Flier, 2001). Thus, the leptin-induced inhibition of food intake results from, at least in part, both the suppression of orexigenic and the induction of anorexigenic neuropeptides.

Leptin Receptor

The leptin receptor is a member of the class I cytokine family (Tartaglia et al., 1995, Tartaglia, 1997) which includes the receptors of IL-6, leukemia inhibitory factor and gp130 (Fruhbeck et al., 2001). The distribution of the leptin receptor is almost universal and most abundant in hypothalamus (Mercer et al., 1996; Scarpace et al., 2000a; Vaisse et al., 1996). The gene coding for leptin receptor is alternatively spliced to produce at least six isoforms, all of which have identical extracellular and transmembrane domains, but different cytoplasmic domains (Tartaglia, 1997; Lee et al., 1996). One of these splice variants, referred to as the long form receptor (ObRb), possesses a large 306 amino acid cytoplasmic domain conferring full signal transduction capability. Other variants, containing only a short portion of the cytoplasmic domain are referred to as the short form receptors. They have limited signal transduction capability and may act as soluble leptin carriers in plasma or across the blood-brain barrier (Fruhbeck et al., 2001). Because of their leptin binding ability, the short form leptin receptors can alter the proportion of leptin circulating in the free versus protein-bound form and may hence serve as important physiological determinants of leptin action (Lammert et al., 2001). The erroneous splicing of the long form leptin receptor in db/db mice yields a truncated receptor, and obesity results (Lee et al., 1996). The obese phenotype of the db/db mice suggests that the ObRb plays an important role in regulation of food intake, energy expenditure and endocrine function.

Leptin Signal Transduction

Leptin receptors generally exist as homo-dimers (Devos et al., 1997). Leptin binds to ObRb in a 1:1 stoichiometry, resulting in the formation of a tetrameric receptor/ligand complex (Devos et al., 1997). Leptin signal in the hypothalamus is mediated through

binding to the leptin receptor and subsequent activation of Janus kinase 2 (JAK2), which is reminiscent of IL-6 signaling. Upon ObRb activation, the subsequent signal events diverge into at least two pathways. One pathway involves phosphorylation of the signal transducer and activator of transcription 3 (STAT3) and initiation of transcription by the activated STAT3 (Bates et al., 2003). The other involves the recently described leptin activation of the insulin receptor substrate (IRS)-phosphatidylinositol-3-OH kinase (PI3K)-mediated signal pathway (Niswender et al., 2001; Zhao et al., 2002). Since PI3K is an essential molecule in mediating insulin responses, thus leptin and insulin by both stimulating PI3K, may modulate each other's function in the control of energy homeostasis. The nature of the interaction between the JAK2-STAT3 and IRS-PI3K pathways is still unclear at present time.

NPY Neurons

NPY is a 36-amino acid peptide that is found in high concentrations in the hypothalamus (Allen et al., 1983). It is synthesized in NPY neurons situated in the arcuate nucleus (ARC). Fibers of these neurons project from ARC to the paraventricular nucleus (PVN), ventromedial nucleus (VMH), and dorsomedial nucleus (DMH) where the peptide is released (Sawchenko and Pfeiffer, 1988). NPY is regarded as the most potent orexigenic peptide. Leptin, as well as insulin, decreases NPY expression and NPY levels via their ARC leptin/insulin receptors (Krysiak et al., 1999; Schwartz et al., 1992) while glucocorticoids stimulate NPY neurons via a glucocorticoid receptor-mediated decrease in CRH expression, which abolishes the inhibitory effect of CRH on NPY expression (Hahn et al., 1998). Six NPY receptors have been cloned. The influence of NPY on feeding is predominantly mediated by the postsynaptic NPY1 and 5 receptors, which are highly expressed in the PVN (Hu et al., 1996).

Central Melanocortin System

Melanocortins

The POMC gene encodes a 31-36-kDa pre-prohormone, from which seven mature peptide hormones are derived via post-translational cleavage by various prohormone convertases. These peptides, collectively called melanocortins (MCs), include adrenocorticotropic hormone (ACTH), α-MSH,β-MSH, γ-MSH, corticotropin-like intermediate lobe peptide (CLIP), β-lipotropin, and β-endorphin (MacNeil et al., 2002). Of these seven bioactive peptides, α-MSH is presumed to be the major regulator of food intake and energy expenditure. This 13-amino-acid peptide represents the most amino terminal portion of ACTH.

MC receptors

Molecular cloning identified five G-protein-coupled receptors which, when activated by melanocortins, signal via $G\alpha_s$ to increase cAMP (Wikberg, 1999). The melanocortin 1 receptor (MC1R) was first recognized as the peripheral α-MSH receptor present in melanocytes, where it regulates the pigmentation of the skin. MC1R is also present in other tissues besides the skin: pituitary, gonad glands, macrophages and monocytes, neutrophils, astrocytes and so on. The MC2R is the ACTH receptor. It is highly expressed in the cortex of the adrenal gland, where it mediates the hormonal corticotropic effect of ACTH. Numerous tissues express the MC5R, and high levels of expression of MC5R are detected in several exocrine glands, notably the lacrimal, harderian and sebaceous glands, suggesting a role in sebaceous gland lipid production. MC3R and MC4R are expressed mainly in the CNS and involved in regulating energy

metabolism. The effects of melanocortins on feeding and energy expenditure are postulated to be mediated by central MC4R, and to a lesser extend, by MC3R.

POMC neurons and MC3 and MC4R expression

Hypothalamic POMC neurons send synapses to PVN and lateral hypothalamic area where α-MSH is released and acts via MC4R mainly to inhibit food intake and increase energy expenditure (Lu et al., 1994; Ollmann et al., 1997). The activity of the central MC system is determined by the balance between the endogenous agonist α-MSH and the endogenous antagonist AgRP. POMC expression is stimulated by leptin, and deficiency of leptin (such as during starvation) inhibits POMC expression. Although both MC3R and MC4R are expressed mainly in the CNS, MC4R is widely distributed throughout numerous brain regions with the highest levels observed in the PVN and the dorsal motor nucleus of the vagus in the caudal brainstem (Cowley et al., 1999). In contrast, expression of MC3R is largely confined to the hypothalamus with ARC and VMH having highest expression levels (Roselli-Rehfuss et al., 1993). It is believed that the regulation of feeding and energy expenditure by melanocortins is mainly mediated by MC4R while MC3R may play a role in feeding efficiency, partitioning of nutrients into fat, and feedback regulation of the activity of the POMC neurons.

Obesity and central MC system

During the last decade, a series of pharmacological and genetic studies have conclusively demonstrated that the central MC system is essential in the homeostatic regulation of feeding and body weight (Cone, 1999). Initial data suggesting a role for melanocortins in body weight regulation came from the study of the obese agouti mouse. Agouti protein is a competitive antagonist of the MC1R. In mammals, agouti is expressed

primarily in the skin where it acts in a paracrine manner to regulate fur pigmentation. Agouti mice with a mutation that lead to ectopic expression of agouti in the brain develop obesity, apparently by antagonism of the MC4R and possibly the MC3R (Lu et al., 1994). AgRP is an endogenous antagonist of the MC3R and possibly an inverse antagonist of the MC4R. Transgenic mice overexpressing AgRP are obese (Ollmann et al., 1997). In addition, POMC knock-out (KO) mice also develop obesity, which can be reversed by treatment with a stable α-MSH analog (Yaswen et al., 1999). Confirmation of the role of the MC4R and MC3R in obesity came from the analysis of MC4R and MC3R KO mice (Butler et al., 2000; Chen et al., 2000; Huszar et al., 1997). MC4R KO mice develop maturity-onset obesity, are hyperphagic, and display reduced oxygen consumption, indicative of a metabolic defect (Butler et al., 2000; Chen et al., 2000). The MC4R KO mice do not respond to the thermogenic effect of a potent nonselective MC receptor agonist melanotan II (MTII) and have a reduced response to the anorexic actions of MTII, suggesting that melanocortins modulate body weight mainly through MC4R (Chen et al., 2000). In contrast to MC4R KO mice, MC3R KO mice are not hyperphagic or significantly overweight, but they have increased adiposity and feeding efficiency (Butler et al., 2000; Chen et al., 2000). Characterization of a variety of obesity models with altered melanocortin signaling suggests that the central MC system may play a significant role in regulating body weight in humans. In fact, two human genome-wide scans found evidence for linkage of obesity to 2p21, a locus that includes POMC. Furthermore, mutations in the POMC gene cause severe obesity in humans (Krude et al., 1998), and up to 4-5% of severe obese humans have defects in the MC4R gene (Farooqi et al., 2000). The ready development of obesity by disruption of the component of the central

melanocortin system underlies the importance of this system in the regulation of body weight and energy homeostasis.

IL-6 and Energy Regulation

IL-6 Signal Transduction

As would be expected from the pleiotropic nature of IL-6's action, many diverse cells express IL-6 receptors, such as lymphocytes, monocytes, hepatocytes, neuronal and glial cells (Kishimoto et al., 1992; Van Wagoner and Benveniste, 1999). The IL-6 receptor (IL-6R), an 80-kDa glycoprotein, is also known as gp80. It is a member of the Class I cytokine receptor family (Fruhbeck et al., 2001). Intriguingly, the intracellular region of IL-6R does not contain any kinase domains, and hence the receptor appears to be incapable of signaling activity (Yamasaki et al., 1988). It is now understood that, IL-6 first binds to IL-6R, forming a low-affinity receptor complex. This complex then associates with the 130-kDa signal-transducing transmembrane glycoprotein gp130 to provide high-affinity binding of IL-6 (Taga et al., 1989; Ward et al., 1994). Dimerization of the intracellular domains of two gp130 molecules recruits JAKs, leading to inter- or intramolecular phosphorylation and subsequent activation. Specific transcription factors STATs are then docked to the stimulated receptor complexes, phosphorylated and activated by receptor-associated JAKs. Activated STATs dimerize and translocate to the nucleus where they bind DNA and stimulate transcription (Hibi et al., 1996; Taga and Kishimoto, 1997). A wide range of evidence shows after the activation of gp130, IL-6 induces a rapid tyrosine phosphorylation of JAK1, JAK2, Tyk2, STAT1, and STAT3. STAT3 in particular, has been indicated to play a key role in IL-6 signal transduction. Recently, several families of proteins involved in the down-regulation of cytokine signaling have been described. Among them suppressor of cytokine signaling-3 (SOCS-

3) protein is shown to act as a negative regulator of the JAK/STAT pathway either by inhibiting JAK activity or by inhibiting binding of STAT factors to SH2 domain of gp130; therefore, preventing the phosphorylation of STATs (Starr et al., 1997; Suzuki et al., 1998). SOCS-3 is hence believed to be an important factor in IL-6 signal transduction.

IL-6 and Weight Regulation

IL-6 has long been considered an inflammatory mediator as well as a stress-induced cytokine (Yudkin et al., 2000). It has pleiotropic effects on a variety of tissues, including stimulation of acute-phase protein synthesis, induction of the proliferation and differentiation of lymphocytes, and increase in the activity of the hypothalamic-pituitary-adrenal axis (HPA). Central and peripheral administrations of IL-6 reportedly induce fever response and/or dose-dependently reduce food intake (Johnson, 1998; Schobitz et al., 1995). Many investigators also believe that IL-6 may play a role in cancer cachexia and some other wasting disorders (Greenberg et al., 1992; Strassmann et al., 1992). Obviously, IL-6 has an impact on energy balance, but the underlying mechanisms are not well understood. Moreover, studies in this regard have mainly focused on only short-term IL-6 treatment, and the results are not always clearcut. First, although IL-6 has, for a long time, been considered an anorexic cytokine, previous reports also showed peripheral administration of IL-6 had no effect on food intake and body temperature (van Haasteren et al., 1994). A recent study also suggests that alterations in food intake in rodents with experimental cancer were not directly related to systemic IL-6 but rather secondary to IL-6-dependent tumor growth (Cahlin et al., 2000). Secondly, IL-6 induces fever response, and intracerebroventricular (icv) injection of IL-6 increases unmasking of GDP binding in brown adipose tissue (BAT) (Busbridge et al., 1989), but the exact mechanisms

underlying enhanced thermogenesis still remain to be elucidated. Finally, the long-term effects of IL-6 administration (more than two weeks) on food intake and body weight have never been examined. Therefore, we employed IL-6 gene delivery to examine some of these questions.

Energy Expenditure

Total body energy expenditure represents the conversion of oxygen and substrate (either food, stored fat, glycogen or protein) to carbon dioxide, water, and energy (either heat or work). Thus, total body energy expenditure can be assessed by whole body oxygen consumption (Lowell and Spiegelman, 2000). Obesity results when energy intake (food) exceeds energy expenditure. There are three components of energy expenditure, obligatory expenditure (required for normal cellular and organ function), physical activity, and adaptive thermogenesis (Lowell and Spiegelman, 2000). The latter occurs mainly in skeletal muscle and brown adipose tissue, and is one mechanism to reduce body weight after hyperphagia and maintain body temperature after exposure to cold (Boss et al., 2000; Himms-Hagen, 1983).

Brown Adipose Tissue and Energy Expenditure

BAT is a specialized fat tissue in mammals heavily innervated by sympathetic nerves. The brown adipocytes contain abundant mitochondria with closely packed cristae that confer the characteristic brown color to this tissue. Thermogenesis in BAT is mainly mediated by norepinephrine activation of sympathetically innervated β_3 adrenoreceptors (Nedergaard et al., 2001). Energy expenditure through brown adipose tissue thermogenesis contributes either to maintenance of body temperature in a cold environment or to consumption of food energy, i.e. cold-induced or diet-induced thermogenesis. Both mechanisms involve a specific and unique protein: the uncoupling

protein-1 (UCP1). UCP1, a 32-kDa protein, is exclusively expressed in mitochondria of brown adipocytes where it uncouples respiration from ATP synthesis and dissipates the proton gradient as heat (Nedergaard et al., 2001).

Skeletal Muscle and Energy Expenditure

Over much of the past century, the skeletal muscle, by virtue of its large size contributing 30–40% of body mass, has been considered the major tissue that enables mammals to adapt to changes in food availability. For example, the rate of heat production during periods of food scarcity is turned down in the skeletal muscle to conserve energy while it is geared up during food abundance to burn excess energy. However, the mechanisms by which skeletal muscle could allow such adaptations remain elusive. UCP3, a UCP1 homologue in muscle, has been proposed to participate in the regulation of thermogenesis and lipid metabolism (Wang et al., 2003). However, several recent studies cast doubt on its physiological relevance to muscle mitochondrial uncoupling (Hesselink et al., 2003; Cadenas et al., 1999; Iossa et al., 2001). Leptin has also been indicated to have direct thermogenic effects in skeletal muscle. Presumably, these effects require both the long form of leptin receptors and PI3K signaling (Dulloo et al., 2002). Muscle-type Carnitine palmitoyltransferase I (M-CPT I) is an important enzyme for energy homeostasis and fat metabolism by modulation of long-chain fatty acid (LCFA) entry into mitochondria, where the LCFAs undergo beta-oxidation (Jeukendrup, 2002). M-CPT I is located in the outer mitochondrial membrane and sensitive to inhibition by malonyl-CoA, which makes it an important site for metabolic regulation. Malony-CoA is the product of a reaction catalyzed by Acetyl-CoA carboxylase (ACC), the first step in fatty acid biogenesis from acetyl-CoA and preserved in nonlipogenic tissues such as skeletal muscles and heart muscle (Jeukendrup, 2002).

The formation of malonyl-CoA may therefore offer a main control point of fatty acid catabolism through inhibition of CPT I in muscle.

Leptin Resistance

One hallmark of diet-induced obesity is leptin resistance. Human obesity as well as many rodent models is associated with elevated serum leptin and leptin resistance, which becomes more pronounced with progressive degrees of obesity (Considine et al., 1996;Halaas et al., 1997; Van Heek et al., 1997; Widdowson et al., 1997). Dr. Scarpace's lab, in particular, has demonstrated that age-related obesity is also associated with leptin resistance (Scarpace et al., 2000b; Scarpace et al., 2000c). The mechanism of leptin resistance with age or obesity is unknown, and most likely is multi-factorial. An early theory of leptin resistance was that leptin was not reaching the target sites in the brain due to a limitation of leptin transport across the blood-brain barrier (peripheral leptin resistance). Evidence supporting this mechanism is the observation that mice with DIO respond better to leptin administered directly into the brain than leptin introduced peripherally (Van Heek et al., 1997; El Haschimi et al., 2000). Our laboratory reported similar findings with age-related obesity. Leptin responses were blunted with either peripheral or central administration of leptin, but to a greater extent following peripheral administration (Scarpace et al., 2000c, 2001; Shek and Scarpace, 2000). Besides the apparent peripheral leptin resistance, central leptin resistance characterized by reduced leptin receptor expression and protein levels and attenuated leptin signal transduction in the hypothalamus may also exist in various obese animal models (El Haschimi et al., 2000; Scarpace et al., 2000c, 2001).

Recombinant Adeno-associated Virus

Adeno-associated virus (AAV) is a single-stranded DNA virus that belongs to the parvovirus family. The viable transfection of AAV requires the presence of a helper virus (Muzyczka, 1992). AAV exists as a latent infection in humans, and so far has not been found to be associated with any human diseases. AAV is capable of infecting non-dividing cells with a site-specific integration (human chromosome 19). Recombinant AAV (rAAV) is derived from AAV and contains only the AAV terminal repeats but not viral coding sequences. rAAV has been uniquely successful as a gene transfer vector (Monahan and Samulski, 2000; Smith-Arica and Bartlett, 2001). The successful use of rAAV-based gene delivery offers clear advantages such as long term, high level *in vivo* expression of transduced genes in several different animal systems (Athanasopoulos et al., 2000; Kaplitt et al., 1994; Xiao et al., 1996). Among various types of rAAV used today, the rAAV type 2 has been uniquely successful as gene transfer vector into the CNS (Xu et al., 2001; Li et al., 2002; Wilsey et al., 2002) .

Based on the lines of information detailed above, we put forward two hypotheses in this dissertation. First, direct activation of the central melanocortin system, which is presumed to be downstream of leptin signaling pathway, can circumvent leptin resistance and reduce body weight and adiposity in the leptin-resistant diet-induced obese animals. The second hypothesis is that IL-6, which shares a similar signal transduction pathway with leptin, can also modulate body weight in normal animals. The goals of this dissertation were, (1) to test the effects of chronic activation of the central MC system by a potent MC3/4-receptor agonist MTII in a diet-induced obese rat model with normal genetic background, (2) to test the effects of long-term activation of central MC system

by rAAV-mediated POMC gene therapy in the genetically obese Zucker (fa/fa) rats with defective leptin receptors, (3) to test the long-term effects of central rAAV-mediated IL-6 gene delivery in the normal rats.

CHAPTER 2
GENERAL METHODS AND MATERIALS

Experimental Animals

Young adult (age 3-4 months) male and female Sprague-Dawley rats, nine-week old male obese Zucker (fa/fa) rats were obtained from Harlan Sprague-Dawley (Indianapolis, IN), Taconic (Germantown, NY) and Charles River (Wilmington, MA), respectively, for all experiments described in this dissertation. Upon arrival, rats were examined and remained quarantined for at least one week. Animals were individually caged with a 12:12 hour light:dark cycle (07:00 to 19:00 hr). Animals were cared for in accordance with the principles of the NIH Guide to the Care and Use of Experimental Animals.

Construction of rAAV Vector Plasmids

pTR-CBA-POMC encodes murine POMC cDNA (a generous gift from Dr. James Roberts) (Uhler and Herbert, 1983) under the control of the hybrid cytomegalovirus immediate early enhancer/chicken β-actin (CBA) promoter (Daly et al., 2001). The woodchuck hepatitis virus post-transcriptional regulatory element (WPRE) is placed downstream of the POMC transgene to enhance its expression (Loeb et al., 1999). A murine IL-6 cDNA (a generous gift by Dr. I.L. Campbell, the Scripps Research Institute, La Jolla, CA) (Raber et al., 1997) was inserted into rAAV vector plasmid pTR-UF12. This plasmid contains the AAV terminal repeats (TRs), the only remaining feature (and 4%) of the wild type AAV genome. Flanked by the TRs, the expression cassette of pTR-UF12 includes the following components, in 5' to 3' order: 1) a 1.7 kb sequence

containing the hybrid cytomegalovirus immediate early enhancer/CBA promoter/exon1/intron (Daly et al., 2001); 2) the internal ribosome entry site (IRES) from poliovirus, which provides for bicistronic expression (Dirks et al., 1993); 3) green fluorescent protein (GFP) (Klein et al., 1998); 4) and the polyA tail from bovine growth hormone. The IL-6 cDNA was inserted between the CBA promoter and the IRES element of the pTR-UF12 to derive the construct pTR-IL-6. The control plasmid, termed pTR-Control, is similar to pTR-CBA-POMC and pTR-IL-6 but only encodes GFP.

In Vitro Analysis of rAAV Plasmids

In vitro Analysis of pTR-CBA-POMC plasmid

The pTR-CBA-POMC construct was tested for *in vitro* expression of POMC by transfecting Human embryonic kidney 293 cells (HEK 293 cells) using FuGENE 6 transfection reagent (Roche Diagnostics, Indianapolis, IN) according to the protocol provided by the manufacturer. One day after the transfection, cells were harvested and total RNA isolated. POMC mRNA levels were analyzed by RT-PCR.

In Vitro Analysis of pTR-IL-6 Plasmid

The pTR-IL-6 construct was tested for *in vitro* expression of IL-6 by mammalian cells. HEK 293 cells were transfected by the calcium-phosphate method, using $2x10^6$ cells and 8 μg DNA per 6 cm dish. One day after transfection, the media were removed and replaced with serum-free media. One day after (2 days after transfection), the media were collected and concentrated 10-fold in Centricon-10 units (Millipore, Bedford, MA, USA). The media samples were then separated on a 15% sodium dodecylsulfate (SDS)-polyacrylamide gel electrophoresis (PAGE) gel (Ready Gel, Bio-Rad, Hercules, CA, USA) and electrotransferred to nitrocellulose membrane, the blot was probed for IL-6 protein using a goat anti-IL-6 polyclonal antibody (Santa Cruz Biotechnology, Santa

Cruz, CA, USA) at a dilution of 1:1000. Purified murine IL-6 (PeproTech, Rocky Hill, NJ, USA) was used as a positive control. Serum-free media samples from untransfected 293 cells were concentrated in a similar manner and examined for IL-6 protein.

Packaging of rAAV Vectors

Vectors were packaged, purified, concentrated, and titered as described previously (Conway et al., 1999). rAAV-POMC was prepared by the Powell Gene Therapy Center at the University of Florida, and rAAV-IL-6 was provided by Dr. Ron Klein of the University of Florida's Department of Pharmacology and Therapeutics. The titers of rAAV-POMC and rAAV-IL-6 were 4.3E11 and 1E11 physical particles/ml, respectively, and the ratios of physical-to-infectious particles for both vectors were less than 30. A mini-adenovirus helper plasmid (pDG) (Grimm et al., 1998) was used to produce rAAV vectors with no detectable adenovirus or wild type AAV contamination. rAAV vectors were purified using iodixanol gradient/heparin-affinity chromatography and were more than 99% pure as judged by PAAG/silver-stained gel electrophoresis (not shown).

rAAV Vector Administration

Rats were anesthetized with either 50mg/kg pentobarbital (IL-6 gene delivery) or 6 mg/kg xylazine and 60 mg/kg ketamine (POMC gene delivery), and heads were prepared for surgery. Animals were placed into a stereotaxic frame and a small incision (1.5 cm) was made over the midline of the skull to expose the landmarks of the cranium (Bregma and Lamda). The following coordinates were used for injecting rAAV-POMC into basal hypothalamus targeting the arcuate nucleus: 3.14mm posterior to bregma, ±0.4mm lateral to the midsaggital suture and 10mm ventral from the skull surface. For rAAV-IL-6 gene delivery, the coordinates for injection into the hypothalamus were 1.8mm posterior to bregma, 1mm lateral to the midsaggital suture and 9mm ventral from the skull surface. A

small hole was drilled through the skull and a 23-gauge stainless steel cannula inserted followed by an injection cannula. Using 10-µl Hamilton syringe, a 2 (for rAAV-IL-6) or 3-µl (for rAAV-POMC) volume of virus stocks was delivered over 5 min, and the needles remained in place at the injection site for 2 additional min.

Surgical Procedures

Surgical Denervation

Rats underwent unilateral surgical denervation of the interscapular BAT under pentobarbital anesthesia as previously described (Scarpace and Matheny, 1998). A transverse incision was made just anterior to the right BAT pad, separating the BAT from the muscles of the right scapula. The scapula was raised to expose the five intercostal nerve bundles entering right BAT pad. A section of each nerve bundle was removed with scissors. The rats were maintained on a heat pad until recovery from the anesthesia. In previous studies, denervation was verified in selected rats by assessing norepinephrine levels in the innervated compared with denervated BAT pads. In all tested cases the denervation was successful (Scarpace and Matheny, 1996).

Intracerebroventricular Cannulation

Under 6 mg/kg xylazine and 60 mg/kg ketamine anesthesia, a cannula (Brain Infusion Kit II; Durect) was stereotaxically placed into the left lateral ventricle using the following coordinates, 0.8 mm posterior to bregma, 1.4 mm lateral to the midsaggital suture and to a depth of 4 mm. The brain infusion cannula was anchored to the skull using acrylic dental cement and a small, stainless steel screw. A catheter was connected from the cannula to the mini-osmotic pump flow moderator. The pump was inserted into a subcutaneous pocket on the dorsal surface.

Oxygen Consumption

O_2 consumption was assessed in up to four rats simultaneously with an Oxyscan analyzer (OXS-4; Omnitech Electronics, Columbus, OH) as described previously (Scarpace et al., 1997). Flow rates were 2 L/min with a 30-s sampling time at 5-min intervals. The rats were placed into the chamber for 150 min with the lowest 6 consecutive O_2 consumption values during this period used in the calculations (basal resting VO_2). Food was not available. Animal rooms were free of human activity and kept as quiet as possible during measurements. All measurements were made between 09:00 and 14:00 hrs. Results were expressed as O_2 consumption relative to metabolic body size ($ml \cdot min^{-1} \cdot kg^{0.75}$).

Tissue Harvesting

Anesthetized rats were sacrificed by cervical dislocation under 85 mg/kg pentobarbital anesthesia. Blood was collected by cardiac puncture and serum was harvested by 15-minute centrifugation in serum separator tubes. The circulatory system was perfused with 30 ml of cold saline. Interscapular BAT, perirenal and retroperitoneal white adipose tissue and hypothalami were excised, weighed, and immediately frozen in liquid nitrogen. The hypothalamus was removed by making an incision medial to piriform lobes, caudal to the optic chiasm, and anterior to the cerebral crus to a depth of 2-3 mm. Tissues were stored at –80 C until analysis.

Serum Measurements

Leptin

Serum leptin is measured using a rat leptin radioimmunoassay kit (Linco Research, St. Charles, MO) or a rodent leptin ELISA kit (Crystal Chem, Chicago IL).

Insulin

Serum insulin was measured using a rat insulin radioimmunoassay kit (Linco Research, St. Charles, MO).

Glucose

Serum glucose was via a colormetric reaction with Trinder, the Sigma Diagnostics Glucose reagent (Sigma, St. Louis MO).

Total cholesterol

Total cholesterol levels were determined by enzymatic colorimetric kits from WAKO Chemicals (Neuss, Germany).

Free Fatty Acids

Serum free fatty acids were measured using the NEFA C colorimetric kit from WAKO Chemicals GmbH (Neuss Germany).

Probes

The UCP-1 probe was a full-length cDNA clone and was obtained from Dr. Leslie Kozak, Pennington Research Center, Baton Rouge, LA. SOCS3 cDNA was a gift from Christian Bjorbaek (Harvard University). The cDNA probes were labeled using a random primer kit (Prime-a-Gene, Promega, Madison, WI). Probes were purified with Nick columns (Pharmacia) and are heat-denatured for 2 minutes. All probes have been verified to hybridize to the corresponding specific mRNAs by Northern Analysis prior to use in Dot Blot assay (below).

RNA Isolation and RNA Dot Blot

Tissue was sonicated in guanidine buffer, phenol extracted, and isopropanol precipitated using a modification of the method of Chomczynski (Chomczynski and Sacchi, 1987). Isolated RNA was quantified by spectrophotometry and integrity was

verified using 1% agarose gels stained with ethidium bromide. For dot blot analysis, multiple concentrations of RNA were immobilized on nylon membranes using a dot blot apparatus (BioRad, Richmond, CA). Membranes were baked in a UV crosslinking apparatus. Membranes were then prehybridized in 10 ml Quickhyb (Stratagene, LaJolla, CA) for 30 minutes followed by hybridization in the presence of a labeled probe and 100 ug salmon sperm DNA. After hybridization for 2 hours at 65 C, the membranes were washed and exposed to a phosphorImaging screen for 24-72 hours (depending on anticipated strength of signal). The screen was then scanned using a Phosphor Imager (Molecular Dynamic, Sunnyvale, CA) and analyzed by ImageQuant Software (Molecular Dynamics).

Relative Quantitative RT-PCR

Relative quantitative RT-PCR was performed using QuantumRNA 18S Internal Standards kit (Ambion, Austin, Tx). Total RNA (2 μg) was treated with RNase-free DNase using a DNA-free kit (Ambion), and first-strand cDNA synthesis generated from 1 μg RNA in a 20 μl volume using random primers (Gibco BRL) containing 200 units of M-MLV reverse transcriptase (Gibco BRL). Relative PCR was performed by multiplexing target gene primers and 18S primers and coamplifying for a number of cycles found to be in the linear range of the target. Linearity for the POMC amplicon, for example, was determined to be between 20 and 29cycles. The optimum ratio of 18S primer to competimer was 1:4 for POMC. PCR was performed at 94°C denaturation for 60 sec, 59°C annealing temperature for 45 sec, and 72°C elongation temperature for 60 sec for 26 cycles. The PCR product was electrophoresed on a 5% acrylamide gel and stained with SYBR green (Molecular Probes, Eugene, OR). Gels were scanned using a

STORM fluorescent scanner and digitized data analyzed using ImageQuant. (Molecular Dynamics).

STAT3/Phospo-STAT3 Assay

Hypothalamus was sonicated in 10 mM Tris-HCL, pH 6.8, 2% SDS, and 0.08 ug/ml okadaic acid plus protease inhibitors (PMFS, benzamidine, and leupeptin) [an aliquot of this sonicate was frozen for RNA analysis]. Sonicate was diluted and quantified for protein using a detergent compatible Bradford Assay. Samples were boiled and separated on an SDS-PAGE gel and electrotransferred to nitrocellulose membrane. Immunoreactivity was assessed on separate membranes with antibodies specific to STAT3 (phosphorylated and unphosphorylated) and antibodies specific to tyrosine 705 phosphorylated STAT3 (antibody kit from New England Biolabs, Beverly, MA). Immunoreactivity was visualized by chemiluminescents detection (Amersham Life Sciences, Piscataway, NJ) and quantified by video densitometry (BioRad, Hercules, CA).

CREB and Phosphorylated CREB (P-CREB) Assay

Immunoreactive CREB and P-CREB were determined with a PhosphoPlus CREB (Ser 133) antibody kit (New England Bio labs, Beverly, MA). Hypothalamic samples (40 μg) prepared as described above were separated on a SDS-PAGE gel and electrotransferred to nitrocellulose membrane. Immunoreactivity was assessed on separate membranes with antibodies specific to CREB (phosphorylated and unphosphorylated) and antibodies specific to serine 133 phosphorylated CREB. Immunoreactivity was visualized by enhanced chemiluminescent detection (Amersham Pharmacia Biotech) and quantified by video densitometry (Bio-Rad).

UCP-1 Protein in Brown Adipose Tissue

Approximately 30 mg of interscapular brown adipose tissue was homogenized in 300 ul 10 mM Tris-HCL, pH 6.8, 2% SDS, and 0.08 ug/mL okadaic acid plus protease inhibitors (PMFS, benzamidine, and leupeptin). Samples were boiled for 5 minutes to and an aliquot of this homogenate was withdrawn and diluted for detergent compatible Bradford protein analysis. Samples were boiled and separated on an SDS-PAGE gel (20 ug protein/lane) and electrotransferred to nitrocellulose membrane. Immunoreactivity was assessed with an antibody specific to UCP-1 (Linco Research, St. Charles, MO). Immunoreactivity was visualized by chemiluminescents detection (Amersham Life Sciences, Piscataway, NJ) and quantified by video densitometry (BioRad, Hercules, CA).

Statistical Analysis

All data are expressed as mean ± standard error of mean. α level was set at 0.05 for all analyses. Data were analyzed by 1-way ANOVA, 2-way ANOVA, or Student's *t*-test, as appropriate. For ANOVA, when the main effect was significant, a *post-hoc* test (either Turkey or Bonferroni Multiple Comparison with the error rate corrected for the number of contrasts) was applied to determine individual differences between means. GraphPad Prism software version 3.0 (San Diego, CA) was used for all statistical analysis and graphing. GraphPad QuickCalc (graphpad.com) was used for post-hoc analysis of all 2-way ANOVA.

CHAPTER 3
EFFECTS OF THE MELANOCORTIN AGONIST MTII IN DIET-INDUCED OBESE SPRAGUE-DAWLEY RATS

Introduction

Melanocortins are bioactive peptides derived from a common pre-hormone, POMC. Among them, α-MSH is a major regulator of feeding and body weight via hypothalamic MC3R, MC4R (Cone, 1999). Central infusion of α-MSH or its synthetic agonists causes anorexia and weight loss (Poggioli et al., 1986; Fan et al., 1997; Grill et al., 1998), whereas infusion of melanocortin receptor blockers or over-production of the endogenous MCR antagonist, AgRP, produces hyperphagia and obesity (Fan et al., 1997; Graham et al., 1997; Ollmann et al., 1997; Hagan et al., 1999). Knockout studies of the central MC3R and MC4R have identified these receptors as important players in energy homeostasis (Chen et al., 2000; Huszar et al., 1997). On one hand, targeted disruption of the MC4 receptor gene leads to overfeeding and obesity (Huszar et al., 1997), whereas MC3 receptor knockouts over-accumulate fat with minimal changes in caloric intake (Chen et al., 2000). Deficiency in POMC also results in increased food intake and morbid obesity in both rodents and humans (Yaswen et al., 1999; Krude et al., 1998). Apparently, the central melanocortin system, which consists of natural agonist α-MSH, the natural antagonist AgRP, and the MC3R and MC4R, has critical functions in the homeostatic regulation of body weight.

Leptin, an adipocyte-derived hormone, acts on satiety and appetite centers in the hypothalamus both to reduce food consumption and increase energy expenditure

(Friedman and Halaas, 1998; Schwartz et al., 1996; Scarpace et al., 1997). Leptin activates POMC- and suppresses AgRP- containing neurons of the ventrolateral and ventromedial ARC, respectively, resulting in an increase in the expression of POMC and a reduction in AgRP (Schwartz et al., 1996, 1997; Cheung et al., 1997; Baskin et al., 1999; Elias et al., 2000). When co-administered with a MC 3/4-receptor antagonist, leptin fails to decrease food intake (Seeley et al., 1997). In addition, the leptin-mediated induction of UCP1, an important thermogenic protein in BAT, is also attenuated with the central MC receptor antagonism (Satoh et al., 1998). These findings suggest that the melanocortin system is located downstream of the hypothalamic leptin signaling pathway and is required to mediate leptin's central responses.

One of the hallmarks of obesity, whether it is genetic, diet-induced or age-related, is leptin resistance. Human obesity, as well as many rodent models of obesity are accompanied by elevated serum leptin and leptin resistance, which becomes more pronounced with progressive degrees of obesity. Diet-induced obese (DIO) rodent models, characterized by hyperleptinemia and hyperinsulinemia, somewhat resemble the onset of human obesity and hence provide a valuable tool for investigating leptin resistance in humans. The nature of leptin resistance associated with DIO animals is not well understood. The blunted responsiveness to both endogenous and exogenous leptin has been in part attributed to defects in blood-brain-barrier transport system (peripheral resistance) (Burguera et al., 2000) and in leptin signal transduction in the hypothalamic leptin-responsive neurons (central resistance) (El Haschimi et al., 2000; Scarpace et al., 2001). It is possible that the central resistance is partially due to a failure of leptin signal to activate POMC or suppress AgRP neurons so that the proper regulation of POMC and

AgRP expression by leptin is lost. As a result, leptin-initiated MC activation is impaired. In support of this notion, α-MSH and the potent melanocortin agonist, MTII were effective in obese Zucker rats with defective leptin receptor signaling and in DIO mice with leptin resistance (Hwa et al., 2001; Cettour-Rose and Rohner-Jeanrenaud, 2002; Pierroz et al., 2002). Chronic impairment in MC activation may generate hypersensitivity (or hyper-responsiveness) of the MC pathway to pharmacological MC stimulation, potentially through homeostatic up-regulation of MC3, 4 receptors. This postulated hypersensitivity has been indicated in two studies, one demonstrating enhanced responses to MTII in obese Zucker rats (Cettour-Rose and Rohner-Jeanrenaud, 2002) and another reporting an acute enhanced anorexic response to α-MSH in leptin-resistant DIO rats (Hansen et al., 2001). These initial clues about central leptin resistance in DIO animals prompted us to address several questions: first, can direct MC activation by MTII circumvent leptin resistance in a DIO rat model with normal genetic background? Second, will the DIO rats respond with hypersensitivity to MTII compared to control rats? Third, does diet-induced obesity alter the expression levels of hypothalamic MC3R and MC4R that may mediate the differential response to MTII in DIO compared to lean animals? Lastly, owing to scarce information on how α-MSH influences energy expenditure and body metabolism (in contrast to plentiful information about the effect of α-MSH and its analogs on food intake), we assessed the thermogenic response as well as fat metabolism in BAT and skeletal muscle following central MTII administration in both lean and DIO rats.

To this end, in this chapter, we examined the effects of 6-day central administration of leptin or MTII on energy balance, BAT thermogenesis and indicators of skeletal

muscle fat metabolism in Chow-fed (CH) lean and DIO Sprague-Dawley rats. Food intake, body weight, adiposity, serum hormone and metabolite levels, oxygen consumption, BAT UCP1 protein, expression of Acetyl-CoA Carboxylase (ACC) and muscle-type carnitine palmitoyltransferase I (M-CPT I) in soleus muscle and MC3R and MC4R in the hypothalamus were measured.

Materials and Methods

Animals and Diets

Fourteen-week old female Sprague-Dawley rats were obtained from Taconic (Germantown, NY). Upon arrival, rats were examined and remained in quarantine for one week. Animals were cared for in accordance with the principles of the NIH Guide to the Care and Use of Experimental Animals. Rats were housed individually with a 12:12 h light: dark cycle (07:00 to 19:00 h). Standard rat chow (15% fat; 3.3 Kcal/g diet 2018; Harlan Teklad, Madison, WI) and water were provided *ad libitum*. At the start of the experiment, 30 rats were maintained on chow (CH), whereas 70 rats were switched to a high-fat (HF) diet (60% fat; 5.2 Kcal/g D12492; Research Diets, New Brunswick, NJ) for ten weeks. Over several weeks, the HF-fed animals were spontaneously divided into two distinct groups: those that were becoming obese on the HF diet (DIO) and those that were not gaining extra weight on the HF diet (Diet Resistant, DR). The top 40% of weight gainers on the HF diet were designated as DIO, whereas the rest were designated DR and removed from the study. DIO and CH animals remained on their respective diets through the conclusion of this study. At the end of the 10-week feeding period, serum leptin (collected from tail) was assessed.

Experiment 1: 6-Day icv Administration of Leptin

CH or DIO rats were infused with either artificial cerebrospinal fluid (ACSF, 6-7 per group) or recombinant mouse leptin (10 μg/day, 5-7 per group) into the left lateral ventricle by mini-osmotic pump (Alzet 2001; Durect, Cupertino, CA) for 6 days. Under 6 mg/kg xylazine (Phoenix Pharmaceutical, St. Joseph, MO) and 60mg/kg ketamine (Monarch Pharmaceuticals, Bristol, TN) anesthesia, a cannula (Brain Infusion Kit II; Durect) was stereotaxically placed into the left lateral ventricle using the following coordinates, 0.8 mm posterior to bregma, 1.4 mm lateral to the midsaggital suture and to a depth of 4 mm. The brain infusion cannula was anchored to the skull using acrylic dental cement and a small stainless steel screw. A catheter was connected from the cannula to the mini-osmotic pump flow moderator. The pump was inserted into a subcutaneous pocket on the dorsal surface. Rats were kept warm until fully recovered and were provided with a highly palatable Jell-O mixture consisting of Jell-O (Kraft Foods, Rye Brook, NY), Ensure Plus (Abbott Laboratories, Columbus, OH), STAT (PRN pharmacal, Pensacola, FL) and Soy Protein Booster (Naturade, Irvine, CA) at day 1 to alleviate the anorexic effect elicited by surgical intervention. Chow or HF diet resumed from day 2, and rats were allowed to access to food *ad libitum*. Food consumption and body weight were recorded for six days. Oxygen consumption was monitored at days 2 and 6. All rats were sacrificed at the end of the dark cycle of day 6 and tissues harvested for analysis.

Experiment 2: 6-Day icv Administration of MTII

CH and DIO rats were infused with either ACSF (control and pair-fed groups, 6-8 per group) or MTII (1 nmol/day, 6-9 per group) into the left lateral ventricle by mini-osmotic pump (Alzet 2001; Durect) for 6 days. Rats were provided with the highly

palatable Jell-O mixture at day 1, and chow or HF diet resumed from day 2. Control and MTII-treated rats were allowed access to food *ad libitum*, whereas pair-fed rats were pair fed to the amount of food consumed by the MTII-treated rats. Daily food consumption and body weight were recorded for six days. Oxygen consumption was monitored at days 2 and 6. All rats were sacrificed at the end of the dark cycle of day 6 and tissues harvested for analysis.

Oxygen Consumption

O2 consumption was assessed in up to four rats simultaneously with an Oxyscan analyzer (OXS-4; Omnitech Electronics, Columbus, OH) as described previously (Scarpace et al., 1992). Flow rates were 2L/min with a 30-s sampling time at 5-min intervals. The rats were placed into the chamber for 150 min with the lowest 6 consecutive O_2 consumption values during this period used in the calculations (basal resting VO_2). Food was not available during the measurement. Results were expressed as mass adjusted consumption ($ml \cdot min^{-1} \cdot kg^{0.75}$).

Tissue Harvesting and Preparation

Rats were sacrificed by cervical dislocation under 85 mg/kg pentobarbital anesthesia. Blood samples were collected by heart puncture and serum was harvested by a 15-min centrifugation in serum separator tubes. The circulatory system was perfused with 30 ml of cold saline, BAT, perirenal and retroperitoneal white adipose tissues (PWAT and RTWAT) and a portion of the red soleus muscle were excised. The hypothalamus was removed by making an incision medial to piriform lobes, caudal to the optic chiasm and anterior to the cerebral crus to a depth of 2-3 mm. Tissues were stored at –80˚C until analysis. For Western analysis, BAT were homogenized in 0.3ml 10 mM

Tris-HCL, pH 6.8, 2% SDS, and 0.08 μg/ml okadaic acid. Protease inhibitors, 1mM phenylmethylsulfonyl fluoride (PMSF), 0.1 mM benzamidine, and 2 μM leupeptin were also present. Homogenates were immediately boiled for 2 min, cooled on ice, and stored frozen at –80˚C. Protein was determined using the DC protein assay kit (Bio-Rad, Hercules, CA). BAT samples were filtered through a 0.45 μm syringe filter (Whatman, Clifton, NJ) to remove lipid particles prior to protein measurements.

Serum Leptin, Insulin, Glucose, and Cholesterol

Serum leptin levels were measured using a rodent leptin ELISA kit (Crystal Chem, Chicago, IL). Serum insulin levels were measured with a rat insulin RIA kits (Linco Research, St. Charles, MO). Total cholesterol was determined by enzymatic colorimetric kits from WAKO Chemicals (Neuss, Germany). Serum glucose was via a colorimetric reaction with Trinder, the Sigma Diagnostics Glucose reagent (St. Louis, MO).

BAT UCP1 Protein

UCP1 levels were determined by immunoreactivity in BAT homogenates. BAT samples (20 μg) prepared as described above were separated on a SDS-PAGE gel and electrotransferred to nitrocellulose membrane. Immunoreactivity was assessed on separate membranes with an antibody specific to rat UCP1 (Linco Research). Immunoreactivity was visualized by enhanced chemiluminescent detection (Amersham Pharmacia Biotech) and quantified by video densitometry (Bio-Rad).

Relative Quantitative RT-PCR

ACC and M-CPT I expression in the soleus muscle and MC3R and MC4R mRNA levels in the hypothalamus were identified by relative quantitative RT-PCR using QuantumRNA 18S Internal Standards kit (Ambion, Austin, TX). Total cellular RNA was extracted as described (Li et al., 2002) and treated with RNase-free DNase (Ambion).

First-strand cDNA synthesis was generated from 2 µg RNA in a 20-µl volume using random primers (Life Technologies, Rockville, MD) containing 200 units of M-MLV reverse transcriptase (Life Technologies). Relative quantitative PCR was performed by multiplexing corresponding primers (ACC sense 5'-*GCTTGCAAACTCGACCTCTC-3', antisense 5'-CTTGATGATGGCGTTCTTGA-3'; M-CPT I sense 5'-GCAAACTGGACCGAGAAGAG-3', antisense 5'-CCTTGAAGAAGCGACCTTG-3'; MC3R sense 5'-AGCAACCGGAGTGGCAGT-3'; antisense 5'-GGCCACGATCAAGGAGAG-3'; MC4R sense 5'-AGTCTCTGGGGAAGGGGCA-3'; antisense5'-CAACTGATGATGATCCCGAC-3')*, 18S primers, and competimers and coamplifying. Linearity for ACC and M-CPT I amplicons was determined to be between 26 and 36 cycles, 18 and 32 for MC3R and 24 to 44 for MC4R. The optimum ratio of 18S primer to competimer was 1:9 for ACC and MC4R, 1:6 for MC3R and 2:15 for M-CPT I. PCR was performed at 94°C denaturation for 60 sec, 59°C annealing temperature for 45 sec, and 72°C elongation temperature for 60 sec for 34 cycles for ACC, 32 for M-CPT1, 28 for MC3R and 40 for MC4R. The PCR product was electrophoresed on acrylamide gel and stained with SYBR green (Molecular Probes, Eugene, OR). Gels were scanned using a STORM fluorescent scanner and data analyzed using ImageQuant (Molecular Dynamics). The relative values of ACC, M-CPT I, MC3R and MC4R mRNA were derived from dividing the signal obtained for corresponding amplicon by that for 18S amplicon.

Statistical Analysis

Results are presented as mean ± SE. Unpaired two-tailed Student's *t* test was employed for analysis of body weight and serum leptin after 10-week feeding and

hypothalamic MC3/4 receptor expression levels, as well as for the comparison of the percent baseline levels of caloric intake between MTII-treated CH and DIO rats at day 2. For all other data, one –way or way-day ANOVA was performed. When the main effect was significant, a *post-hoc* test (either Turkey or Bonferroni Multiple Comparison with the error rate corrected for the number of contrasts) was applied to determine individual differences between means. A value of $P < 0.05$ was considered significant.

Results

Body Weight and Serum Leptin Levels in CH and DIO Rats after 10 Weeks of Diet

At the beginning of HF feeding period, the average body weight of CH and DIO rats were very similar (Table 3-1). By the end of the ten weeks of HF feeding, DIO animals gained almost twice as much weight and became significantly heavier (12%) than CH animals (Table 3-1). Serum leptin levels were markedly elevated in DIO rats by 113% compared with CH rats.

Experiment 1: Effects of 6-Day icv Leptin Infusion on Food Intake and Visceral Adipose Tissues in CH and DIO Rats

To test if the DIO rats are leptin resistant, we examined the responsiveness to central leptin infusion (10μg/day) in CH and DIO rats for 6 days. The dose of 10 μg/day had been previously determined by this laboratory to induce a maximum response in normal chow-fed rats (Scarpace et al., 2001). Leptin induced a sustained suppression in food consumption in CH rats but only a brief anorexic response in DIO rats compared with respective controls (Data not shown). The 6-day cumulative caloric intake decreased by 36 % in leptin-treated CH rats as compared to vehicle (ACSF) controls (Fig. 3-1A), whereas the decrease in cumulative caloric intake failed to reach statistical significance in leptin-treated DIO animals (Fig. 3-1A).

The lipolytic effect of leptin was also investigated in two major visceral fat depots, PWAT and RTWAT. The sum of PWAT and RTWAT of DIO control rats were 3-fold higher than that of CH controls (Fig. 3-1B). This result and the marked elevation of serum leptin levels in the obese rats indicate a dramatic increase in visceral adiposity and presumably total adiposity levels in DIO animals following HF feeding. The 6-day leptin infusion reduced the sum of PWAT and RTWAT expectedly by 59% in CH rats compared with controls (Fig. 3-1B). On the contrary, visceral adiposity levels decreased only slightly in DIO rats given leptin (Fig. 3-1B).

Experiment 2: 6-Day icv MTII Infusion in CH and DIO Rats

Food consumption and body weight

To determine if the DIO rats with leptin resistance are responsive to central melanocortin activation, the melanocortin agonist MTII (1 nmol/day) or ACSF was infused into the lateral ventricle for six days in CH or DIO rats. This dose, 1 nmol/day of MTII was previously demonstrated to elicit a maximum anorexic response in normal chow-fed rats (Clegg et al., 2003). MTII induced a significant reduction in caloric intake in CH rats compared with the ACSF-infused CH animals (Fig. 3-2A). Specifically, the MTII-treated CH rats ate only 38% of calories consumed by CH control rats at day 2, and 66% at day 6. In DIO rats, despite the presence of leptin resistance, MTII also effectively suppressed caloric intake to a similar magnitude (Fig. 3-2B). Moreover, the anorexic response to MTII was enhanced at day 2 of MTII infusion in DIO rats (an 84% reduction in caloric consumption compared to ACSF-infused DIO controls as supposed to a 62% decrease in MTII-infused CH compared to CH control rats) (Fig. 3-2A, B). When caloric intake was calculated as percentage of individual baseline levels (caloric intake at day 0), the difference between CH and DIO animals given MTII at day 2 was significant (18.1 ±

6.3% vs. 5.4 ± 1.2%, P=0.03 by unpaired *t* test). On day 3 and afterwards, however, the decrease in caloric intake in response to MTII became similar between CH and DIO rats (Fig. 3-2A, B).

In addition to the marked anorexia, MTII also reduced body weight significantly in both CH and DIO rats (Fig. 3-2 C, D). MTII-treated CH rats weighed 3.8% less at day 2 compared with *ad libitum*-fed CH controls, and 7.9% less at day 6 (Fig. 3-2C). In DIO rats, the average body mass decreased by 4.2% at day 2 and 6.5% at day 6 compared with *ad libitum*-fed DIO controls (Fig. 3-2D). Pair-feeding in this study revealed that the MTII-induced weight loss was not merely caused by the suppression in food intake. Even though both pair-fed CH and DIO groups lost more body weight than their respective *ad libitum*-fed counterparts at the end of the experiment, the MTII-treated rats on both CH and HF diet exhibited a further reduction in their body weight compared with their respective pair-fed groups (Fig. 3-2 C, D).

Visceral adiposity and serum hormones and metabolites

As shown in Table 2, relative to the respective *ad libitum*-fed controls, central MTII infusion reduced visceral adiposity (represented by the sum of PWAT and RTWAT) significantly in CH (48%) and DIO (44%) rats with similar efficacy. In contrast, pair-feeding failed to produce a significant reduction in visceral fat mass in either CH or DIO rats (Table 3-2). Whilst circulating leptin concentrations were similar between *ad libitum*-fed control and pair-fed groups on either CH or HF diet, serum leptin decreased by 59% and 69% in MTII-treated CH and DIO rats respectively (Table 3-2).

MTII administration also lowered serum insulin levels in CH rats, despite unchanged serum glucose levels (Table 3-2). Pair-feeding, however, only generated a

trend towards reduction in these two parameters in CH animals. On the other hand, pair-feeding significantly decreased serum insulin levels in DIO rats as compared to their *ad libitum*-fed controls. In comparison, MTII exerted a stronger effect on serum insulin than pair-feeding. Conversely, pair-feeding had a greater influence on serum glucose reduction than MTII did in DIO rats. MTII also lowered total serum cholesterol levels by 43% and 18% in CH and DIO rats respectively, whereas pair-feeding induced a similar effect in CH but only a tendency towards a decrease in DIO rats with respect to serum cholesterol levels (Table 3-2).

Energy Expenditure

Whole body oxygen consumption was assessed at day 2 and day 6 following MTII or ACSF infusion by indirect calorimetry in both CH and DIO animals. Oxygen consumption was elevated at day 6 (Fig. 3-3B) but not at day 2 (Fig. 3-3A) in MTII-infused CH rats compared with either *ad libitum*-fed control or pair-fed rats. In contrast, MTII induced a rapid and significant increase in oxygen consumption at day 2 in DIO rats (Fig. 3-3A). The decrease in food intake brought about by MTII should normally suppress energy expenditure, however, elevation of oxygen consumption occurred despite anorexia and persisted through day 6 of MTII infusion (Fig. 3-3B).

Induction of UCP1 in BAT is an important marker for enhanced thermogenesis or energy expenditure in rodents (Scarpace et al., 1997). In present study, we examined the UCP1 protein levels following MTII treatment. DIO control rats had more than 2-fold higher basal BAT UCP1 than CH controls (Fig. 3-4), indicating that high-fat feeding augmented UCP1 levels in BAT. In response to MTII administration, UCP1 levels in both CH and DIO rats increased significantly. UCP1 levels in pair-fed rats remained unchanged as compared with respective *ad libitum*-fed controls (Fig. 3-4).

Expression of Enzymes Regulating Fat Metabolism in Skeletal Muscle

M-CPT I and ACC are two important enzymes involved in fat metabolism in skeletal muscle. Increases in M-CPT I and decreases in ACC are consistent with enhanced fat catabolism (Jeukendrup, 2002). We conducted relative quantitative RT-PCR to determine the expression levels of these two enzymes in red soleus muscle with respect to MTII treatment. The mRNA levels of both enzymes were similar among *ad libitum*-fed, MTII-treated and pair-fed groups in CH rats. However, in DIO rats, MTII infusion prevented the dramatic reduction in M-CPT I expression by pair-feeding (Fig. 3-5A), and it also decreased the mRNA levels of ACC in these rats compared with both *ad libitum*-fed controls and PF rats (Fig. 3-5B). These data suggest that MTII induces fat catabolism in skeletal muscle.

Expression of MC3 and MC4 Receptors in the Hypothalamus

The initial enhanced anorexic and thermogenic responses to MTII in the HF-fed rats prompted us to examine the expression of MC3R and MC4R in the hypothalamus. MC3R and MC4R expression levels were determined by relative quantitative RT-PCR in CH and DIO *ad libitum*-fed control rats. Surprisingly, ten-week HF feeding significantly decreased MC3R and MC4R by 18% and 26%, respectively (Fig. 3-6).

Table 3-1. Body weight and serum leptin levels of chow-fed (CH) and high fat (HF) diet-induced obese (DIO) rats after 10 weeks of diet. Thirty and seventy rats were started on the chow (3.3 Kcal/g) or HF (5.2 Kcal/g) diet, respectively. The top 40% of weight gainers consuming the HF diet at the end of 10-week feeding were designated as DIO (n=27). Serum leptin levels were measured in seven CH and ten DIO rats at end of 10-week feeding. Values are means ± SE. * P <0.01 vs. CH by unpaired *t* test.

	CH	DIO
Body weight (BW)		
Baseline (g)	291.1 ± 4.1	291.9 ± 4.9
Week 10 (g)	333.6 ± 5.5	372.4 ± 7.0 *
BW gain (g)	42.5 ± 4.5	80.6 ± 3.4 *
Serum leptin (ng/ml)	5.32 ± 0.47	11.34 ± 1.50 *

Table 3-2. Effects of 6-day icv MTII administration on visceral adiposity, serum leptin, glucose, insulin, and total cholesterol levels in chow-fed (CH) and diet-induced obese (DIO) rats. MTII (1nmol/day) or vehicle (artificial cerebrospinal fluid) was infused into the left lateral ventricle for 6 days. Control animals were either fed *ad libitum* (Control) or pair-fed to the amount of food consumed by the MTII-treated groups (Pair-fed). Values were measured at the end of the 6-day experimental period. Means ± SE of 6 to 9 animals per group. * $P < 0.05$ vs. Control; † $P < 0.05$ vs. Pair-fed by one-way ANOVA with *post hoc* Turkey's test.

	CH			DIO		
	Control	MTII	Pair-fed	Control	MTII	Pair-fed
PWAT+RTWAT (g)	4.61 ± 0.71	2.41 ± 0.48 *	4.47 ± 1.25	10.91 ±1.45	6.12 ± 0.92 *†	9.91 ± 1.37
Leptin (ng/ml)	2.63 ± 0.47	1.09 ± 0.24 *	2.49 ± 1.12	9.74 ± 2.19	3.02 ± 0.61 *†	7.13 ± 1.51
Glucose (mg/dl)	84.1 ± 2.6	79.9 ± 1.8	73.8 ± 8.2	140.5 ± 9.7	124.2 ± 3.9 †	92.6 ± 5.4 *
Insulin (ng/ml)	3.69 ± 0.56	1.17 ± 0.63 *	2.73 ± 0.54	4.37 ± 0.82	2.05 ± 0.34 *	2.48 ± 0.45 *
Cholesterol (mg/dl)	91.7 ± 8.2	51.9 ± 6.3 *	62.2 ± 5.1 *	120.7 ± 6.0	99.1 ± 5.0 *	109.3 ± 3.9

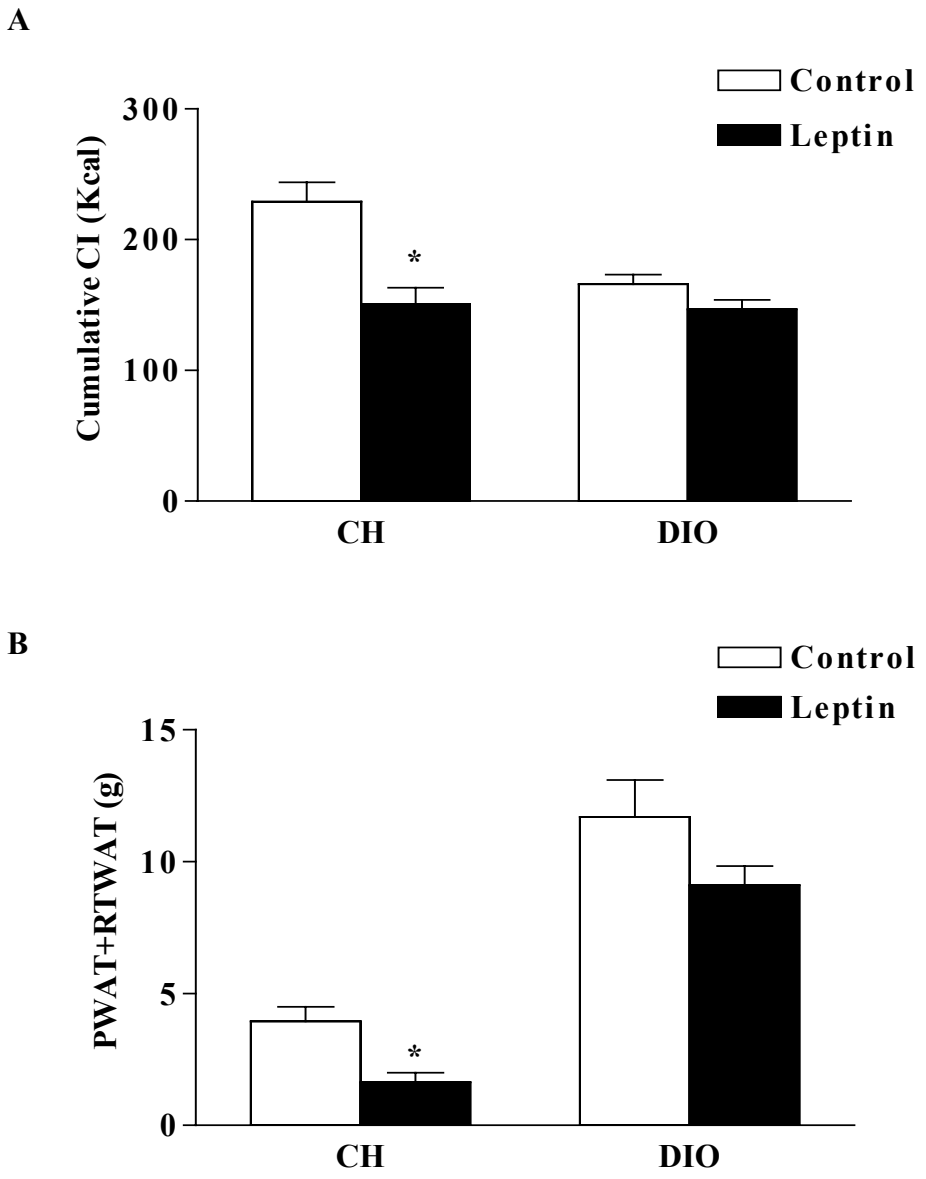

Fig. 3-1. Cumulative caloric intake (CI) (A) and visceral adiposity (B) 6 days following icv administration of vehicle or leptin (10 μg/day) in chow-fed (CH) and DIO rats. The vehicle was artificial cerebrospinal fluid. Values are means ± SE of 5 to 7 animals per group. Visceral adiposity levels are represented by the sum of PWAT and RTWAT. * P <0.05 vs. corresponding controls by two-way ANOVA with *post hoc* Bonferroni's test.

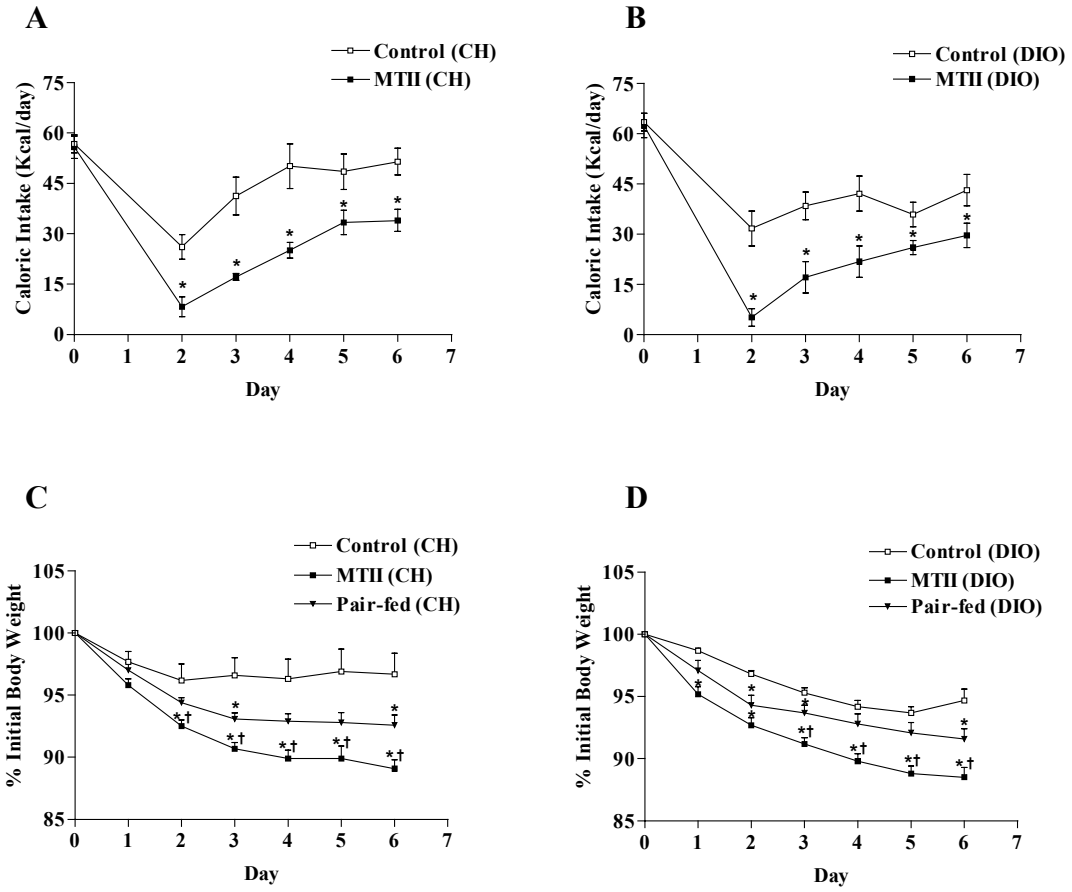

Fig. 3-2. Caloric intake and body weight of chow-fed (CH) (A, C) and DIO (B, D) rats 6 days following icv administration of vehicle or MTII (1 nmol/day). The vehicle was artificial cerebrospinal fluid. Control animals were either fed *ad libitum* (Control) or pair-fed to the amount of calories consumed by the MTII-treated groups (Pair-fed). Body weight is expressed as the percentage of initial body weight prior to the start of the experiment (day 0). Values are means ± SE of 6 to 9 animals per group. During the entire experimental period, caloric intake of pair-fed and MTII-treated rats were significantly different from the controls, and the body weight loss was also significantly different in pair-fed and MTII –treated rats relative to the Controls as well as in MTII groups relative to Pair-fed animals by repeated measures ANOVA. * $P < 0.05$ vs. Controls and † $P < 0.05$ vs. Pair-fed by *post hoc* Turkey's test.

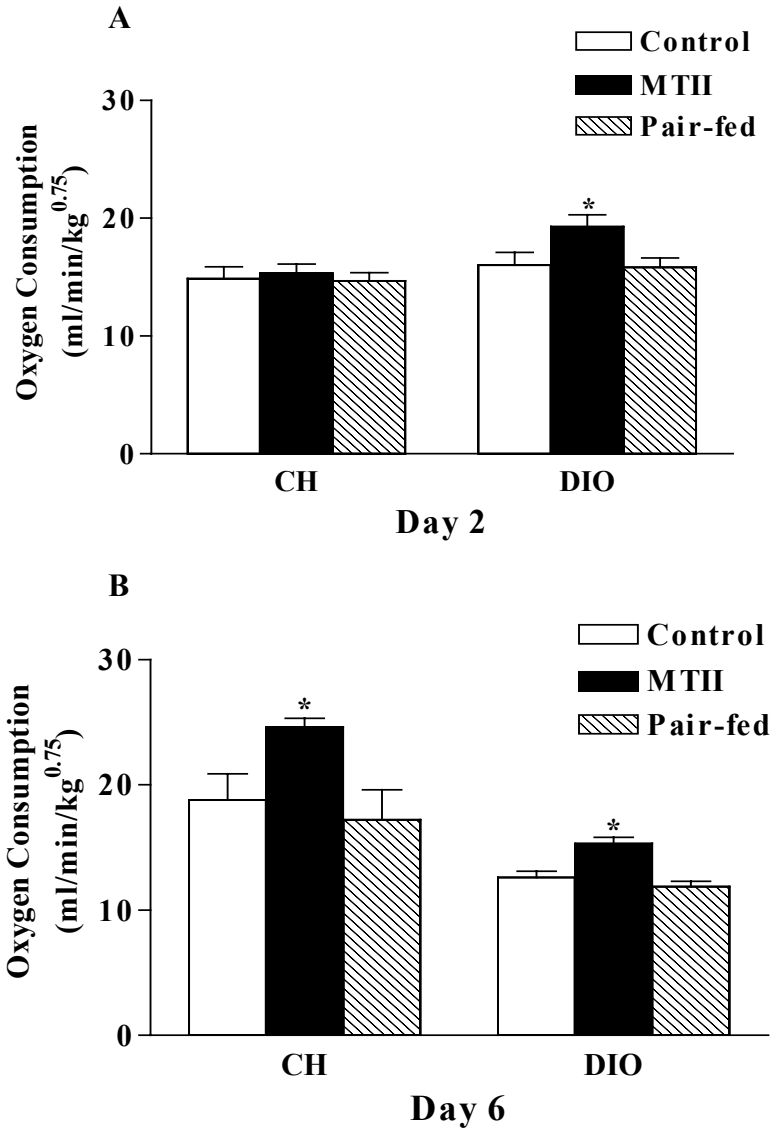

Fig. 3-3. Energy expenditure of chow-fed (CH) and DIO rats 6 days following icv administration of vehicle or MTII (1nmol/day). Control animals were either fed *ad libitum* (Control) or pair-fed to the amount of calories consumed by the MTII-treated groups (Pair-fed). Oxygen consumption was measured at day 2 (A) and day 6(B). Values are means ± SE of 6 to 9 animals per group. * P <0.05 vs. corresponding control and pair-fed groups by one-way ANOVA with *post hoc* Turkey's test.

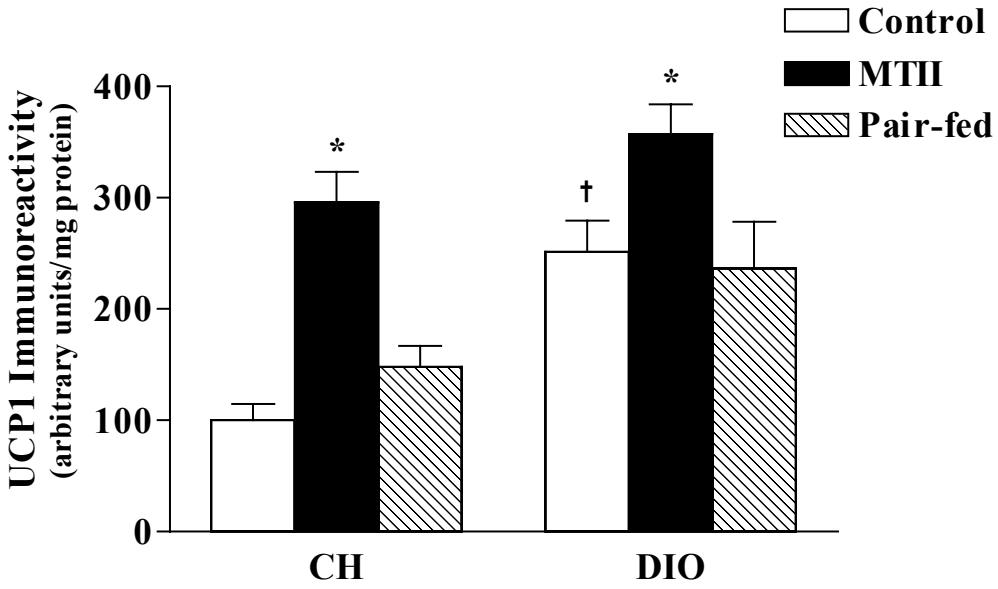

Fig. 3-4. Brown adipose tissue (BAT) uncoupling protein 1 (UCP1) levels in chow-fed (CH) and DIO rats 6 days following icv administration of vehicle or MTII (1nmol/day). The vehicle used was artificial cerebrospinal fluid. Control animals were either fed *ad libitum* (Control) or pair-fed to the amount of calories consumed by the MTII-treated groups (Pair-fed). Values are means ± SE of 6 to 9 animals per group. UCP1 levels are expressed in arbitrary units with levels in CH controls set to 100 and SE adjusted proportionally. * $P < 0.05$ vs. controls and pair-fed; † $P < 0.01$ vs. CH controls by two-way ANOVA with *post hoc* Bonferroni's test.

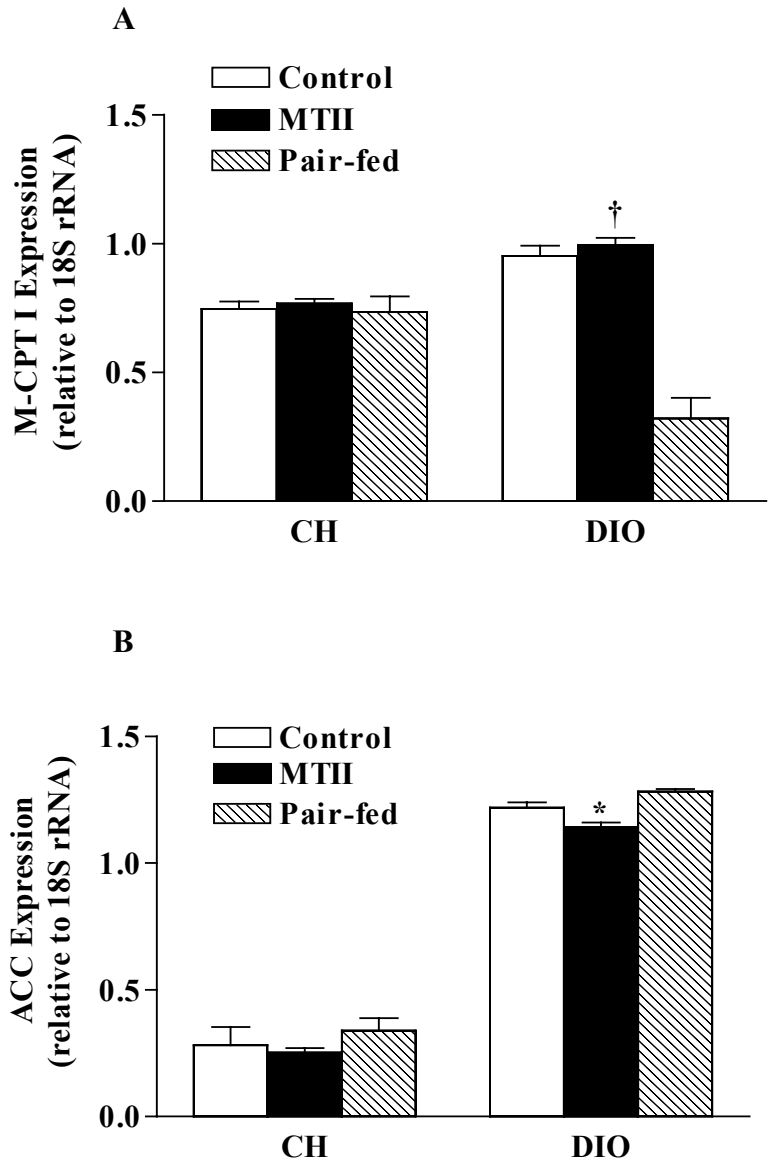

Fig. 3-5. Muscle-type CPT I (A) and ACC (B) expression in red soleus muscle of chow-fed (CH) and DIO rats 6 days following icv administration of vehicle or MTII (1nmol/day). The vehicle used was artificial cerebrospinal fluid. Control animals were either fed *ad libitum* (Control) or pair-fed to the amount of calories consumed by the MTII-treated groups (Pair-fed). Values are means ± SE of 6 to 9 animals per group. Results are normalized to 18S rRNA. * $P < 0.05$ vs. corresponding control and pair-fed groups; † $P < 0.01$ vs. Pair-fed by one-way ANOVA with *post hoc* Turkey's test.

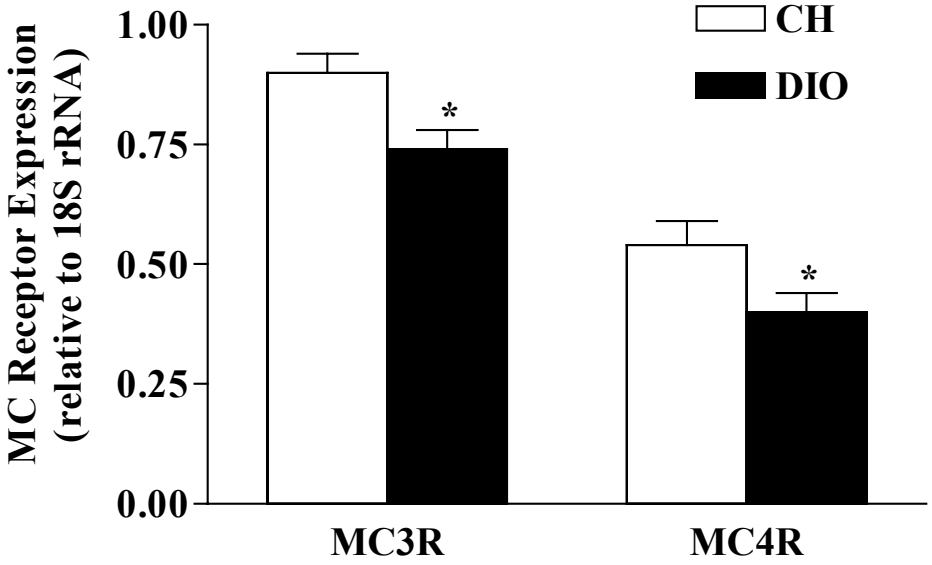

Fig. 3-6. Hypothalamic melanocortin 3 receptor (MC3R) and 4 receptor (MC4R) expression in chow-fed and DIO rats following ten weeks of diet. Values are means ± SE of six animals per group. Results are normalized to 18S rRNA. * $P < 0.05$ vs. controls by unpaired *t* test.

Discussion

The study in this chapter assessed the effects of MTII, a potent MC3/4R agonist, on several aspects of energy regulation in a diet-induced obese rodent model. Selection of adult female Sprague-Dawley rats in this study was based on two considerations. First, the use of mature rats eliminates the potentially confounding variable of normal growth; secondly, female rats have a comparable sensitivity to MTII as males (Clegg et al., 2003), but they typically reach a weight plateau earlier than the male counterparts. After 10 weeks of HF feeding, 40% of the female Sprague-Dawley rats became obese and displayed leptin resistance to centrally infused leptin. However, subsequent central MTII infusion circumvented leptin resistance in these DIO rats, leading to suppressed food intake, reduced body weight and visceral adiposity.

Although in agreement with several earlier reports indicating that DIO animals robustly respond to α-MSH or MTII treatment (Hansen et al., 2001; Pierroz et al., 2002), our study provides an extension of the previous knowledge. First, despite a reduction in hypothalamic MC3R and MC4R expression levels in DIO rats, the animals responded to MTII administration with similar efficacy as that of CH rats. In addition, the initial anorectic response and whole body oxygen consumption (at day 2) was modestly but significantly enhanced in DIO relative to CH rats. There is speculation in literature that central MC receptor up-regulation might contribute to enhanced anorexic response in DIO animals (Hansen et al., 2001). For instance, enhanced responses to MTII in obese Zucker rats are linked to increased MC4R density in certain hypothalamic nuclei (Harrold et al., 1999a). Yet the same study also noted that MC4R densities in specific hypothalamic regions involved in energy regulation were actually diminished in DIO rats

with normal genetic background. Our data together with this report seem to argue against the homeostatic MC3/4R receptor up-regulation theory. Interestingly, protein levels of the endogenous MC3/4R antagonist AgRP were reported to be elevated in DIO animals (Harrold et al., 1999b). Thus, despite the increased MC3/4R antagonist level and reduced MC3/4R expression associated with obesity, there is enhanced initial response to MTII. The possible explanations include up-regulation of components or activity of the post-receptor signaling cascade such as cAMP, protein kinase A, or phosphorylation of the transcription factor cAMP response element binding protein. More studies are needed to identify the precise mechanism for the observed hypersensitivity to MTII in obesity.

The present study also suggests that an increase in energy expenditure contributes to the loss of body weight and visceral adiposity following MTII treatment in both CH and DIO rats. Central MTII infusion markedly reduced body weight and visceral adiposity in obese DIO rats compared to their respective either *ad libitum*-fed or pair-fed animals. Because pair-feeding accounts for changes due to reduced food intake, our observation is suggestive of a food intake-independent component in the fat-trimming effect of MTII. The elevation of oxygen consumption at day 2 in DIO and day 6 in CH and DIO rats during central MTII infusion further argues that an increase in energy expenditure initiated by central MC activation is involved in the regulation of energy balance. Nonshivering thermogenesis in brown adipose tissue represents an essential element in adaptive energy expenditure in rodents, and UCP1 protein level is one indicator of the thermogenic status of BAT (Nedergaard et al., 2001). A previous report indicated that animals treated with MTII had elevated levels of BAT UCP1 expression compared with pair-fed controls (Cettour-Rose and Rohner-Jeanrenaud, 2002). Similarly,

in the present study, MTII greatly enhanced UCP1 protein levels in BAT. This big increase in UCP1 may well be the mediator for the elevated thermogenesis following MTII treatment. The long-term HF feeding (ten weeks) also increased basal BAT UCP1 protein levels by more than 2-fold. This up-regulation of basal UCP1 in BAT may serve as one explanation for the immediate increase in the MTII-induced energy expenditure (at day 2) in DIO rats.

Humans with excessive fat deposition in the body have high risk of various obesity-related disorders. Elevated visceral rather than subcutaneous adiposity is, in particular, associated with type 2 diabetes, heart diseases and stroke (Gasteyger and Tremblay, 2002). MTII produced an impressive reduction in visceral adiposity in the present study, which was not matched by pair-feeding. Even though chronic caloric restriction has been shown to decrease visceral adiposity in rodents and humans (Barzilai et al., 1998; Tchernof et al., 2002), we did not observe a significant decrease in visceral fat mass in either CH or DIO animals that were pair-fed to MTII treatment. Such a discrepancy could result from the transient anorexic response to MTII. Unlike constant food restriction, pair-fed rats in our experiment were restricted to a small amount of food during the initial days of the experiment but then provided with much more food towards later days of the treatment. This pair-feeding pattern resembles caloric restriction followed by partial refeeding. Humans and animals under this kind of feeding pattern often undergo a greater weight gain and fat repletion (Soriguer et al., 2003). In our case, a significant loss in visceral adiposity was likely prevented by this variable pair-feeding corresponding to the transient anorexic response during the course of MTII infusion. In contrast to pair-feeding, MTII treatment clearly reduced visceral adiposity in both CH and DIO groups in

spite of the temporal change in food intake. Therefore, the food-independent effect of MTII, presumably the increased energy expenditure as reflected by both elevated oxygen consumption and BAT UCP1, plays a crucial part in fat catabolism.

Besides its impact on adiposity, MTII has been shown to increase the expression of liver CPT I in lean and obese Zucker rats as compared to their respective pair-fed controls (Cettour-Rose and Rohner-Jeanrenaud, 2002). CPT I is a key enzyme in fat catabolism that controls the transfer of long-chain fatty acyl-CoA molecules into mitochondria where they are oxidized. Another important enzyme is ACC, the rate-limiting enzyme for malonyl-CoA formation. Malonyl CoA is an allosteric inhibitor of CPT I, and thus, a reduction in ACC is consistent with promotion of fat catabolism (Jeukendrup, 2002). In our study, MTII not only prevented the decrease in muscle CPT I expression associated with pair-feeding, but also reduced ACC mRNA in skeletal muscle in DIO rats. The simultaneous changes in the expression of ACC and M-CPT I indicate an overall increase in fatty acid oxidation in skeletal muscles, implying that the increased fat catabolism in muscle could be an additional factor in mediating the fat-reducing action of MTII. Considering the relatively small amount of BAT versus a large volume of skeletal muscles in humans, the MTII-evoked muscle fat metabolism seems to offer a much more promising target for any potential clinical application.

Finally, MTII also appears to improve glucose and cholesterol metabolism and insulin sensitivity. Central MC receptor activation can reduce insulin release from pancreas and enhance glucose metabolism (Fan et al., 1997; Obici et al., 2001). However, the results in obese animal models are controversial: one study suggested that peripheral but not central MTII improved insulin resistance in DIO mice (Pierroz et al., 2002),

whereas another reported that 3-day peripheral MTII administration had no effect on serum insulin in obese Zucker rats (Cettour-Rose and Rohner-Jeanrenaud, 2002). In our present study, central MTII infusion resulted in a significant reduction in serum insulin levels but unchanged serum glucose levels in CH rats. Pair-feeding, however, lowered both serum glucose and insulin levels significantly in only DIO rats, and it generated a downward trend in these two parameters in CH rats. MTII, on the other hand, appeared to be more potent in suppressing serum insulin rather than glucose in DIO rats. The improvement of glucose metabolism in CH and DIO animals may be largely attributed to hypophagia induced by central MTII administration. The potency of MTII against serum insulin may also rely on an additional food-independent mechanism, such as inhibition of insulin release from pancreas by direct central melanocortin receptor activation (Fan et al., 1997;Obici et al., 2001). Besides its impact on insulin and glucose, MTII also reduced total serum cholesterol levels in CH and DIO rats, whereas pair-feeding produced a similar reduction in CH but only a tendency of decrease in DIO rats. How MTII lowers cholesterol is currently unknown. It is conceivable that insulin-mediated stimulation of cholesterol synthesis diminishes following a fall in circulating insulin levels (Horton et al., 2002).

In summary, the study in Chapter 3 has demonstrated that central MC activation by the MC3/4R agonist MTII circumvents leptin resistance associated with DIO, resulting in a reduction in body mass and visceral adiposity. Despite reduced hypothalamic MC3/4R expression, the anorexic and thermogenic responses to MTII are unabated with the initial responses enhanced in DIO versus CH rats. The HF-induced up-regulation of BAT UCP1 in DIO rats may account for the immediate increase in energy expenditure following

central MTII infusion. The sustained thermogenic response to MTII throughout the entire period of infusion was probably mediated, at least in part, by the persistent elevation in BAT UCP1 protein. Furthermore, MTII appears to increase fat catabolism in skeletal muscle, and improve glucose and cholesterol metabolism and insulin sensitivity in both CH and DIO rats. The hypophagia and/or increased energy expenditure are the likely mechanisms underlying these improvements.

CHAPTER 4
EFFECTS OF CENTRAL POMC GENE THERAPY IN GENETICALLY OBESE ZUKCER RATS

Introduction

The central melanocortin system plays a critical role in the homeostatic regulation of body weight (Cone, 1999; Fan et al., 1997; Huszar et al., 1997; Mizuno and Mobbs, 1999; Butler et al., 2000). Melanocortins are bioactive peptides derived from a common precursor, POMC, one of which, α-MSH is a major regulator of feeding and body weight homeostasis. Reduced expression of hypothalamic POMC is associated with obesity syndromes due to mutations in the leptin receptor (Mizuno et al., 1998; Kim et al., 2000) or other genes (tubby, Nhlh2, etc) (Guan et al., 1998; Good et al., 1997), due to hypothalamic damage (Bergen et al., 1998), and, perhaps most commonly, aging (Mobbs et al., 2001). That reduced hypothalamic POMC mRNA could contribute to the obese phenotypes in these models is suggested by the observation that mutations in the POMC gene cause obesity in mice (Yaswen et al., 1999) and humans (Krude et al., 1998). However, it is still unclear if normalization of central POMC tone can reverse obese phenotypes. The present study aims to address this question.

Leptin, an adipocyte-derived hormone, acts on satiety and appetite centers in the hypothalamus to both reduce food consumption and increase energy expenditure (Friedman and Halaas, 1998; Schwartz et al., 1996; Scarpace et al., 1997). Recent evidence suggests that the melanocortin system may be located downstream of the hypothalamic leptin signaling pathway. Leptin activates POMC- and AgRP- containing

neurons of the ventrolateral and ventromedial arcuate nucleus, respectively, resulting in an increase in the expression of POMC and a reduction in AgRP (Schwartz et al., 1996; Schwartz et al., 1997; Cheung et al., 1997; Baskin et al., 1999; Elias et al., 2000). In addition, leptin-induced suppression of food intake is effectively blocked by a MC 3/4 receptor antagonist (Seeley et al., 1997), and the leptin-mediated induction of uncoupling protein 1 (UCP1), an important thermogenic protein in the brown adipose tissue (BAT), is also attenuated by central MC receptor antagonism (Satoh et al., 1998).

Genetically obese fa/fa Zucker rats with a recessive mutation of the leptin receptor gene develop severe, early-onset obesity associated with hyperphagia, hyperleptinemia, and hyperinsulinemia (Bray, 1977; Iida et al., 1996). Using this leptin and insulin resistant rodent model, we examine in Chapter 4 whether overproduction of POMC in the hypothalamus reduces body mass and adiposity and improves glucose metabolism in obese Zucker rats. In addition, some evidence suggest that tachyphylaxis to the MC-mediated reduction in food intake develops following chronic pharmacological treatment of MC agonists in rodents (McMinn et al., 2000; Pierroz et al., 2002, data in Chapter 3). Thus, the second purpose of this study is to examine the consequences of long-term targeted overexpression of POMC on the MC-mediated anorexic response.

Recent successes in using recombinant adeno-associated virus (rAAV) to obtain long-term expression of transgenes provide an opportunity to test our hypotheses (Monahan and Samulski, 2000). There are many advantages of using rAAV, including nonpathogenicity, nonimmunogenicity, high viability of the virion, and most importantly, long-term expression of the delivered transgene. The rAAV type 2 vector has been uniquely successful as gene transfer vector into the CNS (Xu et al., 2001).

In the experiments of Chapter 4, we used a rAAV type 2 vector encoding murine POMC (rAAV-POMC) to assess the long-term consequences of POMC gene delivery on energy balance, BAT thermogenesis and hypothalamic MC signal transduction in obese Zucker rats. To this end, we administered rAAV-POMC or control vectors bilaterally into the arcuate nucleus of the hypothalamus of obese Zucker rats for 38 days, and assessed food intake, body weight, adiposity, serum hormone and metabolite levels, BAT UCP1 protein, hypothalamic POMC, AgRP mRNA levels as well as hypothalamic phosphorylation of the CREB (Montminy et al., 1990).

Materials and Methods

Construction of rAAV Vector Plasmids

pTR-CBA-POMC encodes murine POMC cDNA (a generous gift from Dr. James Roberts) (Uhler and Herbert, 1983) under the control of the hybrid cytomegalovirus immediate early enhancer/chicken β-actin (CBA) promoter (Daly et al., 2001). The woodchuck hepatitis virus post-transcriptional regulatory element (WPRE) is placed downstream of the POMC transgene to enhance its expression (Loeb et al., 1999). The control plasmid, termed pTR-Control, is similar to pTR-CBA-POMC except for the incorporation of the cDNA encoding an enhanced form of green fluorescent protein (GFP) instead of POMC cDNA. The control vector was described previously (Li et al., 2002).

In Vitro Analysis of pTR-CBA-POMC Plasmid

The pTR-CBA-POMC construct was tested for *in vitro* expression of POMC by transfecting HEK 293 cells using FuGENE 6 transfection reagent (Roche Diagnostics, Indianapolis, IN) according to the protocol provided by the manufacturer. One day after

the transfection, cells were harvested and total RNA isolated. POMC mRNA levels were analyzed by RT-PCR.

Packaging of rAAV Vectors

Vectors were packaged, purified, concentrated, and titered as previously described (Zolotukhin et al., 1999). The titers for both rAAV-POMC and rAAV-Control vectors used in this study were $4.26x10^{11}$ physical particles/ml, and the ratios of physical-to-infectious particles for both vectors were less than 30.

Animals

Nine-week old male obese Zucker (fa/fa) rats were obtained from Charles River (Wilmington, MA). Upon arrival, rats were examined and remained in quarantine for two weeks. Animals were cared for in accordance with the principles of the NIH Guide to the Care and Use of Experimental Animals. Rats were housed individually with a 12:12 h light: dark cycle (07:00 to 19:00 h). Standard Purina 5001 rodent diet and water were provided *ad libitum*.

rAAV Vector Administration

Under 6 mg/kg xylazine (Phoenix Pharmaceutical, St. Joseph, MO) and 60mg/kg ketamine (Monarch Pharmaceuticals, Bristol, TN) anesthesia, rats were administered bilaterally ($1.28x10^9$ particles/injection in 3 µl) of rAAV-POMC (n=6) or rAAV-Control (n=6) into the basal hypothalamus with coordinates targeting the arcuate nucleus. The coordinates for injection into the hypothalamus were 3.14mm posterior to bregma, ±0.4mm lateral to the midsaggital suture and 10mm ventral from the skull surface. On each side a small hole was drilled through the skull and a 23-gauge stainless steel cannula inserted followed by an injection cannula. Using 10-µl Hamilton syringe, a 3-µl volume of virus stocks was delivered over 5 min to each site. The needles remained in place at

the injection site for 5 additional min. At the time of surgery, rats were injected with the analgesic Buprenex (0.05mg/kg; Reckitt and Colman, Richmond, VA).

Tissue Harvesting and Preparation

Rats were fasted overnight and sacrificed by cervical dislocation under 85 mg/kg pentobarbital anesthesia. Blood samples were collected by heart puncture and serum was harvested by a 15-min centrifugation in serum separator tubes. The circulatory system was perfused with 30 ml of cold saline, BAT, perirenal and retroperitoneal white adipose tissues (PWAT and RTWAT) were excised. The hypothalamus was removed by making an incision medial to piriform lobes, caudal to the optic chiasm and anterior to the cerebral crus to a depth of 2-3 mm. Tissues were stored at –80˚C until analysis. For Western analysis, hypothalamus and BAT were homogenized in 0.3ml 10 mM Tris-HCL, pH 6.8, 2% SDS, and 0.08 μg/ml okadaic acid. Protease inhibitors, 1mM phenylmethylsulfonyl fluoride (PMSF), 0.1 mM benzamidine, and 2 μM leupeptin were also present. Homogenates were immediately boiled for 2 min, cooled on ice, and stored frozen at –80˚C. Protein was determined using the DC protein assay kit (Bio-Rad, Hercules, CA). BAT samples were filtered through a 0.45 micron syringe filter (Whatman, Clifton, NJ) to remove lipid particles prior to protein measurements.

Serum Leptin, Insulin, Glucose, FFA, and Cholesterol

Serum leptin and insulin were measured using rat radioimmunoassay kits (Linco Research, St. Charles, MO). Serum free fatty acids and total cholesterol were determined by enzymatic colorimetric kits from WAKO Chemicals (Neuss, Germany). Serum glucose was via a colorimetric reaction with Trinder, the Sigma Diagnostics Glucose reagent (St. Louis, MO).

Relative Quantitative RT-PCR

POMC and AgRP expression in the hypothalamus were identified by relative quantitative RT-PCR using QuantumRNA 18S Internal Standards kit (Ambion, Austin, TX). Total cellular RNA was extracted as described (Li et al., 2002) and treated with RNase-free DNase (Ambion). First-strand cDNA synthesis was generated from 2 μg RNA in a 20-μl volume using random primers (Life Technologies, Rockville, MD) containing 200 units of M-MLV reverse transcriptase (Life Technologies). Relative quantitative PCR was performed by multiplexing corresponding primers (POMC sense 5'-GCTTGCAAACTCGACCTCTC-3', antisense 5'-CTTGATGATGGCGTTCTTGA-3'; AgRP sense 5'-AGGGCATCAGAAGGCCTGACCA-3', antisense 5'-CTTGAAGAAGCGGCAGTAGCAC-3'), 18S primers and competimers and coamplifing. Linearity for the POMC and AgRP amplicons was determined to be between 20 and 29 cycles. The optimum ratio of 18S primer to competimer was 1:4 for POMC and 1:9 for AgRP. PCR was performed at 94°C denaturation for 60 sec, 59°C annealing temperature for 45 sec, and 72°C elongation temperature for 60 sec for 26 (POMC) or 24 (AgRP) cycles. The PCR product was electrophoresed on acrylamide gel and stained with SYBR green (Molecular Probes, Eugene, OR). Gels were scanned using a STORM fluorescent scanner and data analyzed using ImageQuant (Molecular Dynamics). The relative values of POMC and AgRP mRNA were derived from dividing the signal obtained for corresponding amplicon by that for 18S amplicon.

CREB and Phosphorylated CREB (P-CREB) Assay

Immunoreactive CREB and P-CREB were determined with a PhosphoPlus CREB (Ser 133) antibody kit (New England Bio labs, Beverly, MA). Hypothalamic samples (40 μg) prepared as described above were separated on a SDS-PAGE gel and

electrotransferred to nitrocellulose membrane. Immunoreactivity was assessed on separate membranes with antibodies specific to CREB (phosphorylated and unphosphorylated) and antibodies specific to serine 133 phosphorylated CREB. Immunoreactivity was visualized by enhanced chemiluminescent detection (Amersham Pharmacia Biotech) and quantified by video densitometry (Bio-Rad).

UCP1 Protein

Immunoreactive UCP1 in BAT homogenates (20 μg) was determined as described for CREB except an antibody specific to rat UCP1 (Linco Research) was used.

Statistical Analysis

Results are presented as mean ± SE. Repeated measures ANOVA was used for analyses of body weight and food intake. When the main effect was significant, a post-hoc *t* test was applied to determine individual differences between means. For all other data, unpaired two-tailed Student's *t* test was employed. A value of $P < 0.05$ was considered significant.

Results

Transient Expression of POMC in HEK 293 Cells

HEK 293 cells were transfected with pTR-CBA-POMC or pTR-Control plasmids (Fig. 4-1). Twenty-four hours after the transfection, total POMC mRNA expression was measured by relative quantitative RT-PCR. The primers used do not discriminate among mouse, rat and human POMC, thus the measured POMC mRNA represents both transgene mouse POMC and endogenous HEK 293 human POMC mRNA. The pTR-CBA-POMC transfection increased POMC expression in HEK 293 cells by more than eight-fold as compared to pTR-Control ($p<0.001$).

POMC Expression in the Hypothalamus of Obese Zucker Rats

To verify the overexpression of the POMC transgene following central viral delivery, POMC mRNA was measured in the hypothalamus by RT-PCR (Fig. 4-2). Thirty eight days after vector delivery, hypothalamic POMC mRNA levels were elevated by four-fold in obese Zucker rats given rAAV-POMC as compared to those given rAAV-Control ($p<0.02$). The ratio of hypothalamic POMC to 18S rRNA expression ranged from 0.061 to 0.073 for control animals and from 0.186 to 0.435 for rAAV-POMC treated rats. Therefore, the POMC mRNA levels were at least two-fold higher in all of the rAAV-POMC rats as compared to the mean levels in the control animals.

Melanocortin Signal Transduction and AgRP mRNA Levels

α-MSH, one of the cleavage products of POMC, is reported to exert its anorexic and thermogenic effects via activation of hypothalamic melanocortin receptors and subsequent phosphorylation of the transcription factor, CREB (P-CREB) (Sarkar et al., 2002). We thus assessed hypothalamic CREB and P-CREB immunoreactivities 38 days post POMC vector delivery. Phosphorylation of CREB was elevated by 62% in the hypothalami of rats with rAAV-POMC treatment whereas total CREB levels were unchanged (Fig. 4-3).

The expression of AgRP, an endogenous antagonist of MC receptors, is presumably regulated by leptin in normal animals (Schwartz et al., 1996; Schwartz et al., 1997; Cheung et al., 1997; Baskin et al., 1999; Elias et al., 2000). RT-PCR revealed that hypothalamic AgRP expression levels were unchanged in rats given rAVV-POMC as compared with control rats at sacrifice (0.927 ± 0.092 vs. 0.995 ± 0.053 relative to 18S rRNA, $P>0.5$).

Body Weight and Food Intake

Bilateral delivery of rAAV-POMC into the basal hypothalamus reduced weight gain and food intake in obese Zucker rats (Fig. 4-4). Before and on the day of vector delivery, average body weight of rAAV-POMC treated rats was comparable to that of control rats (428±18 vs. 403±23g at day 0). After vector delivery, the rats given rAAV-POMC consistently gained less weight, and the difference in body mass between the two groups gradually increased over the thirty-eight days (Fig. 4-4A). Because daily food consumption of obese Zucker rats varied noticeably between individual rats (Fig. 4-4B), daily food intake following vector delivery was also expressed as percent of individual baseline levels, represented by the average daily food intake one week prior to vector administration (Fig. 4-4C). Hypothalamic delivery of rAAV-POMC induced a sustained anorexic response in these obese rats. The inhibition of food intake became statistically significant starting at day 7 post POMC vector delivery and lasted for the duration of the experiment (Fig. 4-4B, C).

Visceral Adiposity and Serum Leptin Levels

Because POMC gene therapy reduced the weight gain of the obese Zucker rats, body adiposity levels were assessed. Thirty-eight days after central POMC gene delivery, there were significant reductions in the visceral adiposity, as reflected by a 24% reduction in the sum of the PWAT and RTWAT ($P<0.05$) in rAAV-POMC-treated compared to control rats (Fig. 4-5A). Fasting serum leptin levels, known to be highly correlated with body fat mass (Frederich et al., 1995), were 43.5% lower in the rAAV-POMC group compared to the control group (Fig. 4-5B).

Fasting Serum Insulin, Glucose, FFA, and Cholesterol

At sacrifice, serum insulin was significantly reduced by rAAV-POMC as compared with rAAV-Control, and serum glucose tended toward a decrease (Fig. 4-6 A, B). The rAAV-POMC delivery also reduced serum total cholesterol levels by 34.5% and increased free fatty acid levels by 33% compared with rAAV-Control (Fig. 4-6 C, D).

Brown Adipose Tissue

Induction of UCP1 in BAT is an important marker for enhanced thermogenesis and thus, energy expenditure in rodents (Scarpace et al., 1997). In present study, we examined the UCP1 protein levels 38 days after POMC gene delivery. Total BAT weight markedly declined with rAAV-POMC treatment whereas the protein concentration (per unit BAT) increased slightly, suggesting the reduction in BAT mass was due to the lipolysis associated with the activation of BAT. This was further supported by a 4-fold increase in BAT UCP1 protein levels in the rAAV-POMC treated compared with control rats (Table 4-1).

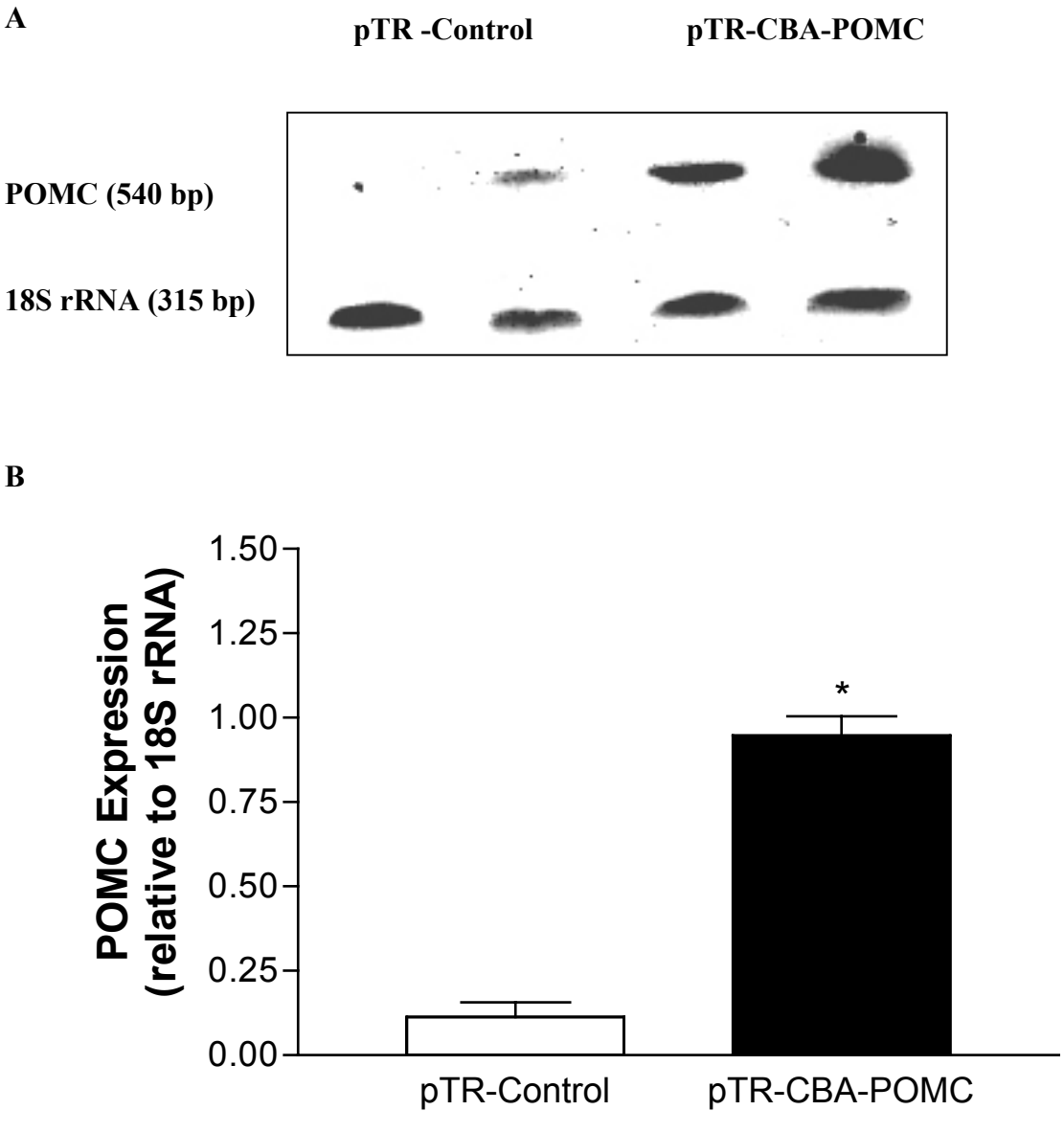

Fig. 4-1. POMC expression in HEK 293 cells 24 hours after pTR-CBA-POMC or pTR-Control transfection. A: Representative image of relative quantitative RT-PCR analysis of POMC mRNA expression with 18S rRNA as an internal standard. B: Quantification of POMC mRNA normalized to 18S rRNA. Data represent mean ± SE from 3 experiments. * $P<0.001$ vs. control by unpaired *t* test.

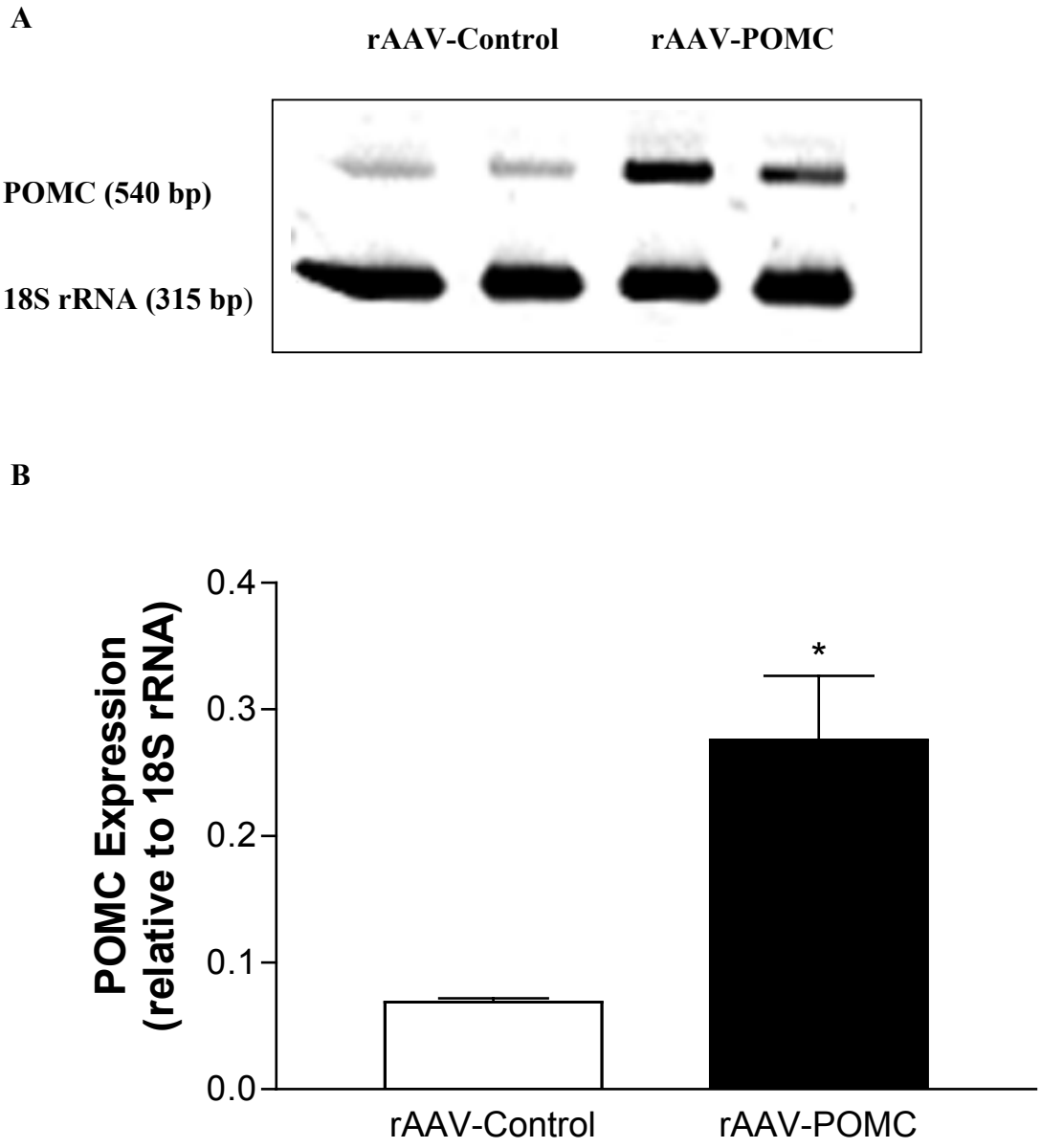

Fig. 4-2. Hypothalamic POMC expression 38 days after rAAV-POMC or control vector delivery in obese Zucker rats. A: Representative image of relative quantitative RT-PCR analysis of hypothalamic POMC mRNA with 18S rRNA as an internal standard. B: Quantification of POMC mRNA normalized to 18S rRNA. Data represent mean ± SE from 6 rats per group. * $P<0.02$ vs. control by unpaired *t* test.

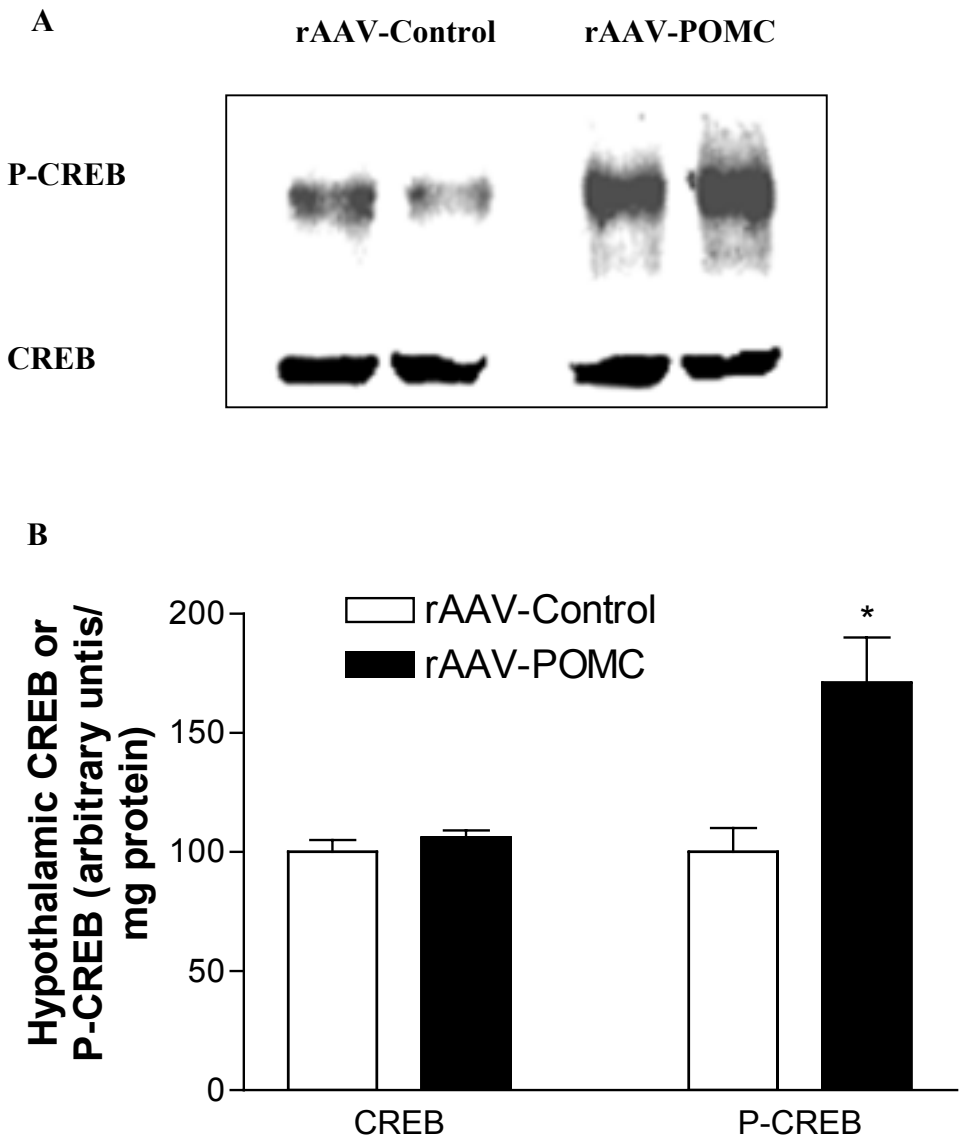

Fig. 4-3. Total CREB and phosphorylated of CREB (P-CREB) in the hypothalamus of obese Zucker rats 38 days post rAAV-POMC or rAAV-Control delivery. A: Representative Western immunoblots using antibodies specific for CREB or P-CREB. B: Quantification of average CREB and P-CREB in 6 control and 6 rAAV-POMC rats. Levels in rAAV-Control rats are set to 100 and SE adjusted proportionally. * $P < 0.05$ vs. control by unpaired *t* test.

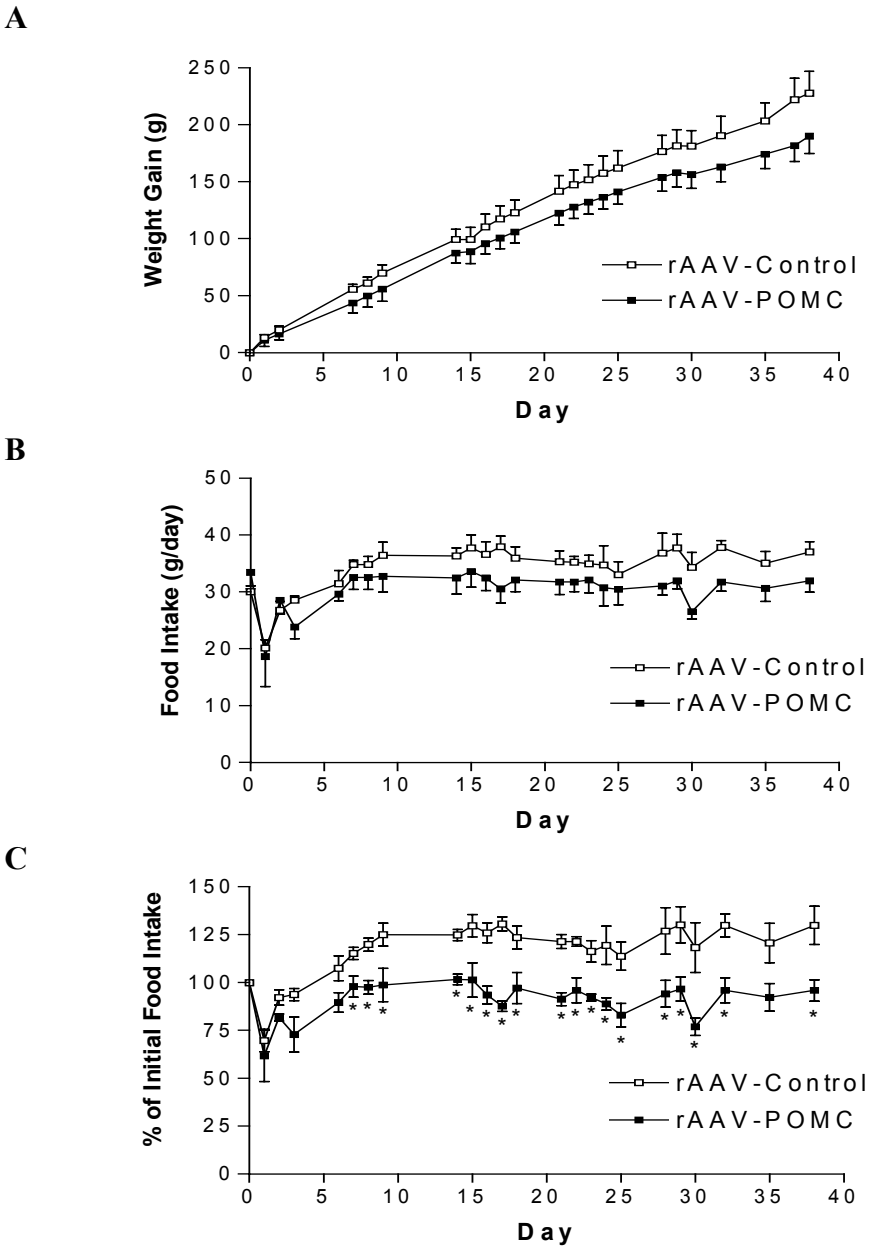

Fig. 4-4. Body weight gain (A), daily food consumption (B), and the percent of initial food intake (C) following rAAV-POMC or rAAV-Control administration in obese Zucker rats. The vectors were injected at day 0. Data represent mean ± SE of 6 rats per group. Initial food intake is the average daily food consumption one week prior to vector delivery. $P<0.0001$ for difference in weight gain (A), food intake (B), or percent of initial food intake (C) with treatment by repeated measures ANOVA. * $P < 0.05$ for difference in food intake between rAAV-POMC and control rats (C) at day 7 through day 38 except day 35.

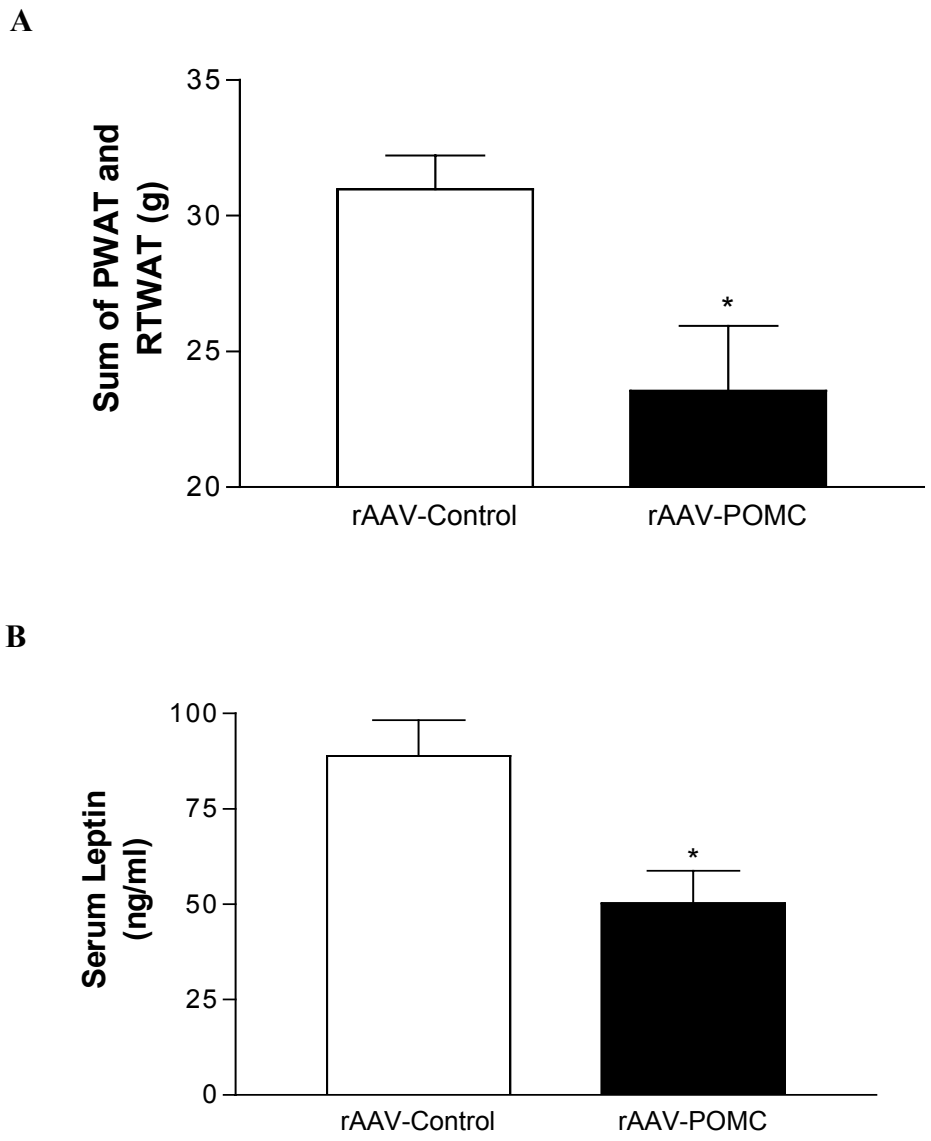

Fig. 4-5. Visceral adiposity (A) and fasting serum leptin (B) 38 days following rAAV-POMC or rAAV-Control administration in obese Zucker rats. Data represent mean ± SE of 6 rats per group. * P<0.05 vs. control by unpaired *t* test.

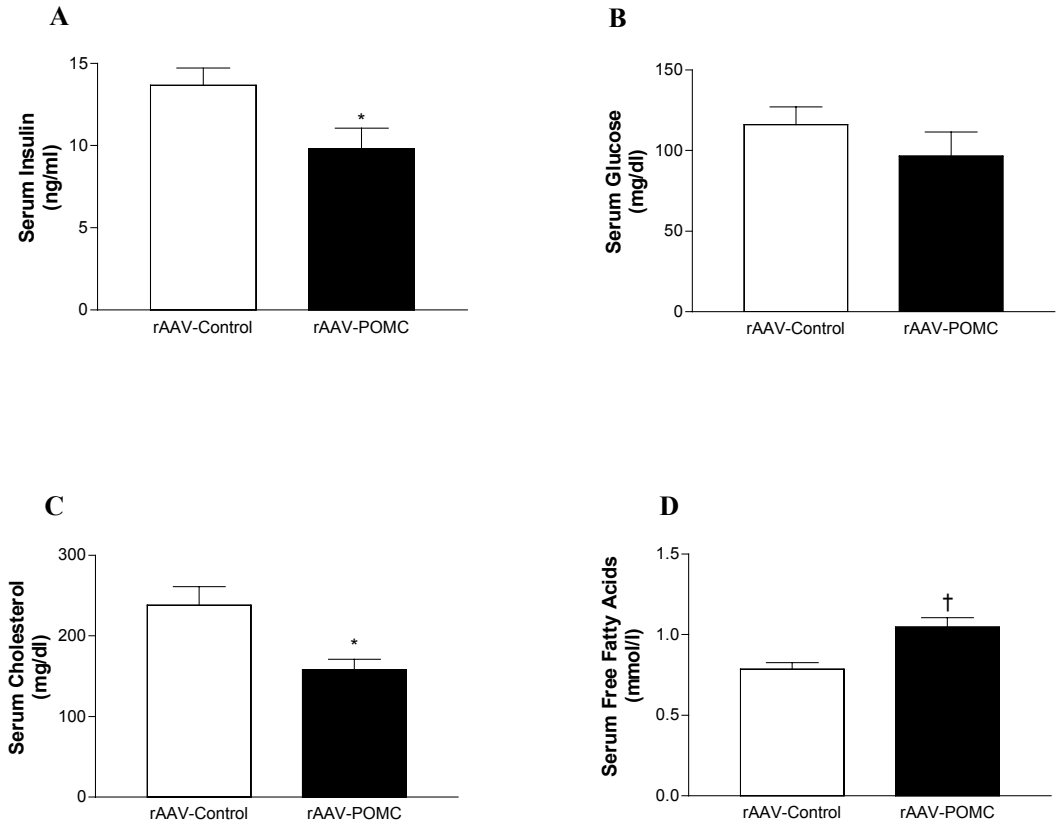

Fig. 4-6. Fasting serum insulin (A), glucose (B), cholesterol (C) and FFA (D) levels 38 days following rAAV-POMC or rAAV-Control delivery in obese Zucker rats. Data represent mean ± SE of 6 rats per group. * $P<0.05$ and † $p<0.01$ vs. control by unpaired *t* test.

Table 4-1. Uncoupling protein 1 and BAT parameters 38 days following rAAV-POMC or rAAV-Control delivery. For UCP1 protein, the levels in rAAV-Control rats are set to 100 and SE adjusted proportionally. Data represent the mean ± SE of 6 rats per group. * P<0.05 and † P<0.01 vs. control by unpaired t test.

	Treatment	
	rAAV-Control	rAAV-POMC
BAT weight (mg)	2193±275	1366±189 *
BAT protein (mg/g BAT)	23.4±1.4	27.2±1.8
BAT protein (mg/total BAT)	50.2±5.2	38.3±7.2
UCP1 protein (arbitrary units/g BAT)	100±17	662±114 †
UCP1 protein (arbitrary units/total BAT)	100±33	412±104 *

Discussion

The study in Chapter 4 examines the long-term consequences of central rAAV-POMC gene therapy in obese Zucker rats with inherent defective leptin receptors and deficient endogenous POMC expression. Our findings are in agreement with several previous pharmacological studies indicating that direct activation of the central MC system is effective in partially reversing the hyperphagia and obesity in obese Zucker rats (Hwa et al., 2001; Cettour-Rose and Rohner-Jeanrenaud, 2002). Our approach, in particular, resulted in long-term overexpression of POMC in the basal hypothalamus, and these obese Zucker rats responded with significant reductions in both food intake and weight gain. The level of hypothalamic P-CREB, the putative active form of the transcriptional factor mediating MC3/MC4 receptor signaling (Montminy et al., 1990; Sarkar et al., 2002), was significantly elevated in the obese Zucker rats whereas hypothalamic AgRP mRNA was unaffected at day 38 post POMC vector delivery. Thus, it appears that long-term POMC gene therapy attenuates weight gain primarily through activation of central MC system characterized by increased hypothalamic POMC mRNA levels, CREB phosphorylation and unchanged AgRP expression. Because POMC vector delivery was aimed at the arcuate nucleus where POMC-expressing neurons are located, it is most likely that POMC overexpression in these neurons is mainly responsible for the observed physiological consequences. However, given the proximity of the third ventricle to the arcuate nucleus, the possibility exists that some of the viral vectors entered the third ventricle. The vectors could also diffuse out of the arcuate nucleus, resulting in the transduction of neurons outside of the arcuate nucleus. The potential ectopic expression of POMC in the brain might account for some of the responses observed. In such cases,

the responses would be expected to be more pharmacological rather than physiological in nature.

The present study in Chapter 4 provides several distinct sets of salient findings. First, our data suggest that an increase in energy expenditure might contribute to the reduced weight gain and visceral adiposity following POMC gene delivery. It is known that pharmacological activation of MC system augments energy expenditure in rodents. For example, normal animals treated with the α-MSH analog, MTII, have elevated levels of BAT UCP1 expression compared with pair-fed controls (Cettour-Rose and Rohner-Jeanrenaud, 2002). The unique UCP1-mediated nonshivering thermogenesis in BAT represents an essential element in adaptive energy expenditure in rodents. An increase in UCP1 protein is indicative of increased BAT-facilitated energy expenditure. Obese Zucker rats, however, have impaired BAT thermogenesis because of the genetically defective leptin receptors (Levin et al., 1984). Despite this inherent problem, we observed a 4-fold increase in BAT UCP1 at 38 days post POMC vector delivery in the obese Zucker rats, indicating markedly stimulated BAT thermogenesis. Although lacking direct measurement of whole body energy expenditure, we speculate based on our observation that, in addition to the hypophagia, an increase in energy expenditure plays a part in mediating the fat and weight-trimming effects of central POMC gene therapy.

Secondly, rAAV-mediated POMC gene delivery produces an impressive reduction in adiposity. For example, by the end of the 38-day POMC gene therapy, PWAT and RTWAT combined were decreased by 24% when compared with controls. In addition, a key indicator of whole body mass (Frederich et al., 1995), fasting serum leptin levels were also reduced by 44%. Central chronic infusion of α-MSH has been shown by one

study to preferentially reduce visceral fat mass as opposed to lean body mass in lean rats (Obici et al., 2001). If such a preference in action is proven to exist, strategies based on MC activation to treat obesity will offer an apparent advantage over some other weight control remedies that indiscriminately reduce both lean and fat body mass through suppression in food consumption.

Thirdly, rAAV-POMC gene delivery appears to improve glucose metabolism. The obese Zucker rats are insulin resistant as indicated by remarkably high levels of serum insulin. Central POMC gene therapy decreased fasting serum insulin, and it also generated a downward trend in serum glucose levels. These data suggest improved glucose metabolism and insulin sensitivity by POMC gene delivery. This observation is consistent with previous findings that central MC receptor activation reduces insulin release from pancreas and enhances glucose metabolism (Fan et al., 1997; Obici et al., 2001). On the other hand, without a pair-fed group to control for the effect of food intake, we are not certain if the improvement in glucose metabolism is directly related to the increased central POMC expression or a consequence of the decreased food consumption and body weight. In addition to its impact on insulin and glucose, POMC gene delivery also lowered total serum cholesterol levels in obese Zucker rats. Thus, central activation of melanocortin system seems to have a cholesterol-reducing effect in these obese animals possessing both leptin and insulin resistance. The mechanism underlying the reduction in cholesterol is currently unknown, and one explanation could be that insulin-mediated stimulation of cholesterol synthesis is impeded following a fall in circulating insulin levels (Horton et al., 2002).

Most surprisingly, present study revealed a sustained anorexic response to rAAV-POMC in the obese Zucker rats throughout the entire 38-day experimental period. This is in sharp contrast to all previous reports in which there was a rapid attenuation of the anorexic response following pharmacological infusions of melanocortins in both normal and DIO rats, and mice (McMinn et al., 2000; Pierroz et al., 2002). The suppression in food intake lasted no longer than four days in any of these studies. In the case of obese Zucker rats, one study noted a three-day anorexic response to chronic pharmacological administration of MTII (Cettour-Rose and Rohner-Jeanrenaud, 2002). Therefore, the sustained anorexic response we observed over 38 days may be unique to central POMC gene delivery. With this procedure, the presumed overproduction of α-MSH is derived from POMC with assistance from a variety of endogenous enzymes such as prehormone convertases, carboxypeptidase E and peptidyl α-amidating mono-oxygenase (Pritchard et al., 2002). This endogenously regulated production of α-MSH may help prevent the rapid desensitization witnessed in previous pharmacological studies. Additionally, obese Zucker rats, in comparison to their lean counterparts, are associated with reduced POMC expression in the arcuate nucleus, lower amount of α-MSH peptide in the paraventricular nucleus, and higher MC4 receptor densities in several hypothalamic regions pivotal to energy regulation (Kim et al., 2000; Harrold et al., 1999a). These factors may also contribute to the prolonged responsiveness to POMC gene delivery in obese Zucker rats. Central MC signaling has been implicated in the development of cachexia (Marks et al., 2003), and we cannot rule out the possibility that the sustained anorexic response by central POMC gene delivery might be in part a mimic of inflammatory-like activities of POMC products. Although in present study, POMC gene delivery appeared to reduce

visceral adiposity to a greater extent as compared with the decrease in whole body mass, an observation inconsistent with cachexigenic action.

In summary, the study in Chapter 4 demonstrates that targeted POMC gene delivery to the hypothalamus suppresses food intake and weight gain and reduces visceral adiposity in genetically obese Zucker rats. This treatment also appears to improve glucose and cholesterol metabolism and insulin sensitivity. The sustained hypophagia and augmentation of thermogenesis in BAT, as also suggested by data from Chapter 3, are the likely mechanisms underlying these improvements.

CHAPTER 5
EFFECTS OF CENTRAL IL-6 GENE THERAPY IN NORMAL MALE SPRAGUE-DAWLEY RATS

Introduction

IL-6 is a multifunctional, proinflammatory cytokine that acts on a wide range of tissues through modulation of cell growth and differentiation. Its pleiotropic effects include stimulation of acute-phase protein synthesis, induction of the proliferation and differentiation of lymphocytes, and an increase in the activity of the hypothalamic-pituitary-adrenal axis (HPA) (Gruol and Nelson, 1997). IL-6 also reduces food intake and increases thermogenic activity in brown adipose tissue (BAT) (Busbridge et al., 1989; Schobitz et al., 1995; Tsigos et al., 1997; Cannon et al., 1998). Thermogenesis in BAT is mediated by norepinephrine activation of sympathetically innervated β_3-adrenergic receptors (β_3ARs) and serves to regulate body temperature and maintain body weight after hyperphagia (Nedergaard et al., 2001). Thus, through modulation of BAT thermogenesis and food intake, IL-6 may have a role in energy homeostasis.

Both immune and nonimmune cells synthesize IL-6. Moreover, as much as one third of the total circulating IL-6 has been estimated to originate from WAT (Mohamed-Ali et al., 1997). Leptin, another WAT-derived cytokine, is considered to be the central afferent signal molecule that indicates the size of fat depots, and this cytokine has important roles in energy homeostasis, mediating both a reduction in food intake and an increase in energy expenditure (Ahima and Flier, 2000). Interestingly, similar to leptin, synthesis of IL-6, as well as systemic concentration, is also positively correlated with

body fat mass (Vgontzas et al., 1997). Both IL-6 and leptin receptors share close structural analogy in the signal transduction domains and have been found in hypothalamic areas involved in energy regulation (Tartaglia et al., 1995; Schobitz et al., 1992). Recent studies demonstrated that IL-6 and leptin activate overlapping signal transduction pathways, notably the JAK/STAT3 pathway (Baumann et al., 1996). Collectively, these data suggest that IL-6 may play a supportive role to leptin in energy homeostasis. However, the underlying mechanisms by which IL-6 enhances thermogenesis are not fully understood.

Most studies concerning IL-6 and energy balance have focused on the IL-6 induced responses associated with infection and wasting diseases, such as cancer cachexia (Greenberg et al., 1992). Moreover, investigations have been limited to effects of short-term administration of IL-6, and the long-term effects of IL-6 treatment on food intake and body weight are unknown. Recent successes in using recombinant adeno-associated virus (rAAV) to obtain long-term expression of transgenes provide an opportunity to examine the chronic effects of IL-6 administration (Monahan and Samulski, 2000). There are many advantages of using rAAV, including the apparent absence of pathogenicity, high viability of the virion, relative independence of infectivity from host chromosome replication and cell cycling, and most importantly, long-term expression of the delivered transgene. The rAAV type 2 vector has been uniquely successful as gene transfer vector into the CNS (Xu et al., 2001).

In present study, we used a rAAV type 2 vector encoding murine IL-6 (rAAV-IL-6) to assess the long-term consequences of IL-6 gene delivery on energy balance, BAT thermogenesis and hypothalamic IL-6 signal transduction. To this end, we administered

rAAV-IL-6 or control viral vectors into the hypothalamus of normal adult male Sprague-Dawley rats for 21 and 35 days, and examined food intake, body weight, adiposity, serum hormonal levels, BAT UCP1 and hypothalamic STAT3 phosphorylation. Furthermore, to test if the IL-6 induced thermogenesis was dependent on sympathetic activation of BAT, we administered rAAV-IL-6 or control viral vectors to rats in which the interscapular BAT was unilaterally denervated, and examined food intake, body weight, as well as BAT UCP1 mRNA and protein levels.

Materials and Methods

Construction of rAAV Vector Plasmids

A murine IL-6 cDNA (a generous gift by Dr. I.L. Campbell, the Scripps Research Institute, La Jolla, CA, USA) (Raber et al., 1997) was inserted into rAAV vector plasmid pTR-UF12. This plasmid contains the AAV terminal repeats (TRs), the only remaining feature (and 4%) of the wild type AAV genome. Flanked by the TRs, the expression cassette of pTR-UF12 includes the following components, in 5' to 3' order: 1) a 1.7 kb sequence containing the hybrid cytomegalovirus immediate early enhancer/chicken β-actin (CBA) promoter/exon1/intron (Daly et al., 2001); 2) the internal ribosome entry site (IRES) from poliovirus, which provides for bicistronic expression (Dirks et al., 1993); 3) green fluorescent protein (GFP) (Klein et al., 1998); 4) and the polyA tail from bovine growth hormone. The IL-6 cDNA was inserted between the CBA promoter and the IRES element of the pTR-UF12 to derive the construct pTR-IL-6. The control plasmid for these studies expresses GFP only and is termed pTR-Control. The control vector was described previously (Klein et al., 1998).

In Vitro Analysis of pTR-IL-6 Plasmid

The pTR-IL6 construct was tested for *in vitro* expression of IL-6 by mammalian cells. Human embryonic kidney 293 cells (HEK 293 cells) were transfected by the calcium-phosphate method, using $2x10^6$ cells and 8 μg DNA per 6 cm dish. One day after transfection, the media were removed and replaced with serum-free media. One day after (2 days after transfection), the media were collected and concentrated 10-fold in Centricon-10 units (Millipore, Bedford, MA, USA). The media samples were then separated on a 15% sodium dodecylsulfate (SDS)- polyacrylamide gel electrophoresis (PAGE) gel (Ready Gel, Bio-Rad, Hercules, CA, USA) and electrotransferred to nitrocellulose membrane, the blot was probed for IL-6 protein using a goat anti-IL-6 polyclonal antibody (Santa Cruz Biotechnology, Santa Cruz, CA, USA) at a dilution of 1:1000. Purified murine IL-6 (PeproTech, Rocky Hill, NJ, USA) was used as a positive control. Serum-free media samples from untransfected 293 cells were concentrated in a similar manner and examined for IL-6 protein.

Packaging of rAAV Vectors

Vectors were packaged, purified, concentrated, and titered as previously described (Zolotukhin et al., 1999). The titers for both rAAV-IL-6 and rAAV-Control vectors used in this study were $1x10^{11}$ physical particles/ml, resulting in $2x10^8$ particles in a 2-μl injection. The ratios of physical-to-infectious particles for both vectors were less than 30. A mini-Ad helper plasmid pDG (Grimm et al., 1998) was used to produce rAAV vectors with no detectable adenovirus or wild type AAV contamination.

Animals

Male Sprague-Dawley rats (330-350 g) around 3.5 months of age were obtained from Harlan Sprague-Dawley (Indianapolis, IN, USA). Upon arrival, rats were examined

and remained in quarantine for one week. Animals were cared for in accordance with the principles of the Guide to the Care and Use of Experimental Animals. All efforts were made to minimize the number of animals and their suffering. Rats were housed individually with a 12:12 h light: dark cycle (07:00 to 19:00 h). Standard Purina 5001 rodent diet and water were provided *ad libitum*.

Surgical Denervation

Rats underwent unilateral surgical denervation of the interscapular BAT under pentobarbital anesthesia as previously described (Scarpace and Matheny, 1998). A transverse incision was made just anterior to the right BAT pad, separating the BAT from the muscles of the right scapula. The scapula was raised to expose the five intercostal nerve bundles entering right BAT pad. A section of each nerve bundle was removed with scissors. The rats were maintained on a heat pad until recovery from the anesthesia. In previous studies, denervation was verified in selected rats by assessing norepinephrine levels in the innervated compared with denervated BAT pads. In all tested cases the denervation was successful (Scarpace and Matheny, 1996).

rAAV Vector Administration

Rats were administered a single dose ($2x10^8$ particles/rat in 2 μl) of rAAV-IL-6 or rAAV-Control into the center of the right side of the anterior hypothalamus under 50mg/kg pentobarbital anesthesia. The coordinates for injection into the hypothalamus were 1.8mm posterior to bregma, 1mm lateral to the midsaggital suture and 9mm ventral from the skull surface. A small hole was drilled through the skull and a 23-gauge stainless steel cannula inserted followed by an injection cannula. Using 10-μl Hamilton

syringe, a 2-µl volume of virus stocks was delivered over 5 min, and the needles remained in place at the injection site for 2 additional min.

Experiment 1

Rats were administered either rAAV-Control (n=9) or rAAV-IL-6 (n=10). Food consumption and body weight were recorded every day for 35 days at which time the rats were sacrificed.

Experiment 2

The interscapular BAT of rats was unilaterally denervated. On the day of surgery, rats were administered either rAAV-IL-6 (n=7) or rAAV-Control (n=7) into the hypothalamus. Daily food intake and body weight were monitored for 21 days at which time the rats were sacrificed.

Tissue Harvesting

Rats were sacrificed by cervical dislocation under 85mg/kg pentobarbital anesthesia. Blood samples were collected by heart puncture. Serum and plasma were harvested by a 10-min centrifugation in serum or plasma separator tubes. The circulatory system was perfused with 20 ml of cold saline, and BAT, perirenal and retroperitoneal white adipose tissues (PWAT and RTWAT) were excised. The hypothalamus was removed by making an incision medial to piriform lobes, caudal to the optic chiasm and anterior to the cerebral crus to a depth of 2-3 mm.

Histochemistry for GFP

Anesthetized animals were perfused with 100 ml of cold phosphate-buffered saline (PBS), followed by 400 ml of cold 4% paraformaldehyde in PBS. After, the brain was removed and equilibrated in a cryoprotectant solution of 30% sucrose/PBS and stored at

4˚C. Coronal sections (30μm) were detected using a fluorescein isothiocyanate (FITC) long-pass filter.

Leptin and Corticosterone RIA

Serum leptin levels were measured with a rat leptin RIA kit (Linco Research, St. Charles, MO, USA). Plasma corticosterone levels were determined by a rat/mouse corticosterone RIA kit (ICN Biomedicals, Costa Mesa, CA, USA).

mRNA Levels

Total cellular RNA was extracted using a modification of the method of Chomczynski (Chomczynski and Sacchi, 1987). The integrity of the isolated RNA was verified using agarose gels (1%) stained with ethidium bromide. The RNA was quantified by spectrophotometric absorption at 260 nm by use of multiple dilution of each sample.

The full-length UCP1 cDNA probe (a cDNA clone obtained from Dr. Leslie Kozak, the Jackson Laboratory, Bar Harbor, ME) (Kozak et al., 1988), the SOCS-3 cDNA probe (a gift from Dr. Christian Bjorbaek) (Bjorbaek et al., 1999) and the full-length human β-actin cDNA (Clontech, Palo Alto, CA, USA) were labeled using a random primer kit (Prime-a-Gene, Promega, Madison, WI, USA). For dot blot analysis, multiple concentrations of RNA were immobilized on nylon membranes using a dot blot apparatus (Bio-Rad, Richmond, CA, USA) and were UV-crosslinked by UV-crosslinker (Fisher Scientific, Pittsburgh, PA, USA). The membranes were prehybridized in 10 ml Quikhyb (Stratagene, La Jolla, CA, USA) for 20 min followed by hybridization in the presence of labeled probe and 100 μg denatured salmon sperm DNA. After hybridization for 2 h at 65°C, the membranes were washed and exposed to a phosphor imaging screen for 48 hours. The latent image was scanned using a Phosphor Imager (Molecular Dynamics, Sunnyvale, CA, USA) and analyzed by ImageQuant Software (Molecular

Dynamics). Levels of mRNA were expressed as the ratio of signal intensity for the target genes relative to that for β-actin.

RT-PCR

IL-6 transgene expression in the hypothalamus was identified by relative quantitative RT-PCR through the use of QuantumRNA 18S Internal Standards kit (Ambion, Austin, TX, USA). Total RNA was treated with RNase-free DNase (Ambion), and first-strand cDNA synthesis generated from 2 μg RNA in a 20-μl volume using random primers (Life Technologies, Rockville, MD, USA) containing 200 units of M-MLV reverse transcriptase (Life Technologies). Relative quantitative PCR was performed by multiplexing murine IL-6 primers (5'-GATGCTACCAAACTGGATATAATC-3', 5'-GGTCCTTAGCCACTCCTTCTGTG-3'), 18S primers and competimers and coamplifing. Linearity for the IL-6 amplicon was determined to be between 20 and 30 cycles. The optimum ratio of 18S primer to competimer was 1:9. PCR was performed at 94°C denaturation for 90 sec, 60°C annealing temperature for 60 sec, and 72°C elongation temperature for 120 sec for 26 cycles. The PCR product was electrophoresed on a 5% acrylamide gel and stained with SYBR green (Molecular Probes, Eugene, OR, USA). Gels were scanned using a STORM fluorescent scanner and data analyzed using ImageQuant (Molecular Dynamics). The relative values of IL-6 mRNA were derived from dividing the signal obtained for IL-6 amplicon by that for 18S amplicon.

UCP1 Protein

UCP1 levels were determined by immunoreactivity in BAT homogenates. BAT samples were homogenized in 10 mM Tris-HCL, pH 6.8, 2% SDS, and 0.08 μg/ml okadaic acid. Protease inhibitors, 1mM phenylmethylsulfonyl fluoride (PMSF), 0.1 mM

benzamidine, and 2 μM leupeptin were also present. BAT homogenates (20 μg) were boiled and separated on a 7.5% SDS-PAGE gel (Ready Gel, Bio-Rad) and electrotransferred to nitrocellulose membrane. UCP1 immunoreactivity was assessed with an antibody specific to rat UCP1 (Linco Research), Immunoreactivity was visualized by enhanced chemiluminescent detection (Amersham Pharmacia Biotech, Buchkinghamshire, England) and quantified by video densitometry.

STAT3 and Phosphorylated STAT3 (P-STAT3) Assay

Immunoreactive STAT3 and P-STAT3 were determined with a PhosphoPlus STAT3 (tyrosine 705) antibody kit (New England Bio labs, Beverly, MA, USA). Hypothalamic samples were prepared in the same manner as BAT in the previous paragraph. Hypothalamic homogenates (40 μg) were separated on a SDS-PAGE gel and electrotransferred to nitrocellulose membrane. Immunoreactivity was assessed on separate membranes with antibodies specific to STAT3 (phosphorylated and unphosphorylated) and antibodies specific to tyrosine 705 phosphorylated STAT3. Immunoreactivity was visualized by enhanced chemiluminescent detection (Amersham Pharmacia Biotech) and quantified by video densitometry. Immunoreactive STAT1 and phosphorylated STAT1 were determined in identical fashion using phosphoPlus STAT1 (tyrosine 701) antibody kit (New England Bio Labs).

Statistical Analysis

Results are presented as mean ± S.E.M. Repeated measures ANOVA was used for analyses of body weight and food intake. BAT UCP1 mRNA and protein levels in the denervation experiment were analyzed by two-way ANOVA with denervation conditions and treatments as variables. When the main effect was significant, a post-hoc test was

applied to determine individual differences between means. For all other data, unpaired Student's t-test was employed. A value of $p < 0.05$ was considered significant.

Results

Transient Expression of IL-6 in HEK 293 Cells

The expression of the pTR-IL-6 construct was assessed *in vitro* by transient transfection of HEK 293 cells with pTR-IL-6. The cells transfected with pTR-IL-6 released robust amount of mouse IL-6 protein into the media (Fig. 5-1, lane 5), whereas no IL-6 was detected in the supernatant of untransfected HEK 293 cells (Fig. 5-1, lane 4).

IL-6 Expression in the Hypothalamus of Rats Given rAAV-IL-6

A GFP reporter gene was incorporated into the control and IL-6 expressing vectors to provide easy identification of cells transduced with rAAV. Thirty-five days after viral delivery, coronal hypothalamic slices were prepared from two rAAV-Control and rAAV-IL-6 treated rats. Both vectors produced similar GFP expression in hypothalamus at 35 days post-injection. GFP-positive cells displayed typical neuron-like morphology and were distributed around the tract of the injection needle (Fig. 5-2, top). To further verify expression of the IL-6 transgene, murine IL-6 mRNA was examined in the hypothalamus by relative quantitative RT-PCR using primers specific for mouse IL-6. Murine IL-6 mRNA was identified in all rAAV-IL-6 treated rats at 21 and 35 days following viral delivery with similar expression levels (100 ± 15 vs. 104 ± 12, $p=0.84$) (Fig. 5-2, bottom). In contrast, IL-6 mRNA was not identified in any of the rAAV-Control administered rats (Fig. 5-2, bottom).

Experiment 1: 35 Days post rAAV-IL-6 Delivery

Body weight and food consumption

Direct delivery of rAAV-IL-6 gene into the hypothalamus reduced weight gain without affecting food intake in normal adult rats (Fig. 5-3). Before and on the day of viral delivery, average body weight of rAAV-IL-6 treated rats was similar to that of control rats (372.9±2.7 vs. 374.1±2.7 g at day 0). Repeated measures ANOVA revealed rAAV-IL-6 suppressed weight gain ($p<0.05$) throughout the duration of the experiment. Body weight difference reached a maximum between day 17 and day 25, after which the weight-reducing effect of IL-6 began to attenuate ($p=0.056\sim0.08$ from day 31 onward) (Fig. 5-3, top). During the same period of time, food consumption was not different between rAAV-IL-6 and control vector treated rats ($P=0.62$) (Fig. 5-3, bottom).

Adiposity and serum leptin levels

Thirty-five days after central IL-6 gene delivery, there were significant reductions in visceral adiposity, including a 20% reduction in PWAT ($p<0.05$) and a 22% decrease in RTWAT ($p<0.05$) in rAAV-IL-6 treated rats compared to control rats (Table 5-1). Serum leptin, another measure of adiposity level, also decreased by 39% in rAAV-IL-6 rats compared with controls (Table 5-1).

Plasma corticosterone levels

IL-6 is known to modulate the activity of HPA (Gruol and Nelson, 1997), and therefore, we measured the basal plasma corticosterone levels in rats. Central IL-6 delivery did not significantly alter plasma corticosterone levels in rAAV-IL-6 rats compared to controls ($p=0.25$) (Table 5-1).

Brown adipose tissue

We examined BAT UCP1 mRNA and protein levels 35 days after IL-6 gene delivery. Total BAT weight was unchanged while total BAT protein increased by 13% ($p=0.28$) (Table 5-2). BAT UCP1 mRNA levels were comparable between these two groups, whereas the UCP1 protein levels in BAT was enhanced by 65% in rAAV-IL-6 treated rats ($p<0.01$) (Table 5-2). The elevated UCP1 protein levels suggest that IL-6 gene delivery increases thermogenesis in BAT.

Experiment 2: 21 Days post rAAV-IL-6 Gene Delivery in Rats with unilaterally Sympathetic Denervation of BAT

Body weight and food intake

In experiment 1, rAAV-IL-6 treatment of intact rats suppressed body weight gain, which became statistically significant as early as day 13 and culminated around week 3 (Fig. 5-3, top). In contrast, following unilaterally sympathetic denervation of BAT, there was no difference between body mass of rAAV-IL-6 and rAAV-Control treated rats throughout the 21-day study ($p>0.5$ by repeated measures ANVOA) (Fig. 5-4, top). Similar to the previous experiment, food intake was comparable between two groups (Fig. 5-4, bottom).

Brown adipose tissue

Experiment 1 demonstrated that chronic expression of murine IL-6 in rat hypothalamus enhanced UCP1 protein levels in BAT. To investigate if the increase in UCP1 is dependent on sympathetic innervation of BAT, we measured UCP1 mRNA expression and the UCP1 protein levels in denervated and intact BAT pads following central rAAV-IL-6 delivery. As expected, in both rAAV-IL-6 and control rats, the levels of UCP1 protein in the denervated pads were dramatically reduced compared with those

in the intact pads (Fig. 5-5A). In the intact BAT pad, rAAV-IL-6 increased UCP1 protein levels by 47% compared to controls ($p<0.05$) (fig. 5-5A). In contrast, IL-6 gene delivery had no effect on UCP1 protein levels in denervated BAT pad (fig. 5-5A).

When UCP1 mRNA levels were examined, a similar picture emerged. In the denervated BAT pads, UCP1 mRNA levels were comparable between rAAV-IL-6 and control rats ($p>0.4$). In contrast, in the innervated BAT pads, rAAV-IL-6 increased UCP1 expression by 64% ($p<0.05$) compared with control rats (Fig 5-5B).

IL-6 Signal Transduction at Day 21 and Day 35

The apparent attenuation of the rAAV-IL-6 induced reduction in weight gain after day 31 in experiment 1 prompted us to examine IL-6 signal transduction during the time of maximum weight gain suppression (day 21) and during the time when the difference in body weight between rAAV-IL-6 and control vector treated rats was no longer statistically significant (day 35). The tyrosine phosphorylation of STAT3 at day 21 and 35 following rAAV-IL-6 delivery was determined in hypothalamic lysates by specific immunoreactivity of P-STAT3. There was a 2.6-fold increase ($p<0.005$) in P-STAT3 levels at day 21 in the rAAV-IL-6 compared with rAAV-Control-treated rats (Fig. 5-6). However, at 35 days post IL-6 gene delivery, there was no longer any increase in P-STAT3 ($P>0.7$) (Fig. 5-6). In addition to the increase in P-STAT3 at day 21, there was a 46% increase in total STAT3 immunoreactivity with rAAV-IL-6 injection ($p<0.05$), but this increase also waned by day 35 ($p=0.35$) (Fig. 5-6). In contrast to STAT3, rAAV-IL-6 did not increase immunoreactive STAT1 or phosphorylated STAT1 at either day 21 or 35 (data not shown).

Suppressor of cytokine signaling-3 (SOCS-3) has shown to be involved in the down-regulation of cytokine signaling and may be a negative regulator of JAK/STAT3

pathway (Starr et al., 1997). SOCS-3 mRNA levels were significantly elevated both at 21 and 35 days following rAAV-IL-6 administration by 57% and 38% respectively (Table 5-3).

Fig. 5-1. Western blot of murine IL-6 protein released from HEK 293 cells transfected with pTR-IL-6 plasmid. Protein samples were prepared from concentrated media. Lanes represent IL-6 protein standards (lane 1-3: 25ng, 2.5ng and 0.25ng respectively), untransfected cells (lane 4) and cells transfected with pTR-IL-6 (lane 5).

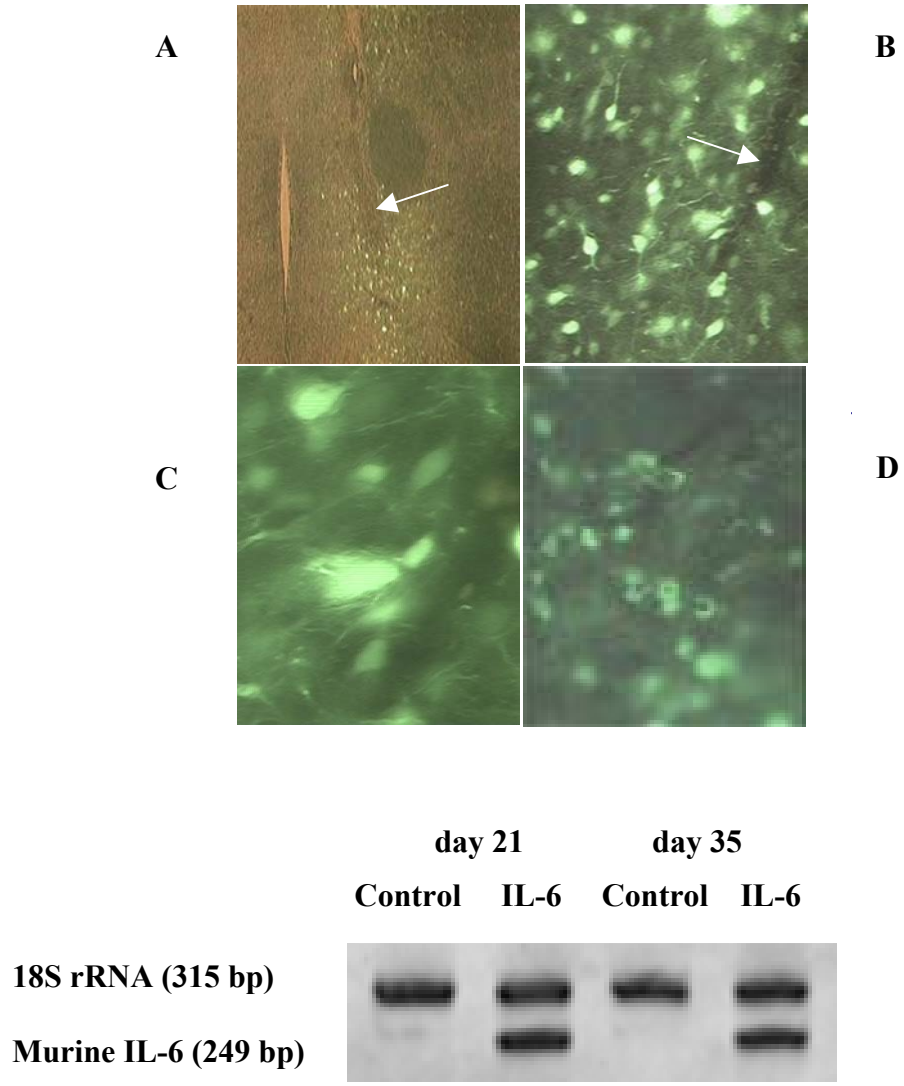

Fig. 5-2. Transgene expression in the hypothalamus after rAAV-IL-6 delivery. (Top) Numerous GFP-positive cells are observed in representative coronal hypothalamic sections following rAAV-IL-6 or rAAV-Control treatment. (A-C) the same hypothalamic section 35 days post rAAV-IL-6 delivery with different magnifications (4x, 20x and 40x respectively). The arrow indicates injection needle tract. (D) A hypothalamic section 35 days post rAAV-Control delivery (20x). (Bottom) Murine IL-6 mRNA, identified by relative quantitative RT-PCR in the hypothalamus, was present in all rAAV-IL-6 treated rats at similar levels, but not in rAAV-Control administered rats. Representative blots of control (lane 1) and rAAV-IL-6 (lane 2) at day 21, and control (lane 3) and rAAV-IL-6 (lane 4) at day 35. Upper bands represent RT-PCR products for 18S rRNA and lower bands for murine IL-6 mRNA. Quantitative results are given in the main text.

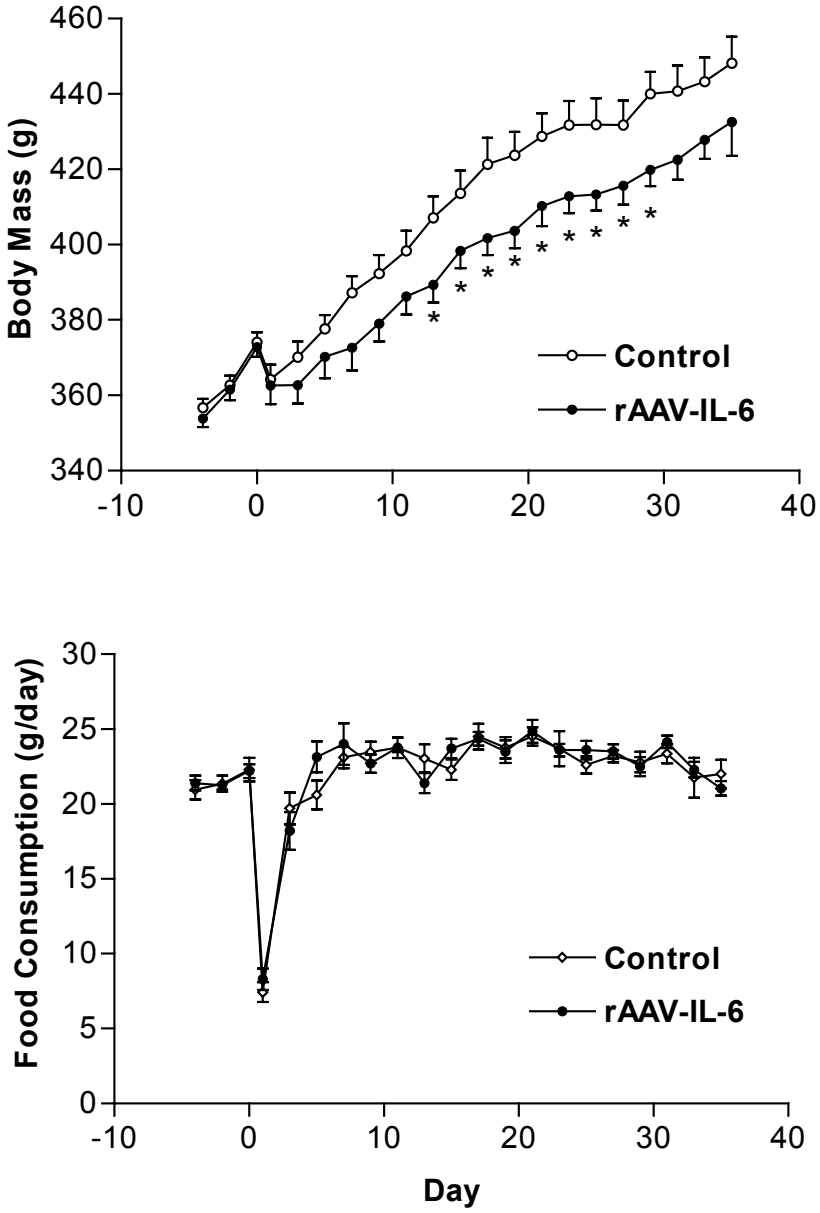

Fig. 5-3. Body weight (top) and daily food consumption (bottom) following rAAV-IL-6 or rAAV-Control administration in adult male Sprague-Dawley rats. The vectors were injected at day 0. Data represent Mean ± S.E.M. of 7-8 rats per group. $p < 0.05$ for difference in body weight with treatment by repeated measures ANOVA. * $p < 0.05$ for difference in body weight between rAAV-IL-6 and control rats by t-test.

Table 5-1. WAT depot weight, serum leptin and plasma corticosterone 35 days following rAAV-IL-6 or rAAV-Control delivery. Data represent the mean ± S.E.M. of 7-8 rats per group. *P<0.05 for difference between control and rAAV-IL-6 treated rats by t-test.

	Treatment	
	rAAV-Control	rAAV-IL-6
PWAT (g)	0.97±0.06	0.78±0.05 *
RTWAT (g)	2.99±0.17	2.34±0.18 *
IWAT (g)	1.43±0.10	1.42±0.09
Serum Leptin (ng/ml)	9.01±1.43	5.46±0.54 *
Plasma corticosterone (ng/ml)	266 ±26	303±19

Table 5-2. Uncoupling protein 1 and BAT parameters 35 days following rAAV-IL-6 or rAAV-Control delivery. For UCP1 mRNA and protein, the levels in rAAV-Control rats are set to 100 and S.E.M. adjusted proportionally. Data represent the mean ± S.E.M. of 7-8 rats per group. *P<0.01 for difference between control and rAAV-IL-6 treated rats by t-test.

	Treatment	
	rAAV-Control	rAAV-IL-6
BAT weight (mg)	314±27	301±24
BAT protein (mg/total BAT)	21.2±1.5	24.0±1.9
UCP1 mRNA (arbitrary units/total BAT)	100±8	107±13
UCP1 protein (arbitrary units/total BAT)	100±15	165±14 *

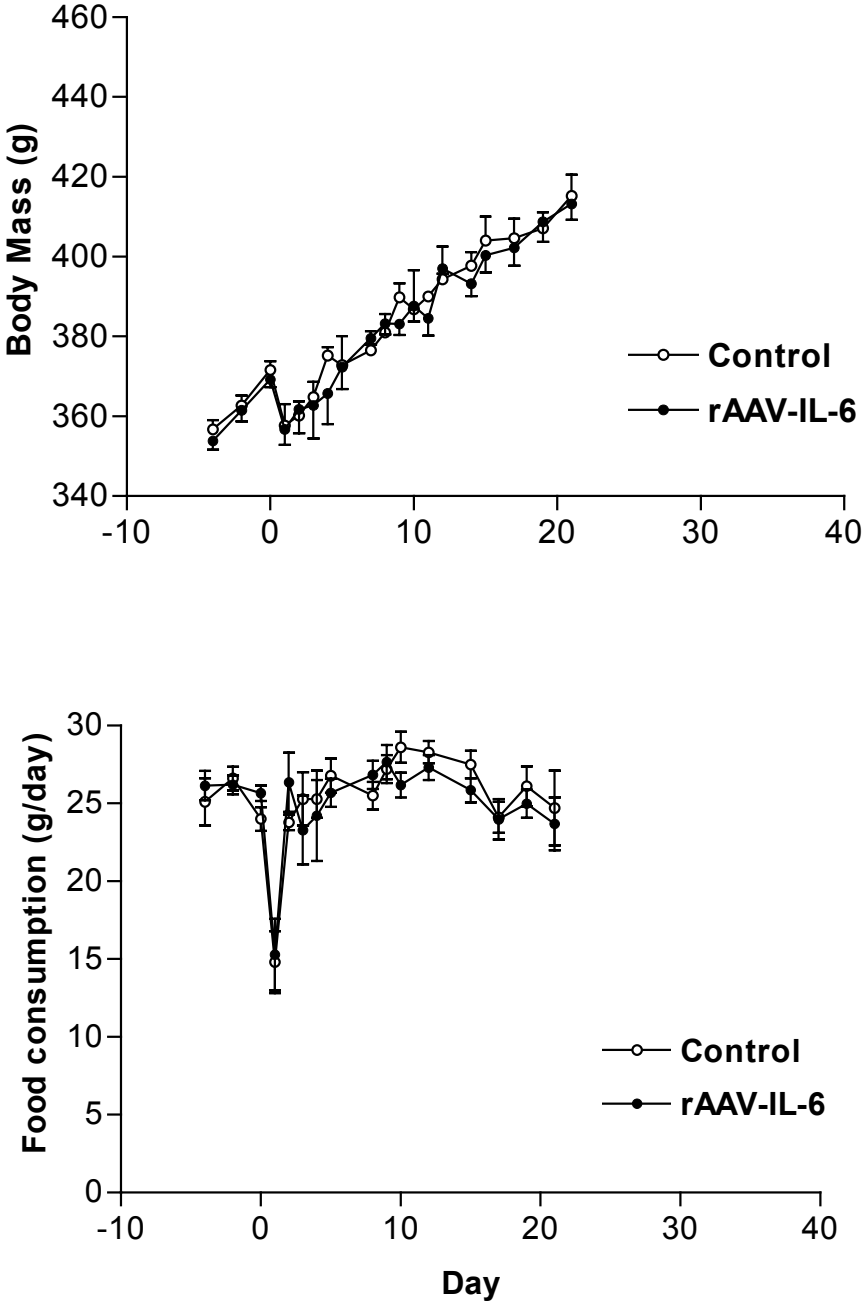

Fig. 5-4. Body weight (top) and daily food consumption (bottom) following rAAV-IL-6 or rAAV-Control administration in adult male Sprague-Dawley rats in which BAT had been unilaterally denervated. Vectors were injected at day 0. Data represent Mean ± S.E.M. of 7 rats per group. There was no significant difference in body weight or food intake between rAAV-IL-6 and control groups.

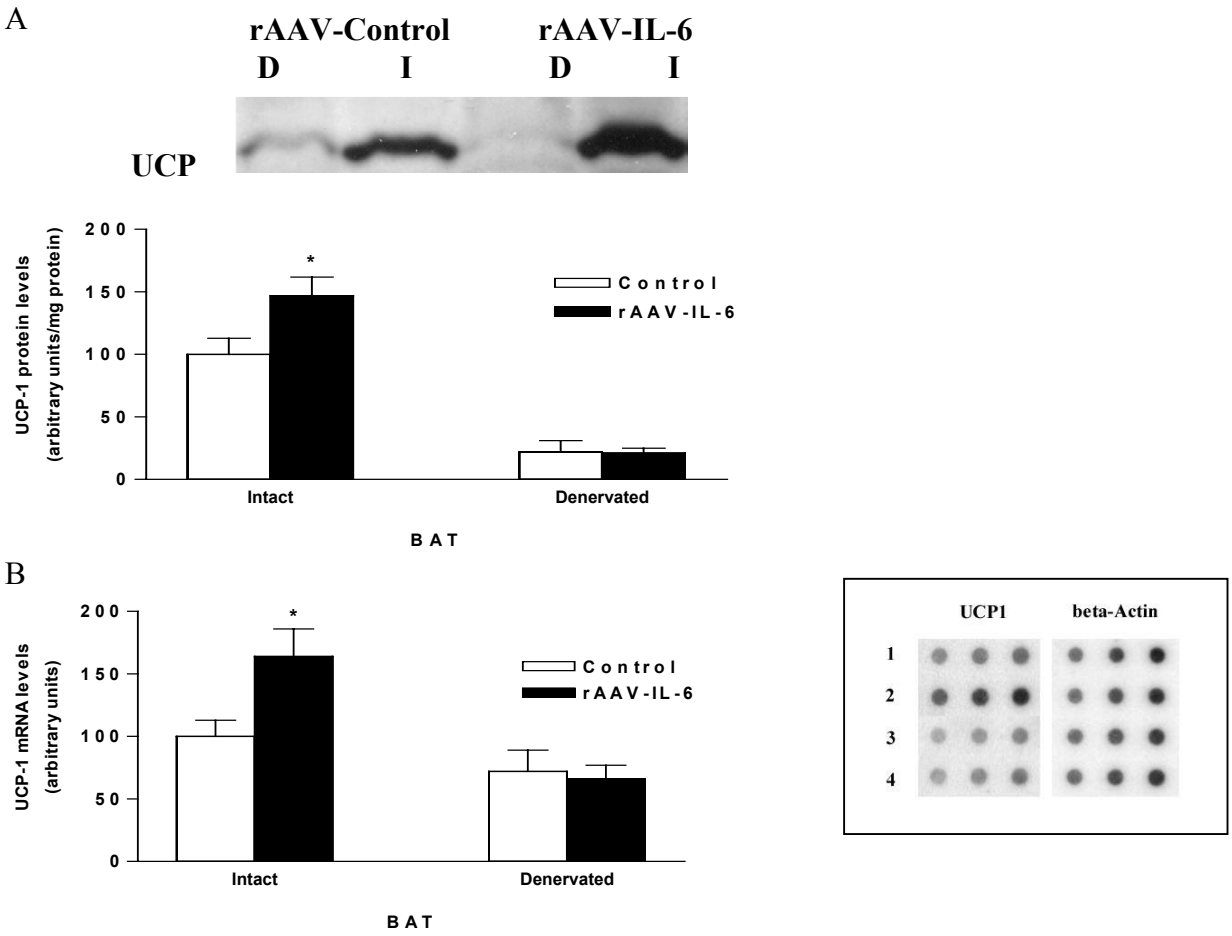

Fig. 5-5. BAT UCP1 protein (A) and mRNA (B) levels 21 days post rAAV-IL-6 or rAAV-Control treatment in rats in which BAT had been unilaterally denervated. Data represent the mean ± S.E.M. of 7 rats per group. UCP1 protein and UCP1 mRNA levels are expressed in arbitrary units with levels in intact pads of control rats set to 100 and S.E.M. adjusted proportionally. A: (Top) Representative western blots using an antibody against UCP1. Lanes represent denervated (D) BAT pads (lane 1,3) and intact (I) BAT pads (lane 2,4) from controls and rAAV-IL-6 treated rats. (Bottom) Quantification of UCP1 based on densitometric scanning. $P < 0.01$ for interaction between rAAV-IL-6 treatment and denervation by two-way ANOVA; * $p < 0.05$ for difference with rAAV-IL-6 treatment in intact BAT pads; $p < 0.05$ for difference with denervation in both control and rAAV-IL-6 treated rats. B: (Left) UCP1 mRNA levels in BAT were determined by dot blot analysis. Levels of mRNA were expressed by comparison of signal intensity for the target genes relative to that for β-actin. $p<0.05$ for interaction between rAAV-IL-6 treatment and denervation by two-way ANOVA; * $p < 0.05$ for difference with rAAV-IL-6 treatment in intact BAT pads. (Right) representative dot blots for UCP1 mRNA: Intact BAT pads from controls (lane 1) and rAAV-IL-6 rats (lane 2), denervated BAT pads from controls (lane 3) and rAAV-IL6 rats (lane 4).

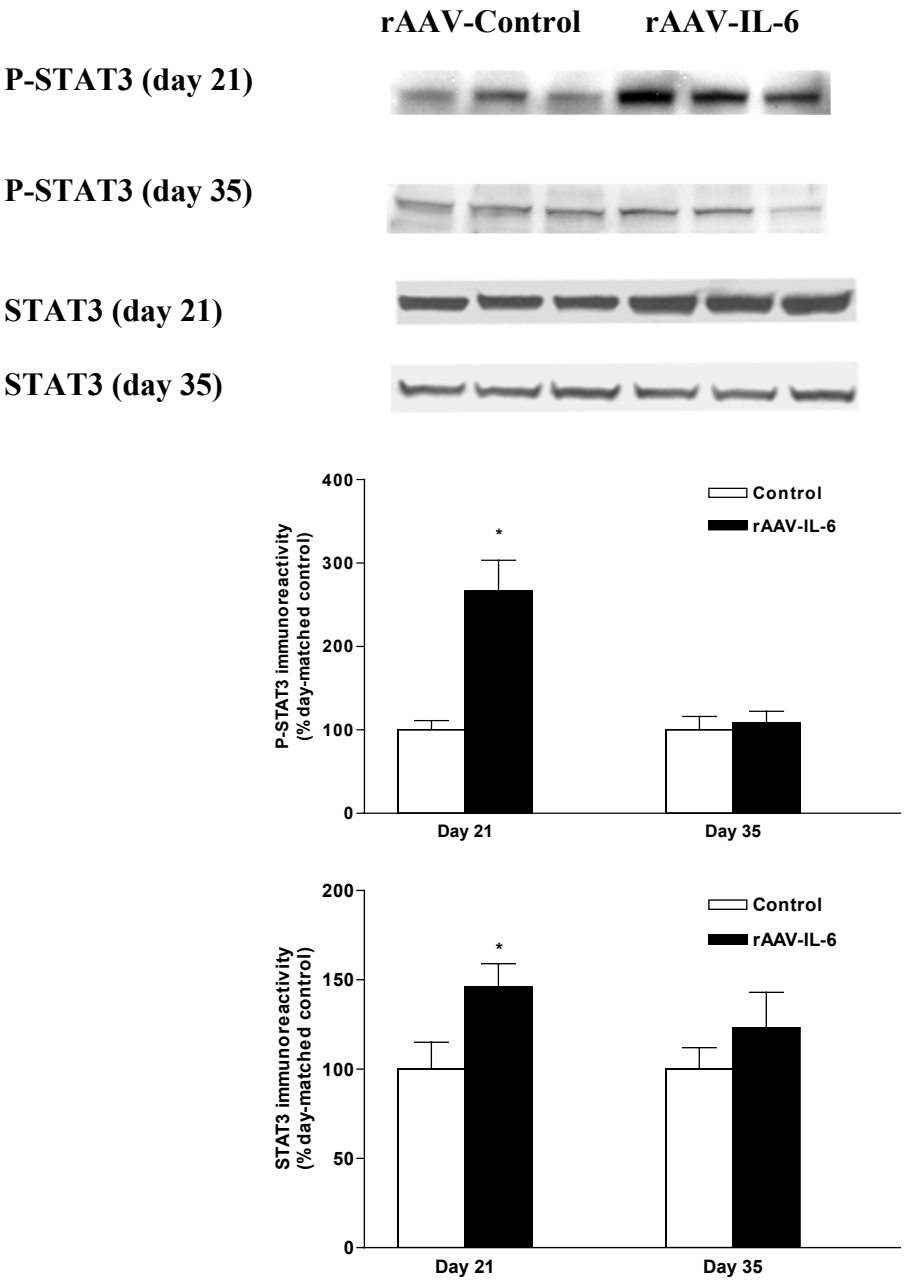

Fig. 5-6. STAT3 phosphorylation identified by P-STAT3 and total STAT3 immunoreactivity in the hypothalamus at 21 or 35 days post rAAV-Control or rAAV-IL-6 delivery. (Top) Western blots using antibodies specific to tyrosine 705 P-STAT3 or STAT3 (phosphorylated and unphosphorylated). Lanes represent the hypothalamus from rAAV-Control (lane 1-3) and rAAV-IL-6 treated (lanes 4-6) rats 21 or 35 days post viral delivery. (Bottom) Quantification of STAT3 and P-STAT3 based on densitometric scanning. Data represent the mean ± S.E.M. of 7 rats per group, with levels in day-matched control rats set to 100 and S.E.M. adjusted proportionally. * $p < 0.005$ (P-STAT3) and $p < 0.05$ (STAT3) vs. rAAV-Control at day 21 by t-test.

Discussion

Central IL-6 Gene Delivery and Weight Regulation

Using central rAAV-IL-6 gene delivery, we demonstrate in Chapter 5 that long-term IL-6 expression in the hypothalamus reduces body weight gain and visceral adiposity without affecting food intake in normal rats. Acute administration of IL-6 activates BAT thermogenesis in rats (Busbridge et al., 1989; Cannon et al., 1998), and in the present experiment, chronic central expression of IL-6 significantly enhances both UCP1 mRNA and UCP1 protein levels in BAT. UCP1 is a unique thermogenic protein in BAT that uncouples oxidative phosphorylation in mitochondria. It allows high rates of substrate oxidation and heat production without phosphorylation of adenosine 5'-diphosphate (Klingenberg and Huang, 1999). Elevated UCP1 protein levels in BAT are indicative of increased thermogenesis in BAT, suggesting that enhanced energy expenditure in BAT may account for the reduction in weight gain following central rAAV-IL-6 gene delivery. This effect of IL-6 is apparently different from the weight loss and fat depletion during cancer and other wasting disorders, which have been attributed to the direct inhibitory effect of IL-6 on lipoprotein lipase activity in adipose tissue (Greenberg et al., 1992; Strassmann et al., 1992). Because the IL-6 transgene was expressed locally in modest amount in hypothalamus, it is unlikely that significant amount of IL-6 protein reached the systemic circulation to produce any peripheral impact.

Our findings in Chapter 5 indicating that rAAV-IL-6 gene delivery did not affect food consumption are inconsistent with previous data indicating an anorexic effect of IL-6 (Johnson, 1998; Schobitz et al., 1995). However, in those studies, the anorexic effect of IL-6 was only apparent in animals and humans when relatively large doses of IL-6 were

employed. IL-6 exerts both beneficial and adverse effects in the CNS (Gruol and Nelson, 1997). To avoid the detrimental consequences of high levels of IL-6 expression in the CNS, we specifically chose a relatively low titer of rAAV-IL-6 to produce sustained yet modest central expression of IL-6 in normal adult rats. Therefore, it is possible that the levels of IL-6 produced by rAAV-IL-6 in hypothalamus were adequate to elicit the thermogenic response but insufficient to produce the anorexic response. Evidence from recent studies also suggests that alterations in food intake in rodents with experimental cancer were not directly related to systemic IL-6 but rather secondary to IL-6-dependent tumor growth (Cahlin et al., 2000). Instead of promoting anorexia in cancer diseases, the elevation of central IL-6 may be secondary to a decline in food intake (Wang et al., 2001). Collectively, these studies suggest that IL-6, when used at low doses, has an insignificant effect on food consumption.

Central IL-6 Gene Delivery and Thermogenesis in BAT

Thermogenesis in BAT is mainly mediated by norepinephrine activation of sympathetically innervated β_3ARs (Nedergaard et al., 2001). Presumably, IL-6 enhances thermogenesis in BAT by a similar mechanism. The present report confirms this supposition by the demonstration that surgical denervation of BAT prevents the IL-6 induced increase in UCP1 gene expression and protein levels. Denervation of BAT also blocked the weight-reducing effect of rAAV-IL-6. These data suggest that sympathetically mediated thermogenesis in BAT is essential for the rAAV-IL-6 mediated reduction in weight gain. It is unlikely that the failure of IL-6 to increase UCP1 in the denervated BAT was due to surgically induced damage, because our previous study

demonstrated that both innervated and denervated BAT pads responded equally to the CGP-12177 (a specific β_3AR agonist) induction of UCP1 (Scarpace and Matheny, 1998).

To our surprise, the unilaterally sympathetic denervation of BAT totally abolished the weight-reducing effect of rAAV-IL-6. In the present study, we delivered the rAAV vector into the right side of the anterior hypothalamus, and the transection of the peripheral nerves innervating interscapular BAT was ipsilateral to the hypothalamic injection. Because the direct projection from the paraventricular nucleus in the hypothalamus to the sympathetic preganglionic neurons in the spinal cord is principally ipsilateral, it is logical that ipsilateral denervation would preferentially block stimulation of the BAT on the right side. However, previous data from this laboratory demonstrated that the same method of viral administration of a rAAV vector encoding leptin activated both BAT pads in intact rats (Nedergaard et al., 2001; Wilsey et al., 2002). This suggests that viral-expressed protein diffused throughout the whole hypothalamus. The increases in UCP1 mRNA and protein levels in contralateral BAT pad in the present study also indicate that this is the case. Nevertheless, it is possible that the degree of the sympathetic activation was not identical in the two BAT pads. The left BAT pad, contralateral to the hypothalamic injection, might be less activated, therefore, the overall IL-6 mediated thermogenic responses in rats with ipsilateral denervation of BAT may be insufficient to elicit a significant effect on body weight. In the future, bilateral denervation of BAT may be more appropriate to address the question whether the reduction in body weight gain by IL-6 gene delivery is dependent on the sympathetic innervation of BAT.

IL-6 is an important modulator of neuroendocrine systems during infectious and traumatic stress and has stimulatory actions on the HPA axis (Gruol and Nelson, 1997).

However, in our experiment, rAAV-IL-6 treatment did not alter basal plasma corticosterone levels. This is consistent with a previous report indicating that basal plasma corticosterone and adrenocorticotrophic hormone (ACTH) were not elevated in IL-6 transgenic mice (Raber et al., 1997). Together with the results from the denervation experiment, these data further suggest that the reduction in weight gain by central IL-6 gene delivery was a specific consequence to IL-6 induced thermogenesis rather than a nonspecific stress response.

Central IL-6 Gene Delivery and IL-6 Signal Transduction

Biological activities of IL-6 are initiated by ligand binding to the IL-6 receptor complex. Subsequently, STAT3 is tyrosine-phosphorylated by JAK kinases that associate with the cytoplasmic portion of the receptor, and translocates to the nucleus and activates transcription (Baumann et al., 1996). In addition to activation of STAT3 protein, IL-6 also activates STAT1 and mitogen-activated protein kinase in neuronal cells (Schumann et al., 1999). Although IL-6 signal transduction has been extensively examined *in vitro* in a variety of cell types, *in vivo* information on this subject is rather limited. It is known that intracerebroventricular application of IL-6 induces nuclear STAT3 translocation in several areas of the hypothalamus (Hubschle et al., 2001). The present study demonstrates that, similar to leptin (Wang et al., 1997;Baumann et al., 1996), central IL-6 gene delivery activates the hypothalamic JAK/STAT3 signal transduction pathway. Moreover, the reversal of the elevated STAT3 phosphorylation between days 21 and 35 post IL-6 gene delivery suggests that hypothalamic IL-6 signal transduction is susceptible to desensitization following chronic central IL-6 stimulation. SOCS-3 is a putative negative regulator of JAK/STAT3 signaling (Starr et al., 1997). The signal molecule may inhibit the JAK-mediated phosphorylation of STAT3, and is usually up-regulated in

response to IL-6 receptor activation. The elevation of SOCS-3 following IL-6 gene delivery may mediate the desensitization of IL-6 signal transduction. However, in present study, when phosphorylation of STAT3 was attenuated, the SOCS-3 levels were still elevated. One possible explanation for this observation is that IL-6, along with many other ligands for the gp130 receptor family such as IL-11, oncostatin M, leukemia inhibitory factor, ciliary neurotrophic factor and leptin, share a common JAK/STAT signaling pathway that promotes phosphorylation of STAT3 (Bjorbaek et al., 1999; Heim, 1999) and perhaps induces SOCS-3. Thus, prolonged IL-6 treatment may change the levels of other gp130-type receptor ligands, such that the elevated SOCS-3 levels, and possibly the attenuation of phosphorylation of STAT3, are a summation of the combined effects from these ligands rather than solely from IL-6. The functional consequence of this desensitization was apparent between days 21 and 35 following central rAAV-IL-6 administration. During this period, body weight in the IL-6 treated rats began to converge with that of the controls, and there was no longer a statistical difference in body weight between control and IL-6 treated rats after day 30. Moreover, UCP1 mRNA levels were elevated at day 21, but returned to control levels by day 35. UCP1 protein levels remained elevated at both 21 and 35 days, but this was most likely the consequence of the unusually long half-life of UCP1 protein (Nedergaard et al., 2001). The parallel desensitization of the JAK/STAT3 signaling, UCP1 mRNA, and convergence of the body weight suggest that activation of the JAK/STAT3 pathway may mediate the rAAV-IL-6 induced thermogenesis in BAT and the subsequent reduction in weight gain.

In conclusion, this study in Chapter 5 demonstrates that chronic elevation of IL-6 in the CNS reduces body weight gain and visceral adiposity without affecting food intake.

The mechanism appears to involve sympathetic induction of UCP1 in BAT and presumably, enhanced thermogenesis in BAT. Unilateral denervation of BAT prevented both the induction of UCP1 and the reduction in body weight gain by rAAV-IL-6. Furthermore, chronic central IL-6 stimulation desensitized IL-6 signal transduction, characterized by attenuation of elevated STAT3 phosphorylation.

CHAPTER 6
GENERAL DISCUSSION

Obesity is a serious health problem in industrialized nations. Its prevalence has been steadily rising during recent years, and this trend is particularly pronounced in children and adolescents (Flegal et al., 2002; Ogden et al., 2002). High availability and consumption of high-energy food on the one hand and a sedentary lifestyle with decreased physical activity on the other hand are likely responsible for this phenomenon. Besides over-accumulation of body fat, obesity is associated with many diseases, such as type 2 diabetes, hypertension, cardiovascular diseases, stroke and certain cancers (Visscher and Seidell, 2001). Therefore, it is essential to control or reduce body weight to prevent or treat these obesity-related complications. Currently, there are few reliable medicines available in the market for the treatment of obesity. Moreover, the two recommended weight-reducing remedies, diet and physical exercise, are not very effective in reducing body weight in many obese patients. An improved understanding of the pathways regulating energy balances is therefore a prerequisite for the optimal use of the existing strategies dealing with obesity and for the design of new effective anti-obesity drugs.

Body weight is maintained through a fine balance between food intake and energy expenditure. Many adipose signal produced by fat cells are believed to serve as afferent signals to the CNS to indicate the body fat status and energy store. Leptin, a cytokine-like molecule, is one such factor that is mainly synthesized by and released from WAT (Friedman and Halaas, 1998; Jequier, 2002). Its production occurs in proportion to

adipose cell size and number. It is released into the blood and reaches its receptors in the brain via facilitated passage across the blood-brain barrier. In the arcuate nucleus of the hypothalamus leptin binds to its long-form cytokine type 1 receptors and initiates the JAK-STAT3 signal transduction (Bates et al., 2003) and possibly the IRS-PI3K pathway (Niswender et al., 2001; Zhao et al., 2002). Central leptin action results in a reduction in food intake and an increase in energy expenditure, involving various mechanisms such as activation of the central MC system and suppression of the NPY system (Friedman and Halaas, 1998; Jequier, 2002). Although leptin is highly effective in reducing body weight and fat mass in lean, young rodents, its effects has been very disappointing in obese humans and animals (Heymsfield et al., 1999; Considine et al., 1996; Scarpace et al., 2000b). In fact, the plasma leptin levels are already greatly elevated in obese humans and animals. A very high dose of exogenous leptin that increased circulating leptin 20-fold above basal levels only resulted in mild and highly variable responses in obese patients (Heymsfield et al., 1999). These observations are consistent with the notion of leptin resistance. The development of leptin resistance in obese patients could be due to the prolonged exposure to increased plasma leptin concentrations. The causes of the leptin resistance are still unclear. Limited access of leptin to its hypothalamic sites of action (Van Heek et al., 1997; Scarpace et al., 2000b) and an impaired intracellular signal transduction in leptin responsive hypothalamic neurons (El Haschimi et al., 2000; Scarpace et al., 2000c; Scarpace et al., 2001) are several of the possible explanations.

Central melanocortin system, as represented by the natural agonist α-MSH, the natural antagonist AgRP, and MC3R and MC4R, has been shown to play a critical role in energy homeostasis. Central infusion of α-MSH or its synthetic agonists causes anorexia

and weight loss (Poggioli et al., 1986; Fan et al., 1997; Grill et al., 1998), whereas infusion of MCR blockers or over-production of AgRP, the endogenous MCR antagonist/inverse agonist produces hyperphagia and obesity (Fan et al., 1997; Graham et al., 1997; Ollmann et al., 1997; Hagan et al., 1999). Knockout studies of the central MC3R and MC4R have identified these receptors as important players in energy homeostasis (Chen et al., 2000; Huszar et al., 1997). On one hand, targeted disruption of the MC4R gene leads to overfeeding and obesity (Huszar et al., 1997), on the other, MC3R knockouts over-accumulate fat with minimal changes in caloric intake (Chen et al., 2000). Deficiency in POMC also results in increased food intake and morbid obesity in both rodents and humans (Yaswen et al., 1999; Krude et al., 1998). Therefore, disruption of any component of the MC system gives rise to obesity. This is in sharp contrast to many other pathways that are also involved in the regulation of body weight. For example, NPY is an important mediator of leptin's action on reducing feeding and increasing energy expenditure. However, neither NPY nor its receptor knockouts result in hypophagia or other expected abnormal phenotypes (Marsh et al., 1998; Palmiter et al., 1998; Pedrazzini et al., 1998). Growing body of evidence suggests that the melanocortin system is located downstream of the hypothalamic leptin signaling pathway and is required to mediate the central effects of leptin. When co-administered with a MC 3/4-receptor antagonist, leptin fails to decrease food intake (Seeley et al., 1997). Moreover, the leptin-mediated induction of UCP1, an important thermogenic protein in the BAT, is also attenuated with the central MC receptor antagonism (Satoh et al., 1998).

IL-6 is a multifunctional, proinflammatory cytokine that acts on a wide range of tissues to modulate cell growth and differentiation. One third of the total circulating IL-6

has been estimated to originate from WAT (Mohamed-Ali et al., 1997). Interestingly, similar to leptin, the systemic concentration of IL-6 is also positively correlated with body fat mass (Vgontzas et al., 1997). Both IL-6 and leptin receptors share close structural analogy in the signal transduction domains, and both have been found in hypothalamic areas involved in energy regulation (Tartaglia et al., 1995; Schobitz et al., 1992). Recent studies demonstrated that IL-6 and leptin activate overlapping signal transduction pathways, notably the JAK-STAT3 pathway (Baumann et al., 1996).

In light of these lines of evidence, we put forward two hypotheses. First, the direct activation of the central melanocortin system can circumvent leptin resistance and reduce body weight and adiposity in the leptin-resistant animals. The second hypothesis is that IL-6, similar to leptin, can also modulate body weight in normal animals. The goals of this dissertation were, (1) to test the effects of chronic activation of the central MC system by a potent MC3/4-receptor agonist MTII in a diet-induced obese rat model with normal genetic background, (2) to test the effects of long-term activation of central MC system by rAAV-mediated POMC gene therapy in the genetically obese Zucker (fa/fa) rats with defective leptin receptors, (3) to test the effects of long-term overexpression of IL-6 in the hypothalamus by rAAV-based gene delivery in the normal rats.

The data in Chapter 3 demonstrate that despite apparent leptin resistance in the HF diet-induced obese female Sprague-Dawley rats, MTII retains a similar efficacy in reducing food intake and increasing energy expenditure. Moreover, the initial responses to MTII are enhanced in obese rats. Rats on ten-week HF feeding gained almost two-fold more weight than CH animals. Serum leptin levels were also increased by 113% compared with CH rats. Six-day central infusion of leptin at a dose (10 μg/day) that has

been previously determined to induce maximum inhibitory effect on feeding resulted in a sustained suppression in food intake in CH rats but only a brief anorexic response in DIO rats. The 6-day cumulative caloric intake markedly decreased in leptin-treated CH rats but not in DIO animals. In these leptin-resistant DIO animals, six-day central infusion of MTII reduced body weight and visceral adiposity compared with *ad libitum*-fed control and pair-fed groups. MTII also markedly suppressed caloric intake both in CH and DIO rats. The anorexic response was enhanced at day 2 in DIO (84% reduction in caloric intake) compared to 62% in CH rats. MTII induced a sustained increase in oxygen consumption in DIO rats at day 2 and 6 but only a delayed response in CH animals (at day 6). In both diet groups, MTII reduced serum insulin and cholesterol compared with controls. HF feeding increased BAT UCP1 by over twofold, and UCP1 levels were further elevated in MTII-treated CH and DIO rats. MTII lowered ACC expression and prevented the reduction in M-CPT I mRNA by pair-feeding in muscle of DIO rats. Compared to CH controls, hypothalamic MC3 and MC4 receptor expression levels were reduced in DIO controls. These studies in Chapter 3 demonstrate that the anorexic and thermogenic responses to MTII are at least similar, if not enhanced, in DIO relative to CH despite reduced central MC3/4 receptor expression. The HF-induced upregulation of UCP1 in BAT may contribute to the immediate increase in MTII-stimulated thermogenesis in DIO rats. MTII may also increase fat catabolism in muscle of DIO rats and improve glucose and cholesterol metabolism in both groups. Both the hypophagia and increased energy expenditure are the likely mechanisms underlying these improvements.

Data from Chapter 3 show that MC agonists are promising agents for reducing body weight and fat mass in leptin resistant obese animals, thus, in Chapter 4 we examined the hypothesis that chronic activation of the central MC system by rAAV-based gene delivery of POMC, the precursor of melanocortins, can also bypass the defective leptin signaling and normalize energy imbalance in obese Zucker rats. Genetically obese fa/fa Zucker rats with a recessive mutation of the leptin receptor gene develop severe, early-onset obesity associated with hyperphagia, hyperleptinemia, and hyperinsulinemia (Bray, 1977; Iida et al., 1996). Using this leptin and insulin resistant rodent model, we have demonstrated that overproduction of POMC in the hypothalamus reduces body mass and adiposity and improves glucose metabolism in these obese Zucker rats. The rAAV encoding POMC or a control vector was delivered bilaterally into basal hypothalamus with coordinates targeting the arcuate nucleus in these obese Zucker rats. Thirty-eight days following POMC gene delivery, hypothalamic POMC expression levels increased by four-fold and melanocortin signaling (indicated by phosphorylation of CREB) increased by 62% with respect to controls. There was a sustained reduction in food intake, a moderated but significant attenuation of weight gain and a 24% decrease in visceral adiposity in rAAV-POMC rats. POMC gene delivery enhanced UCP1 in BAT by over 4-fold. Fasting serum leptin, insulin, and cholesterol levels were also significantly reduced by rAAV-POMC treatment. The experiments in Chapter 4 have demonstrated targeted POMC gene delivery in the hypothalamus suppresses food intake and weight gain and reduces visceral adiposity and hyperinsulinemia in leptin resistant obese Zucker rats. The mechanisms, consistent with the conclusion drawn from Chapter 3, may involve the sustained hypophagia and the augmentation of thermogenesis in BAT.

Together the data from Chapter 3 and 4 support the first hypothesis of this dissertation, that is, activation of the central melanocortin system by either MC agonists or gene delivery of POMC gene can circumvent leptin resistance and reduce body and visceral adiposity in leptin-resistant obese animals. These findings are in agreement with several earlier reports in that obese Zucker rats and DIO rodents robustly respond to α-MSH or MTII treatment (Cettour-Rose and Rohner-Jeanrenaud, 2002a; Hwa et al., 2001; Pierroz et al., 2002). In addition, our studies provide several interesting findings. First, despite reductions in hypothalamic MC3R and MC4R expression levels in DIO rats, the animals responded to MTII administration with similar efficacy as that of CH rats. Furthermore, the initial anorectic response and whole body oxygen consumption were modestly but significantly enhanced in DIO rats. Although we did not measure the hypothalamic MC3R and MC4R protein densities, a previous study noted that MC4R densities in specific hypothalamic regions involved in energy regulation were actually diminished in DIO rats with normal genetic background (Harrold et al., 1999a). Therefore, these data together suggest there are down-regulations of both the central MC receptor expression and protein levels in DIO animals. Interestingly, protein levels of the endogenous MC3/4R antagonist AgRP were shown to be elevated in DIO animals (Harrold et al., 1999b), indicating increased antagonism associated with obesity. Thus, the increased initial anorexic response to MTII in DIO rats may be due to up-regulation of components or activity of the post-receptor signaling cascade such as cAMP, protein kinase A, or phosphorylation of the transcription factor cAMP response element binding protein.

Second, in Chapter 4 we revealed a sustained anorexic response to rAAV-POMC in the obese Zucker rats throughout the entire 38-day experimental period. This is in sharp contrast to all previous reports in which there was a rapid attenuation of the anorexic response following pharmacological injections or infusions of melanocortins in both normal and DIO rats, and mice (McMinn et al., 2000; Pierroz et al., 2002). The suppression in food intake lasted no longer than four days in any of these studies. The studies in Chapter 3 also show that the potent MC3/4R agonist MTII produced an impressive inhibition of food intake at an earlier stage of central administration but its anorexic effect gradually attenuated with time in DIO rats. At the end of the 6-day experiment, the difference in caloric intake was relatively small although still significant between MTII-treated and control rats. In the case of obese Zucker rats, one study noted a three-day anorexic response to chronic pharmacological administration of MTII (Cettour-Rose and Rohner-Jeanrenaud, 2002). Therefore, the sustained anorexic response we observed over 38 days may be unique to central POMC gene delivery. With this procedure, the presumed overproduction of α-MSH is derived from POMC with assistance from a variety of endogenous enzymes such as prehormone convertases, carboxypeptidase E and peptidyl α-amidating mono-oxygenase (Pritchard et al., 2002). This endogenously regulated production of α-MSH may help prevent the rapid desensitization witnessed in previous pharmacological studies. Additionally, obese Zucker rats, in comparison to their lean counterparts, are associated with reduced POMC expression in the arcuate nucleus, lower amount of α-MSH peptide in the paraventricular nucleus, and higher MC4 receptor densities in several hypothalamic regions pivotal to energy regulation (Kim et al., 2000; Harrold et al., 1999a). These factors may also

contribute to the prolonged responsiveness to POMC gene delivery in obese Zucker rats. In summary, these data hint that POMC gene therapy may have some advantage over traditional pharmacological treatment for the long-term maintenance of body weight. However, more studies are warranted to validate the effectiveness of POMC gene therapy in genetically sound rodents. We believe that application of rAAV-POMC vector in DIO animals may be the first and a logic choice based on the results from Chapter 3.

Third, the data from Chapter 3 and 4 also suggest that an increase in energy expenditure contributes to the loss of body weight and visceral adiposity following both MTII administration and POMC gene therapy in respective DIO and obese Zucker rats. Central MTII infusion markedly reduced body weight and visceral adiposity in obese DIO rats compared to their respective either *ad libitum*-fed or pair-fed animals, which is suggestive of a food intake-independent component in the fat-trimming effect of MTII. The elevation of oxygen consumption in CH and DIO rats during central MTII infusion further argues that an increase in energy expenditure initiated by central MC activation is involved in the regulation of energy balance. It is well known that nonshivering thermogenesis in BAT represents an essential element in adaptive energy expenditure in rodents, and UCP1 protein level is an important indicator of the thermogenic status of BAT (Nedergaard et al., 2001). Animals treated with MTII had elevated levels of BAT UCP1 expression compared with pair-fed controls (Cettour-Rose and Rohner-Jeanrenaud, 2002). Similarly, MTII greatly enhanced UCP1 protein levels in BAT in our study. This marked increase in UCP1 may well be the mediator for the elevated thermogenesis following MTII treatment. The long-term HF feeding (ten weeks) also increased basal BAT UCP1 protein levels by more than 2-fold. This up-regulation of basal UCP1 in BAT

may be the underlying mechanism for the immediate increase in the MTII-induced energy expenditure (at day 2) in DIO rats. Obese Zucker rats have impaired BAT thermogenesis because of the genetically defective leptin receptors (Levin et al., 1984). Despite this inherent problem, the data in Chapter 4 revealed a 4-fold increase in BAT UCP1 at 38 days after POMC vector delivery in the obese Zucker rats, indicating markedly stimulated BAT thermogenesis. Although lacking direct measurement of whole body energy expenditure, we speculate based on our observation and the results from Chapter 3 that, in addition to the hypophagia, an increase in energy expenditure plays a part in mediating the fat and weight-trimming effects of central POMC gene therapy.

Fourth, activation of central MC system by either MTII or POMC gene therapy appears to improve glucose and cholesterol metabolism and insulin sensitivity. Central MC receptor activation has been demonstrated to reduce insulin release from pancreas and enhance glucose metabolism (Fan et al., 1997; Obici et al., 2001). However, the results in obese animal models are controversial: one study suggested that peripheral but not central MTII improved insulin resistance in DIO mice (Pierroz et al., 2002), whereas another reported that 3-day peripheral MTII administration had no effect on serum insulin in obese Zucker rats (Cettour-Rose and Rohner-Jeanrenaud, 2002). The experiments in Chapter 3 show central MTII infusion resulted in a significant reduction in serum insulin levels in both CH and DIO rats. The results of pair-feeding groups in these studies indicates the improvement of glucose metabolism in CH and DIO animals may be largely attributed to hypophagia induced by central MTII administration, whereas the potency of MTII against serum insulin may rely on an additional food-independent mechanism, such as inhibition of insulin release from pancreas by direct central melanocortin receptor

activation (Fan et al., 1997; Obici et al., 2001). In Chapter 4, central POMC gene therapy decreased fasting serum insulin, and it also generated a downward trend in serum glucose levels. These data indicate improved glucose metabolism and insulin sensitivity by POMC gene delivery. However, without a pair-fed group to control for the effect of food intake, we are not certain if the improvement in glucose metabolism is directly related to the increased central POMC expression or a consequence of the decreased food consumption and body weight. In addition to modulating glucose metabolism, activation of central MC system by MTII and POMC gene delivery also reduced total serum cholesterol levels in leptin resistant DIO an obese Zucker rats. How MTII lowers cholesterol is currently unknown. It is conceivable that insulin-mediated stimulation of cholesterol synthesis diminishes following a fall in circulating insulin levels (Horton et al., 2002).

Using a rAAV vector expressing murine IL-6 (rAAV-IL-6), we also examined the chronic effects of centrally expressed IL-6 on food intake, body weight and adiposity in male Sprague-Dawley rats, and investigated the underlying mechanisms. The results are shown in Chapter 5. Five weeks after viral delivery, coronary hypothalamic slices were examined by fluoroscopy, and GFP-positive cells displayed typical neuron-like morphology and were distributed around the tract of the injection needle. Furthermore, murine IL-6 mRNA was identified in all rAAV-IL-6-treated rats at 21 and 35 days following viral delivery with similar expression levels but not in any of the rAAV-control-administered rats. Direct delivery of rAAV-IL-6 into rat hypothalamus suppressed weight gain and visceral adiposity without affecting food intake over a 35-day period. rAAV-IL-6 enhanced UCP1 protein levels in interscapular BAT. To investigate if

the induction of UCP1 and the reduction in body weight is dependent on sympathetic innervation of BAT, we administered rAAV-IL-6 or a control vector into the hypothalamus of rats in which the interscapular BAT was unilaterally denervated. Over 21 days, there was no difference in food consumption or body weight between rAAV-IL-6 and control vector treated rats. rAAV-IL-6 delivery increased UCP1 mRNA and protein levels in innervated BAT pads but not denervated BAT pads. Hypothalamic IL-6 signal transduction, indicated by P-STAT3 levels, was elevated by 2.6-fold at day 21, but returned to control levels by day 35. However, the levels of SOCS-3 mRNA, the inhibitory molecule involved in dampening the IL-6 signaling (Starr et al., 1997), was significantly elevated both at day 21 and day 35. These data in Chapter 5 demonstrate that chronic elevation of IL-6 in the CNS reduces body weight gain and visceral adiposity without affecting food intake. The mechanism involves sympathetic induction of UCP1 in BAT and presumably, enhanced thermogenesis in BAT. Furthermore, chronic central IL-6 stimulation desensitizes IL-6 signal transduction characterized by reversal of elevated P-STAT3 levels.

In summary, both MTII administration and POMC gene therapy activated central MC system and reduced body weight, visceral adiposity and improved glucose and cholesterol metabolism in leptin-resistant DIO and obese Zucker rats, respectively. Both hypophagia and increased energy expenditure are the likely underlying mechanisms. Compared with traditional pharmacological intervention, the rAAV-based POMC gene therapy appears to have a prolonged inhibitory effect on appetite and avoids the rapid desensitization witnessed with α-MSH or MTII treatment. Therefore, POMC gene therapy may be valuable for treatment of morbid obesity and long-term maintenance of

body weight. However, more thorough studies in rodents, in large animals such as non-human primates are needed before it can be fathomed in treating human obesity. In addition, using rAAV-IL-6, we also demonstrate IL-6 has a potential role in energy regulation, which involves sympathetic induction of UCP1 in BAT, and presumably, enhanced energy expenditure in BAT.

LIST OF REFERENCES

Ahima RS, Flier JS (2000) Leptin. Annu Rev Physiol 62: 413-437.

Allen YS, Adrian TE, Allen JM, Tatemoto K, Crow TJ, Bloom SR, Polak JM (1983) Neuropeptide Y distribution in the rat brain. Science 221: 877-879.

Athanasopoulos T, Fabb S, Dickson G (2000) Gene therapy vectors based on adeno-associated virus: characteristics and applications to acquired and inherited diseases (review). Int J Mol Med 6: 363-375.

Barzilai N, Banerjee S, Hawkins M, Chen W, Rossetti L (1998) Caloric restriction reverses hepatic insulin resistance in aging rats by decreasing visceral fat. J Clin Invest 101: 1353-1361.

Baskin DG, Hahn TM, Schwartz MW (1999) Leptin sensitive neurons in the hypothalamus. Horm Metab Res 31: 345-350.

Bates SH, Stearns WH, Dundon TA, Schubert M, Tso AW, Wang Y, Banks AS, Lavery HJ, Haq AK, Maratos-Flier E, Neel BG, Schwartz MW, Myers MG, Jr. (2003) STAT3 signalling is required for leptin regulation of energy balance but not reproduction. Nature 421: 856-859.

Baumann H, Morella KK, White DW, Dembski M, Bailon PS, Kim H, Lai CF, Tartaglia LA (1996) The full-length leptin receptor has signaling capabilities of interleukin 6-type cytokine receptors. Proc Natl Acad Sci USA 93: 8374-8378.

Bergen HT, Mizuno TM, Taylor J, Mobbs CV (1998) Hyperphagia and weight gain after gold-thioglucose: relation to hypothalamic neuropeptide Y and proopiomelanocortin. Endocrinology 139: 4483-4488.

Bjorbaek C, El Haschimi K, Frantz JD, Flier JS (1999) The role of SOCS-3 in leptin signaling and leptin resistance. J Biol Chem 274: 30059-30065.

Boss O, Hagen T, Lowell BB (2000) Uncoupling proteins 2 and 3: potential regulators of mitochondrial energy metabolism. Diabetes 49: 143-156.

Bray GA (1977) The Zucker-fatty rat: a review. Fed Proc 36: 148-153.

Burguera B, Couce ME, Curran GL, Jensen MD, Lloyd RV, Cleary MP, Poduslo JF (2000) Obesity is associated with a decreased leptin transport across the blood-brain barrier in rats. Diabetes 49: 1219-1223.

Busbridge, N. J., Dascombe, M. J., Hopkins, S., and Rothwell, N. J. (1989) Acute central effects of interleukin-6 on body temperature, thermogenesis and food intake in the rat. Proc Nutr Soc 48: 48A.

Butler AA, Kesterson RA, Khong K, Cullen MJ, Pelleymounter MA, Dekoning J, Baetscher M, Cone RD (2000) A unique metabolic syndrome causes obesity in the melanocortin-3 receptor-deficient mouse. Endocrinology 141: 3518-3521.

Cadenas S, Buckingham JA, Samec S, Seydoux J, Din N, Dulloo AG, Brand MD (1999) UCP2 and UCP3 rise in starved rat skeletal muscle but mitochondrial proton conductance is unchanged. FEBS Lett 462: 257-260.

Cahlin C, Korner A, Axelsson H, Wang W, Lundholm K, Svanberg E (2000) Experimental cancer cachexia: the role of host-derived cytokines interleukin (IL)-6, IL-12, interferon-gamma, and tumor necrosis factor alpha evaluated in gene knockout, tumor-bearing mice on C57 Bl background and eicosanoid-dependent cachexia. Cancer Res 60: 5488-5493.

Cannon B, Houstek J, Nedergaard J (1998) Brown adipose tissue. More than an effector of thermogenesis? Ann NY Acad Sci 856: 171-187.

Cettour-Rose P, Rohner-Jeanrenaud F (2002) The leptin-like effects of 3-d peripheral administration of a melanocortin agonist are more marked in genetically obese Zucker (fa/fa) than in lean rats. Endocrinology 143: 2277-2283.

Chen AS, Marsh DJ, Trumbauer ME, Frazier EG, Guan XM, Yu H, Rosenblum CI, Vongs A, Feng Y, Cao L, Metzger JM, Strack AM, Camacho RE, Mellin TN, Nunes CN, Min W, Fisher J, Gopal-Truter S, MacIntyre DE, Chen HY, Van der Ploeg LH (2000) Inactivation of the mouse melanocortin-3 receptor results in increased fat mass and reduced lean body mass. Nat Genet 26: 97-102.

Cheung CC, Clifton DK, Steiner RA (1997) Proopiomelanocortin neurons are direct targets for leptin in the hypothalamus. Endocrinology 138: 4489-4492.

Chomczynski P, Sacchi N (1987) Single-step method of RNA isolation by acid guanidinium thiocyanate- phenol-chloroform extraction. Anal Biochem 162: 156-159.

Clegg DJ, Riedy CA, Smith KA, Benoit SC, Woods SC (2003) Differential sensitivity to central leptin and insulin in male and female rats. Diabetes 52: 682-687.

Cone RD (1999) The Central melanocortin system and energy homeostasis. Trends Endocrinol Metab 10: 211-216.

Considine RV, Sinha MK, Heiman ML, Kriauciunas A, Stephens TW, Nyce MR, Ohannesian JP, Marco CC, McKee LJ, Bauer TL, . (1996) Serum immunoreactive-leptin concentrations in normal-weight and obese humans. N Engl J Med 334: 292-295.

Cowley MA, Pronchuk N, Fan W, Dinulescu DM, Colmers WF, Cone RD (1999) Integration of NPY, AGRP, and melanocortin signals in the hypothalamic paraventricular nucleus: evidence of a cellular basis for the adipostat. Neuron 24: 155-163.

Daly TM, Ohlemiller KK, Roberts MS, Vogler CA, Sands MS (2001) Prevention of systemic clinical disease in MPS VII mice following AAV- mediated neonatal gene transfer. Gene Ther 8: 1291-1298.

Devos R, Guisez Y, Van der HJ, White DW, Kalai M, Fountoulakis M, Plaetinck G (1997) Ligand-independent dimerization of the extracellular domain of the leptin receptor and determination of the stoichiometry of leptin binding. J Biol Chem 272: 18304-18310.

Dirks W, Wirth M, Hauser H (1993) Dicistronic transcription units for gene expression in mammalian cells. Gene 128: 247-249.

Dulloo AG, Stock MJ, Solinas G, Boss O, Montani JP, Seydoux J (2002) Leptin directly stimulates thermogenesis in skeletal muscle. FEBS Lett 515: 109-113.

El Haschimi K, Pierroz DD, Hileman SM, Bjorbaek C, Flier JS (2000) Two defects contribute to hypothalamic leptin resistance in mice with diet-induced obesity. J Clin Invest 105: 1827-1832.

Elias CF, Kelly JF, Lee CE, Ahima RS, Drucker DJ, Saper CB, Elmquist JK (2000) Chemical characterization of leptin-activated neurons in the rat brain. J Comp Neurol 423: 261-281.

Fan W, Boston BA, Kesterson RA, Hruby VJ, Cone RD (1997a) Role of melanocortinergic neurons in feeding and the agouti obesity syndrome. Nature 385: 165-168.

Farooqi IS, Yeo GS, Keogh JM, Aminian S, Jebb SA, Butler G, Cheetham T, O'Rahilly S (2000) Dominant and recessive inheritance of morbid obesity associated with melanocortin 4 receptor deficiency. J Clin Invest 106: 271-279.

Flegal KM, Carroll MD, Ogden CL, Johnson CL (2002) Prevalence and trends in obesity among US adults, 1999-2000. JAMA 288: 1723-1727.

Frederich RC, Hamann A, Anderson S, Lollmann B, Lowell BB, Flier JS (1995) Leptin levels reflect body lipid content in mice: evidence for diet- induced resistance to leptin action. Nat Med 1: 1311-1314.

Friedman JM, Halaas JL (1998) Leptin and the regulation of body weight in mammals. Nature 395: 763-770.

Fruhbeck G, Gomez-Ambrosi J, Muruzabal FJ, Burrell MA (2001) The adipocyte: a model for integration of endocrine and metabolic signaling in energy metabolism regulation. Am J Physiol Endocrinol Metab 280: E827-E847.

Gasteyger C, Tremblay A (2002) Metabolic impact of body fat distribution. J Endocrinol Invest 25: 876-883.

Good DJ, Porter FD, Mahon KA, Parlow AF, Westphal H, Kirsch IR (1997) Hypogonadism and obesity in mice with a targeted deletion of the Nhlh2 gene. Nat Genet 15: 397-401.

Graham M, Shutter JR, Sarmiento U, Sarosi I, Stark KL (1997) Overexpression of Agrt leads to obesity in transgenic mice. Nat Genet 17: 273-274.

Greenberg AS, Nordan RP, McIntosh J, Calvo JC, Scow RO, Jablons D (1992) Interleukin 6 reduces lipoprotein lipase activity in adipose tissue of mice in vivo and in 3T3-L1 adipocytes: a possible role for interleukin 6 in cancer cachexia. Cancer Res 52: 4113-4116.

Grill HJ, Ginsberg AB, Seeley RJ, Kaplan JM (1998) Brainstem application of melanocortin receptor ligands produces long- lasting effects on feeding and body weight. J Neurosci 18: 10128-10135.

Grimm D, Kern A, Rittner K, Kleinschmidt JA (1998) Novel tools for production and purification of recombinant adenoassociated virus vectors. Hum Gene Ther 9: 2745-2760.

Gruol DL, Nelson TE (1997) Physiological and pathological roles of interleukin-6 in the central nervous system. Mol Neurobiol 15: 307-339.

Guan XM, Yu H, Van der Ploeg LH (1998) Evidence of altered hypothalamic pro-opiomelanocortin/ neuropeptide Y mRNA expression in tubby mice. Brain Res Mol Brain Res 59: 273-279.

Hagan MM, Rushing PA, Schwartz MW, Yagaloff KA, Burn P, Woods SC, Seeley RJ (1999) Role of the CNS melanocortin system in the response to overfeeding. J Neurosci 19: 2362-2367.

Hahn TM, Breininger JF, Baskin DG, Schwartz MW (1998) Coexpression of Agrp and NPY in fasting-activated hypothalamic neurons. Nat Neurosci 1: 271-272.

Halaas JL, Boozer C, Blair-West J, Fidahusein N, Denton DA, Friedman JM (1997) Physiological response to long-term peripheral and central leptin infusion in lean and obese mice. Proc Natl Acad Sci U S A 94: 8878-8883.

Hansen MJ, Ball MJ, Morris MJ (2001) Enhanced inhibitory feeding response to alpha-melanocyte stimulating hormone in the diet-induced obese rat. Brain Res 892: 130-137.

Harrold JA, Widdowson PS, Williams G (1999a) Altered energy balance causes selective changes in melanocortin-4(MC4- R), but not melanocortin-3 (MC3-R), receptors in specific hypothalamic regions: further evidence that activation of MC4-R is a physiological inhibitor of feeding. Diabetes 48: 267-271.

Harrold JA, Williams G, Widdowson PS (1999b) Changes in hypothalamic agouti-related protein (AGRP), but not alpha- MSH or pro-opiomelanocortin concentrations in dietary-obese and food- restricted rats. Biochem Biophys Res Commun 258: 574-577.

Heim MH (1999) The Jak-STAT pathway: cytokine signalling from the receptor to the nucleus. J Recept Signal Transduct Res 19: 75-120.

Hesselink MK, Greenhaff PL, Constantin-Teodosiu D, Hultman E, Saris WH, Nieuwlaat R, Schaart G, Kornips E, Schrauwen P (2003) Increased uncoupling protein 3 content does not affect mitochondrial function in human skeletal muscle in vivo. J Clin Invest 11: 479-486.

Heymsfield SB, Greenberg AS, Fujioka K, Dixon RM, Kushner R, Hunt T, Lubina JA, Patane J, Self B, Hunt P, McCamish M (1999) Recombinant leptin for weight loss in obese and lean adults: a randomized, controlled, dose-escalation trial. JAMA 282: 1568-1575.

Hibi M, Nakajima K, Hirano T (1996) IL-6 cytokine family and signal transduction: a model of the cytokine system. J Mol Med 74: 1-12.

Himms-Hagen J (1983) Brown adipose tissue thermogenesis in obese animals. Nutr Rev 41: 261-267.

Horton JD, Goldstein JL, Brown MS (2002a) SREBPs: activators of the complete program of cholesterol and fatty acid synthesis in the liver. J Clin Invest 109: 1125-1131.

Hu Y, Bloomquist BT, Cornfield LJ, DeCarr LB, Flores-Riveros JR, Friedman L, Jiang P, Lewis-Higgins L, Sadlowski Y, Schaefer J, Velazquez N, McCaleb ML (1996) Identification of a novel hypothalamic neuropeptide Y receptor associated with feeding behavior. J Biol Chem 271: 26315-26319.

Hubschle T, Thom E, Watson A, Roth J, Klaus S, Meyerhof W (2001) Leptin-induced nuclear translocation of STAT3 immunoreactivity in hypothalamic nuclei involved in body weight regulation. J Neurosci 21: 2413-2424.

Huszar D, Lynch CA, Fairchild-Huntress V, Dunmore JH, Fang Q, Berkemeier LR, Gu W, Kesterson RA, Boston BA, Cone RD, Smith FJ, Campfield LA, Burn P, Lee F (1997) Targeted disruption of the melanocortin-4 receptor results in obesity in mice. Cell 88: 131-141.

Hwa JJ, Ghibaudi L, Gao J, Parker EM (2001) Central melanocortin system modulates energy intake and expenditure of obese and lean Zucker rats. Am J Physiol Regul Integr Comp Physiol 281: R444-R451.

Iida M, Murakami T, Ishida K, Mizuno A, Kuwajima M, Shima K (1996) Substitution at codon 269 (glutamine --> proline) of the leptin receptor (OB-R) cDNA is the only mutation found in the Zucker fatty (fa/fa) rat. Biochem Biophys Res Commun 224: 597-604.

Iossa S, Lionetti L, Mollica MP, Crescenzo R, Botta M, Samec S, Dulloo AG, Liverini G (2001) Differences in proton leak kinetics, but not in UCP3 protein content, in subsarcolemmal and intermyofibrillar skeletal muscle mitochondria from fed and fasted rats. FEBS Lett 505: 53-56.

Jequier E (2002) Leptin signaling, adiposity, and energy balance. Ann N Y Acad Sci 967: 379-388.

Jeukendrup AE (2002) Regulation of fat metabolism in skeletal muscle. Ann N Y Acad Sci 967: 217-235.

Johnson RW (1998) Immune and endocrine regulation of food intake in sick animals. Domest Anim Endocrinol 15: 309-319.

Kaplitt MG, Leone P, Samulski RJ, Xiao X, Pfaff DW, O'Malley KL, During MJ (1994) Long-term gene expression and phenotypic correction using adeno-associated virus vectors in the mammalian brain. Nat Genet 8: 148-154.

Kim EM, O'Hare E, Grace MK, Welch CC, Billington CJ, Levine AS (2000) ARC POMC mRNA and PVN alpha-MSH are lower in obese relative to lean zucker rats. Brain Res 862: 11-16.

Kishimoto T, Akira S, Taga T (1992) Interleukin-6 and its receptor: a paradigm for cytokines. Science 258: 593-597.

Klein RL, Meyer EM, Peel AL, Zolotukhin S, Meyers C, Muzyczka N, King MA (1998) Neuron-specific transduction in the rat septohippocampal or nigrostriatal pathway by recombinant adeno-associated virus vectors. Exp Neurol 150: 183-194.

Klingenberg M, Huang SG (1999) Structure and function of the uncoupling protein from brown adipose tissue. Biochim Biophys Acta 1415: 271-296.

Kozak LP, Britton JH, Kozak UC, Wells JM (1988) The mitochondrial uncoupling protein gene. Correlation of exon structure to transmembrane domains. J Biol Chem 263: 12274-12277.

Krude H, Biebermann H, Luck W, Horn R, Brabant G, Gruters A (1998) Severe early-onset obesity, adrenal insufficiency and red hair pigmentation caused by POMC mutations in humans. Nat Genet 19: 155-157.

Krysiak R, Obuchowicz E, Herman ZS (1999) Interactions between the neuropeptide Y system and the hypothalamic- pituitary-adrenal axis. Eur J Endocrinol 140: 130-136.

Lammert A, Kiess W, Bottner A, Glasow A, Kratzsch J (2001) Soluble leptin receptor represents the main leptin binding activity in human blood. Biochem Biophys Res Commun 283: 982-988.

Lee GH, Proenca R, Montez JM, Carroll KM, Darvishzadeh JG, Lee JI, Friedman JM (1996) Abnormal splicing of the leptin receptor in diabetic mice. Nature 379: 632-635.

Levin BE, Finnegan MB, Marquet E, Sullivan AC (1984) Defective brown adipose oxygen consumption in obese Zucker rats. Am J Physiol 247: E94-100.

Li G, Klein RL, Matheny M, King MA, Meyer EM, Scarpace PJ (2002) Induction of uncoupling protein 1 by central interleukin-6 gene delivery is dependent on sympathetic innervation of brown adipose tissue and underlies one mechanism of body weight reduction in rats. Neuroscience 115: 879-889.

Loeb JE, Cordier WS, Harris ME, Weitzman MD, Hope TJ (1999) Enhanced expression of transgenes from adeno-associated virus vectors with the woodchuck hepatitis virus posttranscriptional regulatory element: implications for gene therapy. Hum Gene Ther 10: 2295-2305.

Lowell BB, Spiegelman BM (2000) Towards a molecular understanding of adaptive thermogenesis. Nature 404: 652-660.

Lu D, Willard D, Patel IR, Kadwell S, Overton L, Kost T, Luther M, Chen W, Woychik RP, Wilkison WO, . (1994) Agouti protein is an antagonist of the melanocyte-stimulating-hormone receptor. Nature 371: 799-802.

MacNeil DJ, Howard AD, Guan X, Fong TM, Nargund RP, Bednarek MA, Goulet MT, Weinberg DH, Strack AM, Marsh DJ, Chen HY, Shen CP, Chen AS, Rosenblum CI, MacNeil T, Tota M, MacIntyre ED, Van der Ploeg LH (2002) The role of melanocortins in body weight regulation: opportunities for the treatment of obesity. Eur J Pharmacol 440: 141-157.

Marks DL, Butler AA, Turner R, Brookhart G, Cone RD (2003) Differential role of melanocortin receptor subtypes in cachexia. Endocrinology 144:1513-1523

Marsh DJ, Hollopeter G, Kafer KE, Palmiter RD (1998) Role of the Y5 neuropeptide Y receptor in feeding and obesity. Nat Med 4: 718-721.

McMinn JE, Wilkinson CW, Havel PJ, Woods SC, Schwartz MW (2000) Effect of intracerebroventricular alpha-MSH on food intake, adiposity, c-Fos induction, and neuropeptide expression. Am J Physiol Regul Integr Comp Physiol 279: R695-R703.

Mercer JG, Hoggard N, Williams LM, Lawrence CB, Hannah LT, Trayhurn P (1996) Localization of leptin receptor mRNA and the long form splice variant (Ob-Rb) in mouse hypothalamus and adjacent brain regions by in situ hybridization. FEBS Lett 387: 113-116.

Mizuno TM, Kleopoulos SP, Bergen HT, Roberts JL, Priest CA, Mobbs CV (1998) Hypothalamic pro-opiomelanocortin mRNA is reduced by fasting and [corrected] in ob/ob and db/db mice, but is stimulated by leptin. Diabetes 47: 294-297.

Mizuno TM, Mobbs CV (1999) Hypothalamic agouti-related protein messenger ribonucleic acid is inhibited by leptin and stimulated by fasting. Endocrinology 140: 814-817.

Mobbs CV, Bray GA, Atkinson RL, Bartke A, Finch CE, Maratos-Flier E, Crawley JN, Nelson JF (2001) Neuroendocrine and pharmacological manipulations to assess how caloric restriction increases life span. J Gerontol A Biol Sci Med Sci 56 Spec No 1: 34-44.

Mohamed-Ali V, Goodrick S, Rawesh A, Katz DR, Miles JM, Yudkin JS, Klein S, Coppack SW (1997) Subcutaneous adipose tissue releases interleukin-6, but not tumor necrosis factor-alpha, in vivo. J Clin Endocrinol Metab 82: 4196-4200.

Monahan PE, Samulski RJ (2000) AAV vectors: is clinical success on the horizon? Gene Ther 7: 24-30.

Montminy MR, Gonzalez GA, Yamamoto KK (1990) Regulation of cAMP-inducible genes by CREB. Trends Neurosci 13: 184-188.

Muzyczka N (1992) Use of adeno-associated virus as a general transduction vector for mammalian cells. Curr Top Microbiol Immunol 158: 97-129.

Nedergaard J, Golozoubova V, Matthias A, Asadi A, Jacobsson A, Cannon B (2001) UCP1: the only protein able to mediate adaptive non-shivering thermogenesis and metabolic inefficiency. Biochim Biophys Acta 1504: 82-106.

Niswender KD, Morton GJ, Stearns WH, Rhodes CJ, Myers MG, Jr., Schwartz MW (2001) Intracellular signalling. Key enzyme in leptin-induced anorexia. Nature 413: 794-795.

Obici S, Feng Z, Tan J, Liu L, Karkanias G, Rossetti L (2001) Central melanocortin receptors regulate insulin action. J Clin Invest 108: 1079-1085.

Ogden CL, Flegal KM, Carroll MD, Johnson CL (2002) Prevalence and trends in overweight among US children and adolescents, 1999-2000. JAMA 288: 1728-1732.

Ollmann MM, Wilson BD, Yang YK, Kerns JA, Chen Y, Gantz I, Barsh GS (1997) Antagonism of central melanocortin receptors in vitro and in vivo by agouti-related protein. Science 278: 135-138.

Palmiter RD, Erickson JC, Hollopeter G, Baraban SC, Schwartz MW (1998) Life without neuropeptide Y. Recent Prog Horm Res 53: 163-199.

Pedrazzini T, Seydoux J, Kunstner P, Aubert JF, Grouzmann E, Beermann F, Brunner HR (1998) Cardiovascular response, feeding behavior and locomotor activity in mice lacking the NPY Y1 receptor. Nat Med 4: 722-726.

Pierroz DD, Ziotopoulou M, Ungsunan L, Moschos S, Flier JS, Mantzoros CS (2002) Effects of acute and chronic administration of the melanocortin agonist MTII in mice with diet-induced obesity. Diabetes 51: 1337-1345.

Poggioli R, Vergoni AV, Bertolini A (1986) ACTH-(1-24) and alpha-MSH antagonize feeding behavior stimulated by kappa opiate agonists. Peptides 7: 843-848.

Pritchard LE, Turnbull AV, White A (2002) Pro-opiomelanocortin processing in the hypothalamus: impact on melanocortin signalling and obesity. J Endocrinol 172: 411-421.

Raber J, O'Shea RD, Bloom FE, Campbell IL (1997) Modulation of hypothalamic-pituitary-adrenal function by transgenic expression of interleukin-6 in the CNS of mice. J Neurosci 17: 9473-9480.

Roselli-Rehfuss L, Mountjoy KG, Robbins LS, Mortrud MT, Low MJ, Tatro JB, Entwistle ML, Simerly RB, Cone RD (1993) Identification of a receptor for gamma melanotropin and other proopiomelanocortin peptides in the hypothalamus and limbic system. Proc Natl Acad Sci U S A 90: 8856-8860.

Saltiel AR (2001) You are what you secrete. Nat Med 7: 887-888.

Sarkar S, Legradi G, Lechan RM (2002) Intracerebroventricular administration of alpha-melanocyte stimulating hormone increases phosphorylation of CREB in TRH- and CRH-producing neurons of the hypothalamic paraventricular nucleus. Brain Res 945: 50-59.

Satoh N, Ogawa Y, Katsuura G, Numata Y, Masuzaki H, Yoshimasa Y, Nakao K (1998) Satiety effect and sympathetic activation of leptin are mediated by hypothalamic melanocortin system. Neurosci Lett 249: 107-110.

Sawchenko PE, Pfeiffer SW (1988) Ultrastructural localization of neuropeptide Y and galanin immunoreactivity in the paraventricular nucleus of the hypothalamus in the rat. Brain Res 474: 231-245.

Scarpace PJ, Matheny M (1996) Thermogenesis in brown adipose tissue with age: post-receptor activation by forskolin. Pflugers Arch 431: 388-394.

Scarpace PJ, Matheny M (1998) Leptin induction of UCP1 gene expression is dependent on sympathetic innervation. Am J Physiol 275: E259-E264.

Scarpace PJ, Matheny M, Borst SE (1992) Thermogenesis and mitochondrial GDP binding with age in response to the novel agonist CGP-12177A. Am J Physiol 262: E185-E190.

Scarpace PJ, Matheny M, Moore RL, Kumar MV (2000a) Modulation of uncoupling protein 2 and uncoupling protein 3: regulation by denervation, leptin and retinoic acid treatment. J Endocrinol 164: 331-337.

Scarpace PJ, Matheny M, Moore RL, Tumer N (2000b) Impaired leptin responsiveness in aged rats. Diabetes 49: 431-435.

Scarpace PJ, Matheny M, Pollock BH, Tumer N (1997) Leptin increases uncoupling protein expression and energy expenditure. Am J Physiol 273: E226-E230.

Scarpace PJ, Matheny M, Shek EW (2000c) Impaired leptin signal transduction with age-related obesity. Neuropharmacology 39: 1872-1879.

Scarpace PJ, Matheny M, Tumer N (2001) Hypothalamic leptin resistance is associated with impaired leptin signal transduction in aged obese rats. Neuroscience 104: 1111-1117.

Schobitz B, Pezeshki G, Pohl T, Hemmann U, Heinrich PC, Holsboer F, Reul JM (1995) Soluble interleukin-6 (IL-6) receptor augments central effects of IL-6 in vivo. FASEB J 9: 659-664.

Schobitz B, Voorhuis DA, De Kloet ER (1992) Localization of interleukin 6 mRNA and interleukin 6 receptor mRNA in rat brain. Neurosci Lett 136: 189-192.

Schumann G, Huell M, Machein U, Hocke G, Fiebich BL (1999) Interleukin-6 activates signal transducer and activator of transcription and mitogen-activated protein kinase signal transduction pathways and induces de novo protein synthesis in human neuronal cells. J Neurochem 73: 2009-2017.

Schwartz MW, Seeley RJ, Campfield LA, Burn P, Baskin DG (1996) Identification of targets of leptin action in rat hypothalamus. J Clin Invest 98: 1101-1106.

Schwartz MW, Seeley RJ, Woods SC, Weigle DS, Campfield LA, Burn P, Baskin DG (1997) Leptin increases hypothalamic pro-opiomelanocortin mRNA expression in the rostral arcuate nucleus. Diabetes 46: 2119-2123.

Schwartz MW, Sipols AJ, Marks JL, Sanacora G, White JD, Scheurink A, Kahn SE, Baskin DG, Woods SC, Figlewicz DP, . (1992) Inhibition of hypothalamic neuropeptide Y gene expression by insulin. Endocrinology 130: 3608-3616.

Schwartz MW, Woods SC, Seeley RJ, Barsh GS, Baskin DG, Leibel RL (2003) Is the energy homeostasis system inherently biased toward weight gain? Diabetes 52: 232-238.

Seeley RJ, Yagaloff KA, Fisher SL, Burn P, Thiele TE, van Dijk G, Baskin DG, Schwartz MW (1997) Melanocortin receptors in leptin effects. Nature 390: 349.

Shek EW, Scarpace PJ (2000) Resistance to the anorexic and thermogenic effects of centrally administrated leptin in obese aged rats. Regul Pept 92: 65-71.

Smith-Arica JR, Bartlett JS (2001) Gene therapy: recombinant adeno-associated virus vectors. Curr Cardiol Rep 3: 43-49.

Soriguer F, Moreno F, Rojo-Martinez G, Cardona F, Tinahones F, Gomez-Zumaquero JM, Garcia-Fuentes E, Morcillo S (2003) Redistribution of abdominal fat after a period of food restriction in rats is related to the type of dietary fat. Br J Nutr 89: 115-122.

Spiegelman BM, Flier JS (2001) Obesity and the regulation of energy balance. Cell 104: 531-543.

Starr R, Willson TA, Viney EM, Murray LJ, Rayner JR, Jenkins BJ, Gonda TJ, Alexander WS, Metcalf D, Nicola NA, Hilton DJ (1997) A family of cytokine-inducible inhibitors of signalling. Nature 387: 917-921.

Strassmann G, Fong M, Kenney JS, Jacob CO (1992) Evidence for the involvement of interleukin 6 in experimental cancer cachexia. J Clin Invest 89: 1681-1684.

Suzuki R, Sakamoto H, Yasukawa H, Masuhara M, Wakioka T, Sasaki A, Yuge K, Komiya S, Inoue A, Yoshimura A (1998) CIS3 and JAB have different regulatory roles in interleukin-6 mediated differentiation and STAT3 activation in M1 leukemia cells. Oncogene 17: 2271-2278.

Sweeney G (2002) Leptin signalling. Cell Signal 14: 655-663.

Taga T, Hibi M, Hirata Y, Yamasaki K, Yasukawa K, Matsuda T, Hirano T, Kishimoto T (1989) Interleukin-6 triggers the association of its receptor with a possible signal transducer, gp130. Cell 58: 573-581.

Taga T, Kishimoto T (1997) Gp130 and the interleukin-6 family of cytokines. Annu Rev Immunol 15: 797-819.

Tartaglia LA (1997) The leptin receptor. J Biol Chem 272: 6093-6096.

Tartaglia LA, Dembski M, Weng X, Deng N, Culpepper J, Devos R, Richards GJ, Campfield LA, Clark FT, Deeds J, . (1995) Identification and expression cloning of a leptin receptor, OB-R. Cell 83: 1263-1271.

Tchernof A, Nolan A, Sites CK, Ades PA, Poehlman ET (2002) Weight loss reduces C-reactive protein levels in obese postmenopausal women. Circulation 105: 564-569.

Tsigos C, Papanicolaou DA, Defensor R, Mitsiadis CS, Kyrou I, Chrousos GP (1997) Dose effects of recombinant human interleukin-6 on pituitary hormone secretion and energy expenditure. Neuroendocrinology 66: 54-62.

Uhler M, Herbert E (1983) Complete amino acid sequence of mouse pro-opiomelanocortin derived from the nucleotide sequence of pro-opiomelanocortin cDNA. J Biol Chem 258: 257-261.

Vaisse C, Halaas JL, Horvath CM, Darnell JE, Jr., Stoffel M, Friedman JM (1996) Leptin activation of Stat3 in the hypothalamus of wild-type and ob/ob mice but not db/db mice. Nat Genet 14: 95-97.

van Haasteren GA, van der Meer MJ, Hermus AR, Linkels E, Klootwijk W, Kaptein E, van Toor H, Sweep CG, Visser TJ, de Greef WJ (1994) Different effects of continuous infusion of interleukin-1 and interleukin-6 on the hypothalamic-hypophysial-thyroid axis. Endocrinology 135: 1336-1345.

Van Heek M, Compton DS, France CF, Tedesco RP, Fawzi AB, Graziano MP, Sybertz EJ, Strader CD, Davis HR, Jr. (1997) Diet-induced obese mice develop peripheral, but not central, resistance to leptin. J Clin Invest 99: 385-390.

Van Wagoner NJ, Benveniste EN (1999) Interleukin-6 expression and regulation in astrocytes. J Neuroimmunol 100: 124-139.

Vgontzas AN, Papanicolaou DA, Bixler EO, Kales A, Tyson K, Chrousos GP (1997) Elevation of plasma cytokines in disorders of excessive daytime sleepiness: role of sleep disturbance and obesity. J Clin Endocrinol Metab 82: 1313-1316.

Visscher TL, Seidell JC (2001) The public health impact of obesity. Annu Rev Public Health 22: 355-375.

Vozarova B, Weyer C, Hanson K, Tataranni PA, Bogardus C, Pratley RE (2001) Circulating interleukin-6 in relation to adiposity, insulin action, and insulin secretion. Obes Res 9: 414-417.

Wang W, Lonnroth C, Svanberg E, Lundholm K (2001) Cytokine and cyclooxygenase-2 protein in brain areas of tumor-bearing mice with prostanoid-related anorexia. Cancer Res 61: 4707-4715.

Wang Y, Kuropatwinski KK, White DW, Hawley TS, Hawley RG, Tartaglia LA, Baumann H (1997) Leptin receptor action in hepatic cells. J Biol Chem 272: 16216-16223.

Wang Z, Kontani Y, Sato Y, Mizuno T, Mori N, Yamashita H (2003) Muscle type difference in the regulation of UCP3 under cold conditions. Biochem Biophys Res Commun 305: 244-249.

Ward LD, Howlett GJ, Discolo G, Yasukawa K, Hammacher A, Moritz RL, Simpson RJ (1994) High affinity interleukin-6 receptor is a hexameric complex consisting of two molecules each of interleukin-6, interleukin-6 receptor, and gp-130. J Biol Chem 269: 23286-23289.

Widdowson PS, Upton R, Buckingham R, Arch J, Williams G (1997) Inhibition of food response to intracerebroventricular injection of leptin is attenuated in rats with diet-induced obesity. Diabetes 46: 1782-1785.

Wikberg JE (1999) Melanocortin receptors: perspectives for novel drugs. Eur J Pharmacol 375: 295-310.

Wilsey J, Zolotukhin S, Prima V, Shek EW, Matheny MK, Scarpace PJ (2002) Hypothalamic delivery of doxycycline-inducible leptin gene allows for reversible transgene expression and physiological responses. Gene Ther 9: 1492-1499.

Xiao X, Li J, Samulski RJ (1996) Efficient long-term gene transfer into muscle tissue of immunocompetent mice by adeno-associated virus vector. J Virol 70: 8098-8108.

Xu R, Janson CG, Mastakov M, Lawlor P, Young D, Mouravlev A, Fitzsimons H, Choi KL, Ma H, Dragunow M, Leone P, Chen Q, Dicker B, During MJ (2001) Quantitative comparison of expression with adeno-associated virus (AAV- 2) brain-specific gene cassettes. Gene Ther 8: 1323-1332.

Yamasaki K, Taga T, Hirata Y, Yawata H, Kawanishi Y, Seed B, Taniguchi T, Hirano T, Kishimoto T (1988) Cloning and expression of the human interleukin-6 (BSF-2/IFN beta 2) receptor. Science 241: 825-828.

Yaswen L, Diehl N, Brennan MB, Hochgeschwender U (1999) Obesity in the mouse model of pro-opiomelanocortin deficiency responds to peripheral melanocortin. Nat Med 5: 1066-1070.

Yudkin JS, Kumari M, Humphries SE, Mohamed-Ali V (2000) Inflammation, obesity, stress and coronary heart disease: is interleukin-6 the link? Atherosclerosis 148: 209-214.

Zhao AZ, Huan JN, Gupta S, Pal R, Sahu A (2002) A phosphatidylinositol 3-kinase phosphodiesterase 3B-cyclic AMP pathway in hypothalamic action of leptin on feeding. Nat Neurosci 5: 727-728.

Zolotukhin S, Byrne BJ, Mason E, Zolotukhin I, Potter M, Chesnut K, Summerford C, Samulski RJ, Muzyczka N (1999b) Recombinant adeno-associated virus purification using novel methods improves infectious titer and yield. Gene Ther 6: 973-985.

BIOGRAPHICAL SKETCH

Gang Li was born in Shaoxing, Zhejiang, China, on the 29th of July 1971, to Yantang Li and Xuehua Tang. He attended Zhejiang Medical University (now School of Medicine at Zhejiang University), Hangzhou, Zhejiang, China, where he received his Bachelor of Medicine degree in 1996. He continued his outstanding academic achievement at Peking Union Medical College (PUMC), Beijing, China, graduating with an M.D. degree in 1997 and became a resident surgeon at the PUMC Hospital, Beijing, China. After two years of vigorous clinical training, Gang Li went on to join the University of Florida's interdisciplinary Program in biomedical sciences in August 1999, where he pursued doctoral studies under the guidance of Dr. Philip J. Scarpace in the Department of Pharmacology and Therapeutics. Gang Li married Qin Dong in May 1999 in China, and they have spent three happy years together in Gainesville, Florida. In the future, he is looking forward to have a successful career in medical sciences with his medical professional experiences and research skills.